The PHILOSOPHICAL MAGAZINE

FIRST PUBLISHED IN 1798

L. 45 SEVENTH SERIES No. 371 December 1954

UNIVERSITY OF HAWAII
LIBRARY
JAN 10 '55

A Journal of Theoretical Experimental and Applied Physics

EDITOR
PROFESSOR N. F. MOTT, M.A., D.Sc., F.R.S.

EDITORIAL BOARD
SIR LAWRENCE BRAGG, O.B.E., M.C., M.A., D.Sc., F.R.S.
SIR GEORGE THOMSON, M.A., D.Sc., F.R.S.
PROFESSOR A. M. TYNDALL, C.B.E., D.Sc., F.R.S.

PRICE 15s. 0d.
Annual Subscription £8 0s. 0d. payable in advance

AND PUBLISHED BY TAYLOR & FRANCIS LTD., RED LION COURT, FLEET ST., LONDON, E.C.4.

Commemoration Number

To mark the 150th Anniversary of the

PHILOSOPHICAL MAGAZINE

Natural Philosophy through the
Eighteenth Century & Allied Topics

CONTENTS

The Philosophical Magazine. By ALLAN FERGUSON, M.A., D.Sc., and JOHN FERGUSON, M.A., B.D.

Astronomy through the Eighteenth Century. By Sir H. SPENCER-JONES, F.R.S.

Physics in the Eighteenth Century. By Prof. HERBERT DINGLE, D.Sc.

Chemistry through the Eighteenth Century. By Prof. J. R. PARTINGTON, D.Sc.

Mathematics through the Eighteenth Century. By J. F. SCOTT, Ph.D.

Engineering and Invention in the Eighteenth Century. By Engineer-Captain EDGAR C. SMITH, O.B.E., R.N.

Scientific Instruments in the Eighteenth Century. By ROBERT S. WHIPPLE, M.I.E.E., F.Inst.P.

The Scientific Periodical from 1665 to 1798. By DOUGLAS McKIE, D.Sc., Ph.D.

Scientific Societies to the end of the Eighteenth Century. By DOUGLAS McKIE, D.Sc., Ph.D.

The Teaching of the Physical Sciences at the end of the Eighteenth Century. By F. SHERWOOD TAYLOR, Ph.D.

ALERE FLAMMAM

viii + 164 pages

15/6

POST FREE

TAYLOR & FRANCIS, LTD.
RED LION COURT, FLEET ST., LONDON, E.C.4
PRINTERS & PUBLISHERS FOR OVER 150 YEARS

CXXXVIII. *Concentration Contours in Grain Boundary Diffusion*

By R. T. P. Whipple
Atomic Energy Research Establishment, Harwell, Berks.*

[Received June 10, 1954]

Abstract

Formulae are obtained for the concentration in a poorly diffusing half space bisected by a thin well-diffusing slab, at different times after the edge of the half-space has been suddenly raised from zero to unit concentration.

This represents a simplified model for studying 'grain boundary' diffusion of one metal into another. The problem also has obvious application to the study of heat flow in a poorly conducting solid with a metallic fin.

§ 1. Introduction

If two different metals, A and B are in contact along a plane surface (the surface $y=0$) and are then heated, it is found that the metals diffuse into one another. Barnes (1950) has developed a technique by means of which concentration contours may be made visible : the penetration can also be studied by 'tracer' technique. It is found that the penetration takes place much more readily along the 'grain boundaries' than elsewhere. It is the object of this paper to investigate this problem mathematically.

In the idealized problem it is assumed that the half space $y>0$ is filled with a material of diffusivity D, except for a thin slab of width $2a$ parallel to the y axis, which has diffusivity D' $(D'\gg D)$. At times $t<0$ the concentration C of the other metal is everywhere zero. At time $t=0$ the concentration on the plane $y=0$ is suddenly raised to unity and maintained at this value. The problem is to find the concentration $C=C(x, y, t)$ elsewhere.

In the slab $C=C'$ satisfies

$$D'\nabla^2 C'=\frac{\partial C'}{\partial t}. \qquad (1.1)$$

Outside the slab

$$D\nabla^2 C=\frac{\partial C}{\partial t}. \qquad (1.2)$$

The boundary conditions at the edges of the slab $(x=\pm a)$ are

$$C'=C, \qquad (1.3)$$

$$D'\frac{\partial C'}{\partial x}=D\frac{\partial C}{\partial x}. \qquad (1.4)$$

---

* Communicated by the Author.

When $y=0$

$$C=C(x,0,t)=H(t) \qquad (1.5)$$

where $H(t)$ is the Heaviside unit function.

In actual fact the D's are functions of the concentration C, so that the differential eqns. (1.1) and (1.2) are non-linear. It is not proposed to consider this complication here.

The problem as stated above is obviously equivalent to a heat flow problem, where a thin well-conducting fin projects into a block of poorly conducting material. In this case the equations would be exact.

The same problem has been considered by Fisher (1951), but his solution appears to be incorrect. Roe (1951) has also done some calculations on this problem. He considers the case of a number of parallel grain boundaries. His calculations have not as yet been published.

§ 2. APPROXIMATION WITHIN THE SLAB

C' is evidently an even function of x. Hence if $y \gg a$ it is a fair approximation to take

$$C'(x,y,t)=C_0'(y,t)+\frac{x^2}{2}C_2'(y,t). \qquad (2.1)$$

Then (1.1) gives

$$D'\left(\frac{\partial^2 C_0'}{\partial y^2}+C_2'\right)=\frac{\partial C_0'}{\partial t}.$$

Neglecting terms of order a^2, the boundary conditions (1.3) and (1.4) gives

$$C=C_0'$$

$$D\frac{\partial C}{\partial x}=D'aC_2'.$$

Hence eliminating C_0' and C_2'

$$D'\frac{\partial^2 C}{\partial y^2}+\frac{D}{a}\frac{\partial C}{\partial x}=\frac{\partial C}{\partial t} \qquad (2.2)$$

This represents a single homogeneous boundary condition satisfied by C when $x=a$. Using (1.2) it can also be written

$$D'\frac{\partial^2 C}{\partial x^2}-\frac{D}{a}\frac{\partial C}{\partial x}=\left(\frac{D'}{D}-1\right)\frac{\partial C}{\partial t}. \qquad (2.2.1)$$

§ 3. EXACT SOLUTION BY MEANS OF A FOURIER–LAPLACE TRANSFORM

Let

$$\psi(x,\mu,\lambda)=\int_0^\infty \exp(-\lambda t)\,d\lambda\int_0^\infty \sin\mu y C(x,y,t)\,dy. \qquad (3.1)$$

Then from the theory of Fourier and Laplace transforms

$$C(x,y,t)=\frac{1}{\pi}\int_{-\infty}^{\infty}\sin\mu y\,d\mu\frac{1}{2\pi i}\int_{-i\infty}^{i\infty}\exp(\lambda t)\psi(x,\mu,\lambda)\,d\lambda \qquad (3.2)$$

when the λ path of integration is to the right of all singularities of $\psi(\lambda)$.

Multiplying eqn. (1.2) by $\exp(-\lambda t)\sin\mu y$ and integration with respect to t and y

$$\frac{\partial^2\psi}{\partial x^2}-\left(\mu^2+\frac{\lambda}{D}\right)\psi+\int_0^\infty \exp(-\lambda t)\,dt\left[\sin\mu y\frac{\partial C}{\partial y}-\mu\cos\mu y\,C\right]_{y=0}^{\infty}$$

$$-\frac{1}{D}\int_0^\infty \sin\mu y\,dy\,[\exp(-\lambda t)\,C]_{t=0}^{\infty}=0.$$

But on using the boundary condition (1.5)

$$\left[\sin\mu y\frac{\partial C}{\partial y}-\mu\cos\mu y\,C\right]_{y=0}^{\infty}=\mu C(x,0,t)=\mu H(t).$$

While

$$[\exp(-\lambda t)\,C]_{t=0}^{\infty}=-C(x,y,0)=0.$$

Hence

$$\frac{\partial^2\psi}{\partial x^2}-\left(\mu^2+\frac{\lambda}{D}\right)\psi=-\frac{\mu}{\lambda}. \tag{3.3}$$

The boundary condition (2.2.1) transforms into

$$D'\frac{\partial^2\psi}{\partial x^2}-\frac{D}{a}\frac{\partial\psi}{\partial x}-\left(\frac{D'}{D}-1\right)\lambda\psi=0 \tag{3.4}$$

when $x=a$.

The solution of (3.3), consistent with (3.4), and having ψ finite when $x\to\infty$ is

$$\psi=\psi_1+\psi_2, \tag{3.5}$$

where

$$\psi_1=\frac{\mu}{\lambda(\mu^2+\lambda/D)}, \tag{3.6}$$

$$\psi_2=\frac{(D'/D-1)\,\mu\exp\left[-\sqrt{\left(\mu^2+\frac{\lambda}{D}\right)}\,(x-a)\right]}{\left(D'\mu^2+\frac{D}{a}\sqrt{\left(\mu^2+\frac{\lambda}{D}\right)}+\lambda\right)\left(\mu^2+\frac{\lambda}{D}\right)}. \tag{3.7}$$

At this stage it is convenient to introduce the following dimensionless parameters

$$\left.\begin{aligned}\xi=\frac{x-a}{\sqrt{Dt}}\qquad \eta&=\frac{y}{\sqrt{Dt}},\\ \alpha&=\frac{a}{\sqrt{Dt}},\\ \Delta&=D'/D,\\ \beta&=(\Delta-1)\,\alpha.\end{aligned}\right\} \tag{3.8}$$

Then applying (3.2) and replacing μ by $\mu/\sqrt{Dt}$, λ by λ/t

$$C=C_1+C_2, \tag{3.9}$$

where $$C_1=\frac{1}{2\pi^2 i}\int_{-\infty}^{\infty}\sin(\mu\eta)\mu\,d\mu\int_{-i\infty}^{i\infty}\frac{\exp\lambda\;d\lambda}{(\mu^2+\lambda)\;\lambda}, \tag{3.10}$$

and $$C_2=\frac{\Delta-1}{2\pi^2 i}\int_{-\infty}^{\infty}\sin(\mu\eta)\mu\,d\mu\int_{-i\infty}^{i\infty}\frac{\exp(\lambda-\sqrt{\mu^2+\lambda}\;\xi)\,d\lambda}{(\mu^2+\lambda)\left(\Delta\mu^2+\frac{1}{\alpha}\sqrt{\mu^2+\lambda}+\lambda\right)}. \tag{3.11}$$

3.1. *Evaluation of* C_1

C_1, which is independent of ξ, evidently represents the concentration which would be found in the absence of the slab.

In fact, performing the λ integration

$$C_1=\frac{1}{\pi}\int_{-i\infty}^{i\infty}(1-\exp[-\mu^2])\sin\mu\eta\,\frac{d\mu}{\mu}$$

$$=1-\frac{1}{\pi}\int_0^{\eta}d\eta'\int_{-\infty}^{\infty}\exp(-\mu^2)\cos\mu\eta'\,d\mu$$

$$=\frac{1}{\sqrt{\pi}}\int_{\eta}^{\infty}\exp(-\eta'^2/4)\,d\eta'=\operatorname{erfc}\eta/2. \quad . \quad . \quad . \quad (3.12)$$

§ 4. TRANSFORMATION OF INTEGRAL FOR C_2

Although not directly expressible in terms of elementary functions, the integral for C_2 can be transformed into a form which is more convenient for numerical computation.

Let $\lambda=\nu^2-\mu^2$. The path of integration for λ can be taken from $\infty\exp(-i\pi)$ to $\infty\exp(i\pi)$, passing to the right of all singularities of the integrand. Hence keeping μ fixed, the path of integration for ν is from $\infty\exp(-i\pi/2)$ to $\infty\exp(i\pi/2)$, keeping to the right of all singularities. Thus

$$C_2=\frac{1}{\pi^2 i}\int_{-\infty}^{\infty}\sin\mu\eta\exp(-\mu^2)\,\mu d\mu\int_{-i\infty}^{i\infty}\frac{\exp(\nu^2-\xi\nu)}{\mu^2+\frac{\nu}{\beta}+\frac{\nu^2}{\Delta-1}}\,\frac{d\nu}{\nu}. \qquad (4.1)$$

Noting that

$$\mu\sin\mu\eta=-\frac{1}{2}\frac{d}{d\eta}(\exp[i\mu\eta]+\exp[-i\mu\eta])$$

$$\frac{\exp(-\nu\xi)}{\nu}=\int_{\xi}^{\infty}\exp(-\nu\xi')\,d\xi'$$

$$\frac{1}{\mu^2+\frac{\nu}{\beta}+\frac{\nu^2}{\Delta-1}}=\exp\left(\mu^2+\frac{\nu}{\beta}+\frac{\nu^2}{\Delta-1}\right)\int_1^{\infty}\exp\left[-\left(\mu^2+\frac{\nu}{\beta}+\frac{\nu^2}{\Delta-1}\right)\sigma\right]d\sigma,$$

one can write

$$C_2=-\frac{\partial}{\partial\eta}\int_{\xi}^{\infty}d\xi'\int_1^{\infty}d\sigma\,.\,\frac{1}{\pi}\int_{-\infty}^{\infty}\exp(-\mu^2\sigma+i\mu\eta)\,d\mu$$

$$\times\frac{1}{i\pi}\int_{-i\infty}^{i\infty}\exp\left[\nu^2\frac{\Delta-\sigma}{\Delta-1}-\nu\left(\xi'+\frac{\sigma-1}{\beta}\right)\right]d\nu.$$

Noting that the last integral vanishes if $\sigma>\Delta$, and performing the third and fourth integrations

$$C_2=-\frac{1}{\pi}\frac{\partial}{\partial\eta}\int_{\xi}^{\infty}d\xi'\int_1^{\Delta}\frac{d\sigma}{\sqrt{\sigma}}\sqrt{\frac{\Delta-1}{\Delta-\sigma}}\exp\left[-\frac{1}{4}\left\{\frac{\eta^2}{\sigma}+\frac{\Delta-1}{\Delta-\sigma}\left(\xi'+\frac{\sigma-1}{\beta}\right)^2\right\}\right]$$

$$=\frac{\eta}{2\sqrt{\pi}}\int_1^{\Delta}\frac{d\sigma}{\sigma^{3/2}}\exp(-\eta^2/4\sigma)\operatorname{erfc}\left[\frac{1}{2}\sqrt{\frac{\Delta-1}{\Delta-\sigma}}\left(\xi+\frac{\sigma-1}{\beta}\right)\right] \quad . \quad (4.2)$$

which is in a form suitable for numerical integration.

As a check, suppose $\Delta \to \infty$, whilst $\alpha = a/\sqrt{Dt} = \beta/(\Delta-1)$ remains finite. Then for finite σ the last factor is simply erfc $\xi/2$. For large values of σ the last factor is unity, and the integral converges owing to the factor $\sigma^{-3/2}$. Hence

$$C_2 \simeq \operatorname{erfc}\frac{\xi}{2} \cdot \frac{\eta}{2\sqrt{\pi}} \int_1^\infty \exp(-\eta^2/4\sigma)\frac{d\sigma}{\sigma^{3/2}}$$

$$= \operatorname{erfc}\frac{\xi}{2} \operatorname{erf}\frac{\eta}{2}$$

i.e.

$$C = C_1 + C_2 = 1 - \operatorname{erf}\frac{\xi}{2} \operatorname{erf}\frac{\eta}{2}$$

Thus $C=1$ when $\xi=0$ or $\eta=0$, i.e., $x=a$ or $y=0$, and $C \to 0$ when $\xi \to \infty$ and $\eta \to \infty$, i.e., $x \to \infty$ and $y \to \infty$. This is clearly correct, since if $\Delta \to \infty$ whilst α remains finite, the slab can be regarded as a perfect diffuser, and hence attains unit concentration immediately.

If $\Delta \to \infty$, whilst $\beta = \alpha\,(\Delta - 1)$ remains finite, (4.2) simplifies to

$$C_2 = \frac{\eta}{2\sqrt{\pi}} \int_1^\infty \frac{d\sigma}{\sigma^{3/2}} \exp(-\eta^2/4\sigma) \operatorname{erfc}\frac{1}{2}\left(\frac{\sigma-1}{\beta} + \xi\right)$$

$$= \frac{\eta}{\sqrt{\pi}} \int_0^1 \exp\left(-\frac{\eta^2\tau^2}{4}\right) \operatorname{erfc}\left[\frac{1}{2}\left(\frac{1}{\tau^2\beta} - \frac{1}{\beta} + \xi\right)\right] d\tau. \quad . \quad . \quad (4.3)$$

Under certain conditions the integral (4.2) can be approximated by the method of steepest descents. It is found, however, that this method is only applicable in regions where the concentration is already very small. The formulae are given in the next section, and the analysis, which is rather tedious, is given in the Appendix.

§ 5. SUMMARY AND RESULTS

We have considered an idealized problem in which a slab of width $2a$ and diffusion constant D' bisects the half space $y>0$, the rest of which consists of material of diffusion constant D.

It is found that if the concentration on the plane $x=0$ is suddenly raised to unity at time $t=0$ and maintained at this value, the concentration in the quadrant $y>0$, $x>a$ at time t is a function of the four dimensionless variables ξ, η, β, Δ

$$\xi = \frac{x-a}{\sqrt{Dt}}, \qquad \eta = \frac{y}{\sqrt{Dt}},$$

$$\beta = \left(\frac{D'}{D} - 1\right)\frac{a}{\sqrt{Dt}} \quad \text{and} \quad \Delta = D'/D,$$

and is given explicitly by the formula

$$C = \operatorname{erfc}\eta + \frac{\eta}{2\sqrt{\pi}} \int_1^\Delta \frac{d\sigma}{\sigma^{3/2}} \exp\left(-\frac{\eta^2}{4\sigma}\right) \operatorname{erfc}\frac{1}{2}\sqrt{\frac{\Delta-1}{\Delta-\sigma}}\left(\frac{\sigma-1}{\beta} + \xi\right). \quad . \quad (5.1)$$

Fig. 1

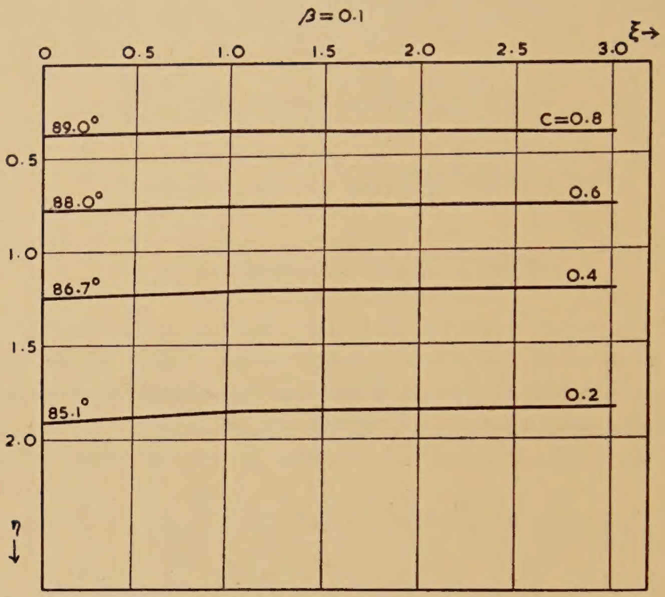

Concentration contours for $\beta=0\cdot1$.

Fig. 2

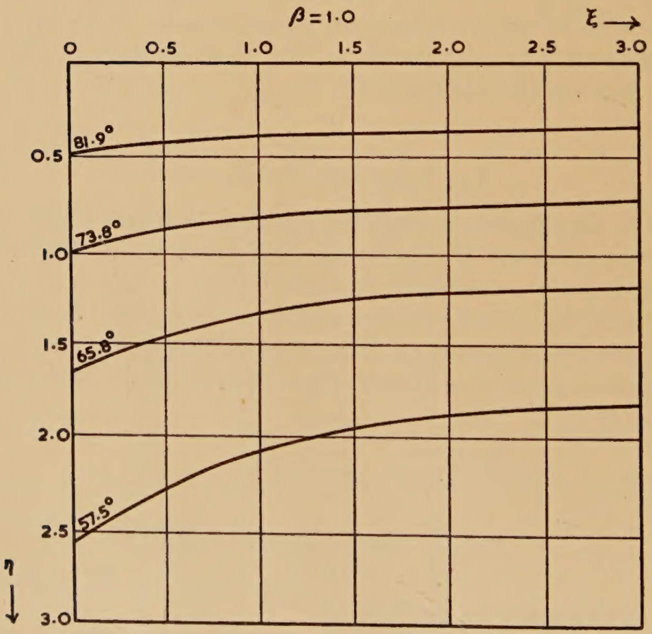

Concentration contours for $\beta=1\cdot0$.

Fig. 3

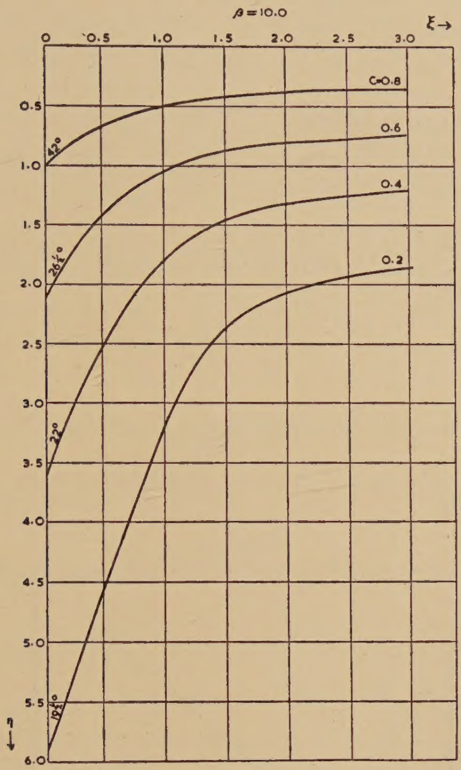

Concentration contours for $\beta=10{\cdot}0$.

Fig. 4

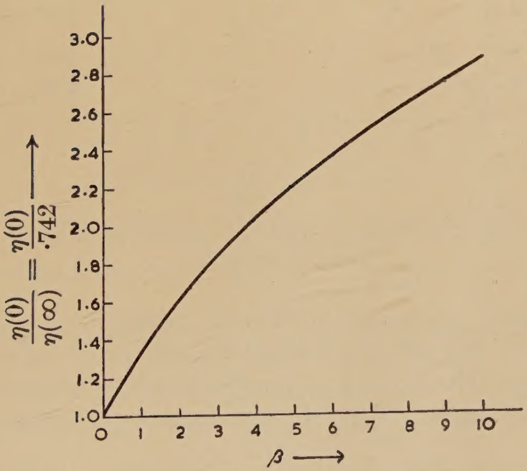

Penetration of $C=0{\cdot}6$ contour along grain boundary. Graph shows ratio of penetration along grain boundary to penetration far from boundary as function of $\beta=(\Delta-1)\dfrac{a}{\sqrt{(Dt)}}$.

Unless η is comparable with Δ this simplifies to

$$C=\operatorname{erfc}\eta+\frac{\eta}{2\sqrt{\pi}}\int_1^\infty\frac{d\sigma}{\sigma^{3/2}}\exp\left(-\frac{\eta^2}{4\sigma}\right)\operatorname{erfc}\frac{1}{2}\left(\frac{\sigma-1}{\beta}+\xi\right)$$

$$=\operatorname{erfc}\eta+\frac{\eta}{\sqrt{\pi}}\int_0^\infty\exp\left(-\frac{\eta^2\tau^2}{4}\right)\operatorname{erfc}\frac{1}{2}\left(\frac{1}{\tau^2\beta}-\frac{1}{\beta}+\xi\right)d\tau. \quad (5.2)$$

and this integral is convenient for numerical calculations.

If ξ is rather small, and $\eta\gg 1$ but $\ll\Delta^3/\beta$ the integral may be approximated by the ' method of steepest descents ', and we obtain

$$C_2\simeq 1{\cdot}159\,\beta^{1/3}\eta^{-2/3}\exp-[0{\cdot}473\,\beta^{-2/3}\eta^{4/3}-0{\cdot}396\,\beta^{-4/3}\eta^{2/3}(1-\beta\xi)$$
$$+O(\beta^{-2}(1-\beta\xi)^2)]. \quad (5.3)$$

To the same degree of approximation the gradient of the concentration contours is

$$\left(\frac{d\eta}{d\xi}\right)_c=\tan\theta\simeq-0{\cdot}63\,\eta^{1/3}\beta^{-2/3}(1-0{\cdot}421\,(\eta\beta)^{-2/3}(1-\beta\xi)). \quad (5.4)$$

These formulae are only valid, however, in regions where the concentration is already very small.

Fig. 5

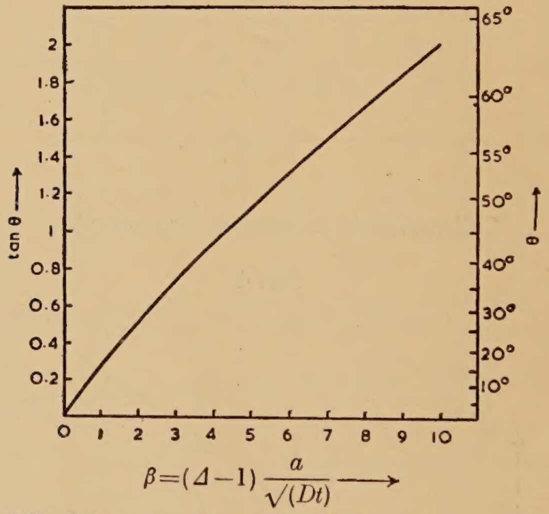

Gradient of $C=0{\cdot}6$ contour at point of contact with grain boundary as function of β

The formula (5.2) does not involve Δ explicitly, but only through $\beta=(\Delta-1)\,a/\sqrt{Dt}$. By plotting a series of contours $C=$constant in the ξ, η plane for various values of β it is possible to follow the history of a given system at different times. This follows since at a given time

$$\beta=(\Delta-1)\frac{a}{\sqrt{Dt}}=\text{constant},$$
$$x-a=\sqrt{Dt}\,\xi,$$
$$y=\sqrt{Dt}\,\eta,$$

so that at later times β diminishes, and the diagrams may be regarded as maps of the actual concentration contours on a diminishing scale.

In figs. 1, 2, 3 the contours $C=0{\cdot}2$, $0{\cdot}4$, $0{\cdot}6$, $0{\cdot}8$, $1{\cdot}0$ have been plotted in the ξ, η plane for $\beta=0{\cdot}1$, 1, 10.*

Figure 4 is a graph of the ratio of the ordinates ($\eta(0)$ and $\eta(\infty)$) for the $C=0{\cdot}6$ contour where it meets the slab and far from the slab, plotted as a function of β. It illustrates the extra penetration along the grain boundary.

Figure 5 is a graph of θ, the angle at which the contour $C=0{\cdot}6$ meets the η axis, plotted as a function of β. (The contour $C=0{\cdot}6$ has been chosen as this is the contour rendered visible by Barnes' technique.)

APPENDIX

Application of Method of Steepest Descents

Under certain conditions the integral (4.2) can be approximated by the method of steepest descents.

If X is large,

$$\operatorname{erfc} X=\frac{2}{\sqrt{\pi}}\int_x^\infty \exp(-n^2)\,dn\approx\frac{1}{\sqrt{\pi}}\frac{\exp(-X^2)}{X}. \quad . \quad . \quad (\text{A.1})$$

Hence in (4.2), if the argument of the error function is large for those values of σ which make the most important contribution to the integral as a whole

$$C_2\simeq\int_1^\Delta g(\sigma)\exp[-f(\sigma)]\,d\sigma, \quad . \quad . \quad . \quad . \quad . \quad (\text{A.2})$$

where

$$g(\sigma)=\frac{\eta}{\pi}\sqrt{\frac{\Delta-\sigma}{\Delta-1}}\,\frac{1}{\sigma^{3/2}\left(\dfrac{\sigma-1}{\beta}+\xi\right)}, \quad . \quad . \quad . \quad . \quad (\text{A.3})$$

$$f(\sigma)=\frac{1}{4}\left\{\frac{\eta^2}{\sigma}+\frac{\Delta-1}{\Delta-\sigma}\left(\frac{\sigma-1}{\beta}+\xi\right)^2\right\}. \quad . \quad . \quad . \quad . \quad (\text{A.4})$$

Now η^2/σ is a monotonically decreasing function of σ in $(1, \Delta)$. When $\sigma=1$ its gradient is $-\eta^2$. Also $\dfrac{\Delta-1}{\Delta-\sigma}\left(\dfrac{\sigma-1}{\beta}+\xi\right)^2$ is a monotonically increasing function of σ in $(1, \Delta)$. When $\sigma=1$ its gradient is $\xi\left(\dfrac{2}{\beta}+\dfrac{\xi}{\Delta-1}\right)$.

Hence provided

$$\eta^2>\xi\left(\frac{2}{\beta}+\frac{\xi}{\Delta-1}\right), \quad . \quad . \quad . \quad . \quad . \quad . \quad . \quad . \quad (\text{A.5})$$

---

* The asymptotic formulae were not used in computing for these figures and in fact it was found that they would only be useful for values of C considerably less than 0·1.

$f(\sigma)$ has a minimum in the range $(1, \varDelta)$, say at $\sigma=\sigma_0$. Then if this minimum is 'sufficiently sharp'

$$C_2 \simeq \sqrt{2\pi}\, g(\sigma_0)\, \{f''(\sigma_0)\}^{-1/2} \exp[-f(\sigma_0)]. \quad . \quad . \quad . \quad \text{(A.6)}$$

It is not easy to state in precise terms the conditions under which the steepest descents formula is valid : it depends on the variation of $g(\sigma)$. However, a fairly good criterion is that

$$\frac{f''(\sigma_0)^3}{f'''(\sigma_0)^2} \gg \frac{2}{9}. \quad . \quad . \quad . \quad . \quad . \quad . \quad . \quad . \quad . \quad \text{(A.7)}$$

In addition it is necessary that

$$X(\sigma_0)=\frac{1}{2}\sqrt{\frac{\varDelta-1}{\varDelta-\sigma_0}}\left(\frac{\sigma_0-1}{\beta}+\xi\right) \gg 1 \quad . \quad . \quad . \quad . \quad \text{(A.8)}$$

before the approximation (A.1) is valid.

To the same degree of accuracy as (A.6)

$$\frac{\partial C_2}{\partial \xi} \approx -\frac{\partial f}{\partial \xi} C_2 = -\frac{1}{2}\,\frac{\varDelta-1}{\varDelta-\sigma_0}\left(\frac{\sigma_0-1}{\beta}+\xi\right) C_2, \quad . \quad . \quad . \quad \text{(A.9)}$$

$$\frac{\partial C_2}{\partial \eta} \approx -\frac{\partial f}{\partial \eta} C_2 = -\frac{1}{2}\,\frac{\eta}{\sigma_0} C_2 \quad . \quad . \quad . \quad . \quad . \quad . \quad . \quad . \quad . \quad \text{(A.10)}$$

so that the gradient of the contours of equal concentration is given by

$$\tan\theta=\frac{d\eta}{d\xi}=-\frac{\partial C_2/\partial \xi}{\partial C_2/\partial \eta}=-\frac{\varDelta-1}{\varDelta-\sigma_0}\left(\frac{\sigma_0-1}{\beta}+\xi\right)\frac{\sigma_0}{\eta}. \quad . \quad . \quad \text{(A.11)}$$

A complete discussion of all possible cases would be rather involved. For simplicity we confine ourselves to the practically important case when $\varDelta$ is large but $\beta=(\varDelta-1)\,\alpha=(\varDelta-1)\,a/\sqrt{Dt}$ is of order unity. It is easy to see that if

$$\eta \ll \max\left(\varDelta^{3/2}\beta^{-1};\ \varDelta\left(\frac{\xi}{\beta}\right)^{1/2}\right)$$

the minimum of $f(\sigma)$ occurs for values of $\sigma \ll \varDelta$, and in this case the factor $(\varDelta-1)/(\varDelta-\sigma)$ occurring in (A.4) and (A.3) may be replaced by unity, without appreciable loss of accuracy, i.e.,

$$g(\sigma) \simeq \frac{\eta}{\pi}\,\frac{1}{\sigma^{3/2}\left(\dfrac{\sigma-1}{\beta}+\xi\right)}, \quad . \quad . \quad . \quad . \quad . \quad . \quad . \quad \text{(A.12)}$$

$$f(\sigma) \simeq \frac{1}{4}\left\{\frac{\eta^2}{\sigma}+\left(\frac{\sigma-1}{\beta}+\xi\right)^2\right\}. \quad . \quad . \quad . \quad . \quad . \quad \text{(A.13)}$$

Thus

$$f'(\sigma_0)=0$$

if

$$\sigma_0^2\,(\sigma_0-1+\beta\xi)=\frac{\eta^2\beta^2}{2}.$$

In particular, if

$$|1-\beta\xi| \ll (\eta\beta)^{2/3}, \quad . \quad . \quad . \quad . \quad . \quad . \quad . \quad . \quad \text{(A.14)}$$

$$\sigma_0 \simeq \left(\frac{\eta\beta}{\sqrt{2}}\right)^{2/3}+\tfrac{1}{3}(1-\beta\xi)+\ldots \quad . \quad . \quad . \quad . \quad . \quad \text{(A.15)}$$

In substituting in $g(\sigma_0)$, $f''(\sigma_0)$ and $f'''(\sigma_0)$ we may neglect the second term in σ_0. Then

$$g(\sigma_0)\simeq\frac{\eta\beta}{\pi}\sigma_0^{-5/2}=\frac{2^{5/6}}{\pi}(\eta\beta)^{-2/3}+0(\eta\beta)^{-4/3}, \quad \ldots\ldots\ldots \quad \text{(A.16)}$$

$$f(\sigma_0)=\frac{3}{2^{8/3}}\beta^{-2/3}\eta^{4/3}-\frac{1}{2^{4/3}}\beta^{-4/3}\eta^{2/3}(1-\beta\xi)+0\,\beta^{-2}(1-\beta\xi)^2. \quad . \quad \text{(A.17)}$$

Applying formula (A.6)

$$C_2\simeq 2^{11/6}\,3^{-1/2}\,\pi^{-1/2}\,\beta^{1/3}\,\eta^{-2/3}\exp\left[-f(\sigma_0)\right]. \quad \ldots\ldots \quad \text{(A.18)}$$

To the same degree of accuracy

$$\frac{\partial C_2}{\partial\xi}\simeq-\frac{1}{2}\frac{1}{\beta}(\sigma_0-1-\beta\xi)\,C_2=-\frac{1}{2^{4/3}}\eta^{2/3}\beta^{-1/3}\left(1-\frac{2}{3}\left(\frac{\sqrt{2}}{\eta\beta}\right)^{2/3}(1-\beta\xi)\right)C_2, \quad \ldots\ldots\ldots \quad \text{(A.19)}$$

$$\frac{\partial C_2}{\partial\eta}\simeq-\frac{1}{2}\frac{\eta}{\sigma_0}C_2=-\frac{1}{2^{2/3}}\eta^{1/3}\beta^{-2/3}\left(1-\frac{1}{3}\left(\frac{\sqrt{2}}{\eta\beta}\right)^{2/3}(1-\beta\xi)\right)C_2. \quad . \quad \text{(A.20)}$$

If $C_2\gg C_1$, then the gradient of the concentration contours is

$$\tan\theta=-\frac{\partial C/\partial\xi}{\partial C/\partial\eta}\simeq-\frac{\partial C_2/\partial\xi}{\partial C_2/\partial\eta}$$

$$=-\frac{1}{2^{2/3}}\eta^{1/3}\beta^{1/3}\left(1-\frac{1}{3}\left(\frac{\sqrt{2}}{\eta\beta}\right)^{2/3}(1-\beta\xi)\right). \quad \ldots\ldots \quad \text{(A.21)}$$

This implies that in the region where the above approximations hold the steepness of the concentration contours gradually increases with η, i.e., with y.

Now consider the range of validity of the above approximations. From (A.5) the method of steepest descents is certainly not valid unless

$$\eta>\sqrt{\xi\left(\frac{2}{\beta}+\frac{\xi}{\Delta-1}\right)}. \quad \ldots\ldots\ldots \quad (a)$$

We have restricted ourselves to the case

$$\eta\ll\max\left(\Delta^{3/2}\beta^{-1};\ \Delta\left(\frac{\xi}{\beta}\right)^{1/2}\right) \quad \ldots\ldots \quad (b)$$

and from (5.15) we have further restricted ourselves to the case

$$\eta\gg\frac{|1-\beta\xi|^{3/2}}{\beta}. \quad \ldots\ldots\ldots \quad (c)$$

The approximation to the error function is not valid unless

$$X(\sigma_0)\approx\frac{1}{2}\frac{\sigma_0}{\beta}\approx\frac{1}{2^{4/3}}\eta^{2/3}\beta^{-1/3}\gg1,$$

i.e.,

$$\eta\gg\beta^{1/2}. \quad \ldots\ldots\ldots \quad (d)$$

Now to the same order of approximation

$$f(\sigma_0)=3X(\sigma_0)^2$$

so this condition also implies that C_2 itself is small.

Combining conditions (*c*) and (*d*), it follows that if $\xi=0$ we must have

$$\eta > \max\left(\frac{1}{\beta}\ ;\ \beta^{1/2}\right)$$

so that in any case $\eta \gg 1$. In this case $C_2 \gg C_1$, since

$$C_1 = \operatorname{erfc}\frac{\eta}{2} \simeq \frac{1}{\sqrt{\pi}}\,\frac{\exp(-\eta^2/4)}{\eta}$$

for large η and this tends to zero more rapidly with η than

$$\exp(-f(\sigma_0)) \simeq \exp(-0{\cdot}473\,\beta^{-2/3}\,\eta^{4/3}).$$

The steepest descents method is only valid if

$$\frac{9}{2}\,\frac{f''(\sigma_0)^3}{f''(\sigma_0)^2} \approx \frac{27}{8\times 2^{2/3}}\,\frac{1}{\beta^2}\,(\eta\beta)^{4/3} = \tfrac{9}{2}f(\sigma_0) \gg 1 \quad . \quad . \quad . \quad . \quad (e)$$

and this is essentially equivalent to (*d*).

Since, by condition (*d*), $C_2 \gg C_1$ in the region of validity of the approximations, we are justified in replacing C by C_2 in the formula (A.21) for $\tan\theta$.

Summarizing, the formula (A.18), (A.19), (A.20), (A.21) are only valid if ξ is rather small, $\eta \gg 1$ but $\ll \Delta^3/\beta$, and under these conditions $C_2 \gg C_1$, but $\ll 1$. In order to investigate the region where C_2 is comparable with unity, numerical integration of (4.2) or (4.3) is required.

Using the approximate boundary condition (2.2), Fisher derives the asymptotic formula

$$C \approx \exp\left\{\frac{1}{\pi^{1/4}}\,\frac{\eta}{\beta^{1/2}}\right\} \operatorname{erfc}\xi/2.$$

As stated above, this formula appears to be incorrect.

REFERENCES

BARNES, R. S., 1950, *Nature, Lond.*, **166**, 1032.
FISHER, J. C., 1951, *J. Appl. Phys.*, **22**, 74.
ROE, G. M., 1951, *Phys. Rev.*, **83**, 871 (Note).

CXXXIX. *The Physical Nature of a Metal Surface in Conduction Theory*

By H. A. Müser*

British Council Fellow at H. H. Wills Physical Laboratory, University of Bristol†

[Received July 20, 1954]

Summary

A metal electron striking the surface of the metal from inside will be reflected into the metal. In the present paper this process of reflection will be treated as a phenomenon of electron diffraction. The atoms in a metal surface form a regular array, and this array may be considered as a cross-grating. As all free electrons in a metal have practically the same (Fermi) energy, their wavelength is uniform, and the ratio between this wavelength and the cube-edge of a face- or body-centred cubic lattice can be calculated. This gives a relation between the electron wavelength and the dimensions of the cross-grating, and formulae for the distribution of intensity over the various orders of diffraction can be derived. The main result is that the specular reflection is generally suppressed over a wide range of angles of incidence. This is true for any angle between the crystal axes and the surface. Generally most of the intensity is deflected to the first order of diffraction, but in the case of glancing electrons (i.e. electrons striking the surface at very small angles) most of the reflected intensity is found at a direction almost perpendicular to the surface.

§ 1. Introduction

Recent experimental results on electrons in metals involving the effect of the metal surface on the mean free path have been accounted for theoretically on the basis of a simple free electron model, in which the reflection of electrons at the surface is assumed to be non-specular (Sondheimer 1952). This means that the simple idea of electrons in a box made of smooth walls (i.e. potential walls) has to be supplemented by the assumption of some mechanism which deflects the electrons. It is recognized of course, that even the best polish technically possible may leave a submicroscopic roughness. If that is so, specular reflection by the plane of the macroscopic surface of the metal cannot be expected, but by improving the technique of polishing we might hope for a gradual approach to the ideal case. The object of this paper is to suggest a mechanism of electron

---

[*] Communicated by the Author.

[†] Formerly and now Physikalisches Institut der Universität Frankfurt-Main, Germany.

diffraction, which would lead to the conclusion that specular reflection is rendered impossible even in the case of a ‘ perfect ’ polish, i.e., a polish leaving only the natural atomic roughness of the surface atoms.

§ 2. ELECTRON WAVELENGTH AND INTERATOMIC DISTANCE

For a metal with one electron per atom the free electron model yields for the wavelength of an electron having Fermi limiting energy in a cubic lattice

$$\lambda_\zeta = \sqrt[3]{\frac{8\pi}{3n}}\,a, \qquad \dots\dots\dots \qquad (1)$$

where a is the length of the cube-edge and n the number of atoms per elementary cube, i.e., $n=4$ for a face-centred lattice. We focus our attention on this case and find numerically

$$\lambda_\zeta = 1{\cdot}279\,a.$$

The distance between nearest neighbours being $a/\sqrt{2}$, λ_ζ is too big to allow any diffraction to occur, but only by a factor of less than two.

Fig. 1

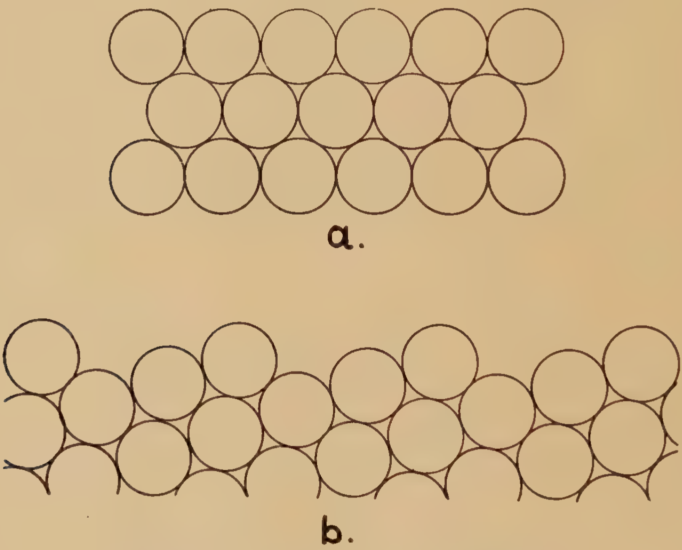

Arrangement of atoms in metal surface.

Even ‘ perfect ’ polish as defined above, however, will not produce a regular sequence of nearest neighbours in the metal surface. A slab of metal will consist of crystallites of random direction, i.e., in a two-dimensional picture a plane will look like fig. 1 (*b*) rather than 1 (*a*). This gives a regular array of atoms in the surface which looks roughly like what is known as an echelette grating in infra-red technique ; the grating constant is obviously bigger than the distance between nearest neighbours, and electron diffraction becomes possible.

The resistance of a metal is determined by the scattering of electrons with energies very nearly equal to the Fermi limit, and thus with wavelengths very nearly equal to λ_ζ. If in the Schrödinger equation the energy is a constant, it becomes analogous to the differential equation of an optical wave, and the electron waves behave like optical waves in a medium of constant refractive index. Therefore we may use the well-known optical formulae for echelette gratings, especially for the distribution of intensities among the different orders of diffraction. We are interested in the question, how much of the intensity is to be expected outside the zero order.

§ 3. QUALITATIVE ARGUMENT (FACE-CENTRED CUBIC LATTICE)

A qualitative argument will show that there is a fair chance of finding a considerable part of the intensity in the first order of diffraction rather than in the zero order.

Let s, d and ϕ define the dimensions of one element of an echelette grating as indicated in fig. 1 (*b*), and let us idealize it as indicated in fig. 2. Looking at the left part first, we find the condition that the zero order will be suppressed by the usual procedure used in optics: we combine 'beam' 1 with 'beam' 2, 3 with 4 etc., and find the path length difference between any two of them is simply $\varDelta=s$. The corresponding beams will cancel each other, if $\varDelta=\lambda/2$, $3\lambda/2$, . . . etc.

Fig. 2

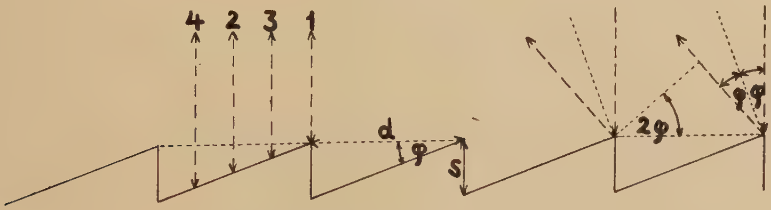

Echelette grating as surface model.

With an echelette grating we find a maximum of intensity in one order, if the direction of the diffraction order coincides with the direction of specular reflection from the planes of the lamellae, i.e., a direction at the angle ϕ from the plane of the grating. The right part of fig. 2 shows that the path length difference $\varDelta$ in the case of this specular reflection is $\varDelta=d\sin 2\phi$; if this is to be a direction of diffraction, $\varDelta$ must be equal to λ, 2λ, . . . etc. Now $d\sin 2\phi=2d\sin\phi\cos\phi$, or, as $s=d\tan\phi$, $\varDelta=2s\cos^2\phi$. Hence the condition for suppression of the zero order is

$$\lambda=2s, \qquad . \quad . \quad . \quad . \quad . \quad . \quad . \quad . \quad . \quad . \quad . \quad (2\,a)$$

and for strong intensity in the first order

$$\lambda=2s\cos^2\phi. \qquad . \quad . \quad . \quad . \quad . \quad . \quad . \quad . \quad . \quad . \quad (2\,b)$$

ϕ is a small angle, so the two conditions give nearly the same answer.

Looking back at fig. 1 (*b*) for a moment we find that the depth s of the furrows of the grating is roughly the distance between two (111)-planes for a face-centred cubic lattice, i.e., $a/\sqrt{3}$ or $0{\cdot}577\,a$. Comparing $s \simeq 0{\cdot}577\,a$ and $\lambda_\zeta = 1{\cdot}279\,a$, we find our conditions for annihilation of the zero order and high intensity in the first order nearly fulfilled ; this statement is true for a wide range of angles ϕ. ϕ must not be too big, of course, but if ϕ is big, d becomes small, and if $d < \lambda_\zeta$, there will be no diffraction anyhow.

§ 4. Quantitative Argument

Let us represent the plane surface of a face-centred metal by the intersection of an (*hkl*)-plane with the lattice. If the centre of a certain atom is a point of this plane, the same will be true for others, and all the atoms in the (*hkl*)-plane will form a regular array (fig. 3). There are various ways of arranging the points into parallelograms (some ways indicated in fig. 3) ; if there are only atoms in the corners and none inside the parallelogram, the areas of all these parallelograms are obviously equal. The area can be shown to be

Fig. 3

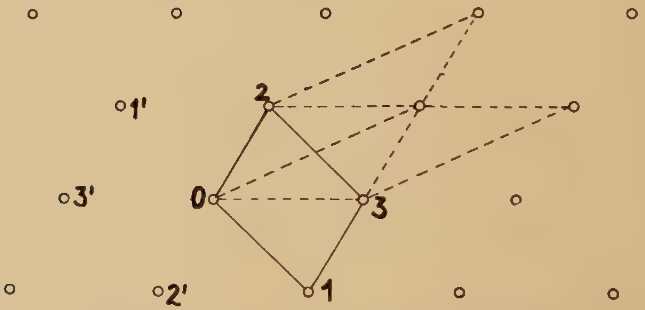

Array of atoms in (*hkl*)-plane ; proper combination to parallelograms (see text).

$$F = \tfrac{1}{4}a^2\sqrt{(h^2+k^2+l^2)}, \quad \ldots\ldots\ldots \quad (3\,a)$$

if h, k, l are all odd numbers ; otherwise it is

$$F = \tfrac{1}{2}a^2\sqrt{(h^2+k^2+l^2)}. \quad \ldots\ldots\ldots \quad (3\,b)$$

Any of our parallelograms may be considered as the basic cell of a cross-grating ; we choose the appropriate parallelogram in the following way. Starting from an arbitrary atom and calling it atom no. 0, we look for the nearest neighbours having a (111)-plane in common with point 0. There are two of them ; we call them 1 and 1′. Then we choose among the atoms of the next row parallel to 1′01 the atom 2 in such a way that the angle 102 is as nearly as possible 90° ; again there is a corresponding atom 2′ in the parallel row on the other side. To make the choice unambiguous, we may add the condition $\sphericalangle(102) \geqslant 90°$, leaving only the identical parallelograms (0132) and (01′3′2′) as basic cells of the cross-grating. Figure 4 shows such a parallelogram in the case of a (431)-plane chosen arbitrarily as an example. Beside the atoms in the corners it shows the atoms inside the parallelogram as seen from the surface, but lying slightly below it.

Fig. 4

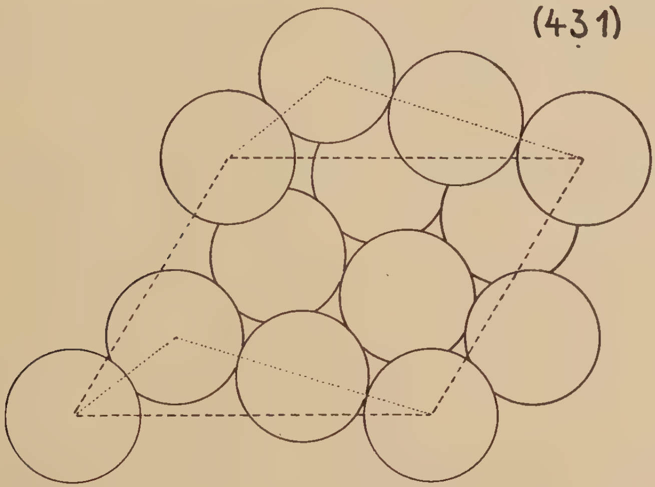

Basic cell of surface grating, for (431)-plane as an arbitrary example.

In the (111)-plane the atoms are tightly packed, and their distance is smaller than λ_ζ. Consequently, from now on we consider the (111)-planes as ‘ optically ’ dense reflecting planes. By so doing we may draw fig. 5 as a picture of the two-dimensional grating we have to consider. It is a series of flat* kinked steps. We may neglect the kinks, if the steps are broad enough, but we shall simplify the problem in a less serious manner : we neglect the small blackened area indicated in fig. 5, cutting off a triangular area at the bottom of the basic cell of our cross-grating and adding it on the top. For the resulting arrangement of plane lamellae the distribution of intensities among the various orders of diffraction can be calculated from well-known optical principles given in any advanced textbook on optics (e.g. Sommerfeld). If the directions of x- and y-axis are chosen as indicated in fig. 5, the z-axis perpendicular to the plane of the grating, maxima of intensity will be found, if

$$\alpha=\alpha_0+n_1\frac{\lambda}{a} \quad \text{and} \quad \beta=\beta_0+n_1\frac{\lambda}{a}\cot\psi+n_2\frac{\lambda}{b\sin\psi}. \qquad (4)$$

Here α_0, β_0, γ_0 are the direction cosines of the incident radiation, α, β, γ the direction cosines for the maxima, λ the wavelength of the radiation, a, b, ψ

---

* Generally they are flat ; it can be shown that there are sub-steps, if $(h-k)$ and $(k-l)$ have a common denominator other than the factor 2 occurring if h, k, l are all odd numbers.

as shown in fig. 5, n_1 and n_2 any positive or negative integers so that $\alpha^2+\beta^2\leqslant 1$. Obviously we have

$$\gamma_0=-\sqrt{(1-\alpha_0{}^2-\beta_0{}^2)} \qquad \text{and} \qquad \gamma=\sqrt{(1-\alpha^2-\beta^2)}.$$

For the directions given by (4) the intensities become

$$J=C[(\gamma-\gamma_0)-(\beta-\beta_0)\tan\phi]^2$$
$$\times\left\{\sin^2\left[\pi(\gamma-\gamma_0)\frac{s}{\lambda}\right]\sin^2\left[\pi\frac{a}{b}\frac{\sin\delta}{\sin(\delta+\psi)}\left(n_2+(\gamma-\gamma_0)\frac{s}{\lambda}\right)\right]\right\}\Big/$$
$$\left\{\left[n_2+(\gamma-\gamma_0)\frac{s}{\lambda}\right]^2\left(n_1+\frac{a}{b}\frac{\sin\delta}{\sin(\delta+\psi)}\left[n_2+(\gamma-\gamma_0)\frac{s}{\lambda}\right]\right)^2\right\}. \quad \dots \quad (5)$$

C is a constant, given by the condition that the sum of all diffracted intensities must be equal to the incident intensity, the other quantities being defined as before. We see that J will have its maximum value, if $n_2=-(\gamma-\gamma_0)\,s/\lambda$ and $n_1=0$, because in this case both factors in the denominator become zero. From our qualitative argument we expected strong intensity in the first order for $\lambda=2s\cos^2\phi$. Now we find the same condition again: in the case of perpendicular incidence, which we assumed there, $\alpha_0=\beta_0=0$, $\gamma_0=-1$; with $n_1=0$ and $n_2=-1$ we have from (4): $\alpha=0$, $\beta=-\lambda/b\sin\psi$, or, as $b\sin\psi$ corresponds to our grating constant d from fig. 2: $\beta=-\lambda/d$; hence $\gamma=+\sqrt{(1-\lambda^2/d^2)}$. To make the denominators of (5) 0, we must have

Fig. 5

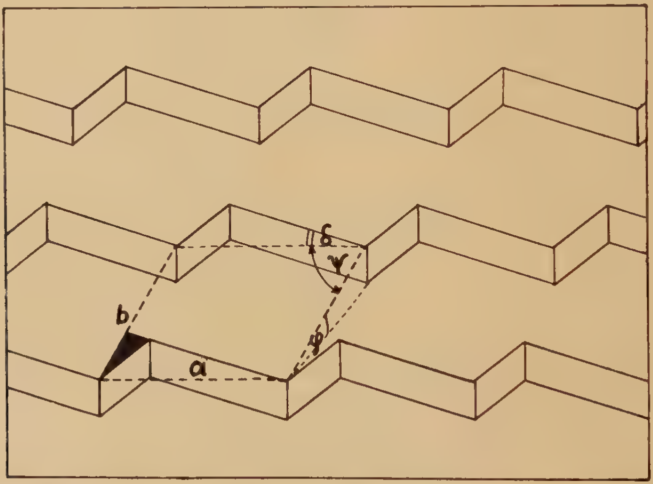

Idealized surface grating. Blackened area neglected in calculations.

$$\lambda=s\,(\gamma-\gamma_0)=s\,[1+\sqrt{(1-\lambda^2/d^2)}].$$

Solving this equation, we find

$$\lambda=\frac{2s}{1+(s/d)^2}.$$

Since $s/d=\tan\phi$, this is exactly condition (2 b).

Apart from this simple case eqn. (4) is too complicated to be visualized easily. An example may illustrate its results. Figure 6 shows the percentage of intensity in the zero order, i.e., in the direction of specular reflection, for two values of β_0, viz. 0 and $\frac{1}{2}$, as a function of $\cos^{-1}\alpha_0$, i.e., the angle towards the x-axis. The values are calculated again for the (431)-plane used as an example above. Figure 7 shows the intensity for $n_1=0$, $n_2=-1$, under the same conditions. For angles above about $\pm 20°$ and $\beta_0=0$ the condition $\alpha^2+\beta^2\leqslant 1$ is no longer fulfilled, the first order does not occur. The figures show that specular reflection is strongly suppressed over a considerable range of angles of incidence; specular reflection is not the predominant behaviour of electrons striking the metal surface even if there is only the natural atomic roughness of the surface, and even if the most perfect polish imaginable has been applied.

§ 5. RANGE OF VALIDITY OF THE APPROXIMATION

This conclusion is more general than the special example of the (431)-plane might suggest. Calculations of other cases show qualitatively the same results in spite of quantitative differences. This is to be expected, as the quantity s, the depth of the grating furrows, mainly determines the conditions (2 a) and (2 b), and this is the same for any (hkl). Generally it may be said that the range of angles of incidence, over which specular reflection disappears, increases with increasing area of the basic cell of the grating.

Another objection against the calculations might be that the steps with their sharp edges are an inadmissible idealization of the actual form of the boundary of the metal. This is not too serious, however. In an early treatment of diffraction problems Voigt (1911) showed for the case of the one-dimensional grating that the exact form of the grating is meaningless to a first approximation. He expands the periodic function determining the cross section of the grating into a Fourier series, and shows that only the first N terms of the series influence the diffraction phenomena if N orders of diffraction occur; the higher orders of the series are negligible to a first approximation. In other words, alterations of the form of the grating elements can be neglected as long as they remain below the order of magnitude of the wavelength. In this form we may use Voigt's argument for the two-dimensional case: as the diameter of the atoms is smaller than λ_ζ, it does not matter whether we consider sharp steps or some rounded-off structure, which would certainly be nearer to the truth.

A more serious objection is this. The optical formulae used for the calculations are based on Kirchhoff's treatment of diffraction. This implies the assumption that the incident radiation reaches the grating undisturbed. This is true only if $\lambda \ll d$, in other words our calculations may lose their quantitative character in the case of small (hkl), where the dimensions of the grating elements are bigger than, but still comparable to the wavelength. But even then the calculations will be a fairly good approximation, since no major discrepancies between theory and experiment are known from infra-red technique, where the same formulae have been used successfully for the design of echelette gratings, and the condition $\lambda \ll d$ is by no means fulfilled either.

Fig. 6

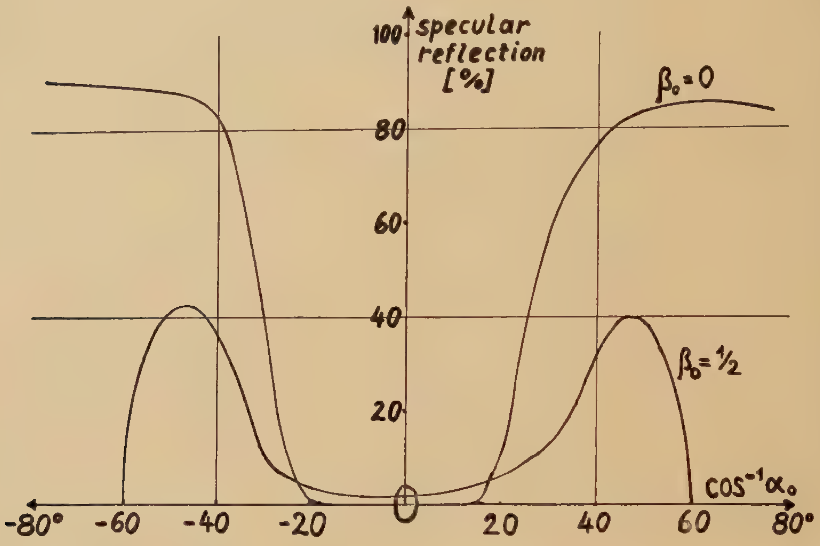

Percentage of intensity in the zero order (specular reflection) for different angles of incidence, (431)-plane as an example.

Fig. 7

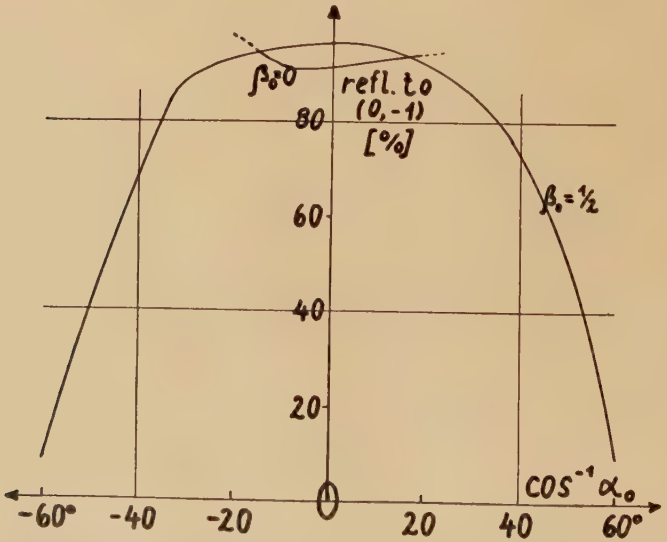

Percentage of intensity in the $(0\,;\ -1)$ order for different angles of incidence ; (431)-plane as an example.

§ 6. Glancing Electrons

Finally it is a shortcoming of the calculations that they do not include the case $\gamma_0 \simeq 0$, i.e., the so-called ‘ glancing electrons ’, which are the most important ones in certain surface phenomena (Pippard 1947). Obviously we must take into account the fact that a considerable part of each element of a grating is ‘ shadowed ’ by the preceding one (fig. 8). We can try to overcome this difficulty by leaving the shadowed parts out of the integration leading to formula (4). It must be realized, however, that this procedure makes the difficulties of the preceding paragraph all the more serious. Very narrow beams are cut out of the wave front by each grating element now, and the width of such a beam may now easily be smaller than λ_ξ. In this case diffraction by the edge of the $(n-1)$st element precedes the reflections by the nth element of the grating. Bearing this in mind we work out the following formula for the limiting case $\gamma_0 \simeq 0$, extending the integration over the parts not shadowed. As the result will be only qualitative anyway, we omit the kinks of fig. 5 and write down the formula only for the one-dimensional grating with furrows of width d :

Fig. 8

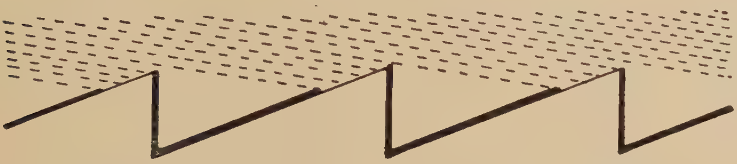

‘ Shadowed ’ parts of grating under glancing incidence.

$$J=C\left[(\gamma-\gamma_0)\frac{d}{\lambda}-n\tan\phi\right]^2\frac{\pi^2\gamma_0^2}{\alpha_0^2\tan^2\phi}. \qquad (6)$$

As the zero order is now to be found at a glancing angle, only negative n are possible in this case. For the case of specular reflection we have $n=0$, $\gamma=-\gamma_0$, hence

$$J_0=C\frac{4\pi^2\gamma_0^4 d^2}{\lambda^2\alpha_0^2\tan^2\phi}.$$

We obtain a simple expression for J/J_0 :

$$\frac{J}{J_0}=\frac{\lambda^2}{4\gamma_0^2 d^2}\left[(\gamma-\gamma_0)\frac{d}{\lambda}-n\tan\phi\right]^2. \qquad (7)$$

The predominant term is $\gamma d/\lambda$: the first order $(n=-1)$ is no longer preferred ; there is a strong preference for those orders reflected almost perpendicular to the grating $(\gamma\simeq 1)$. That means that the glancing electrons will preferably be thrown down into the metal at large angles from the surface.

§ 7. THE BODY-CENTRED LATTICE

So far we have dealt with the face-centred cubic lattice. We found in § 2 that the main condition for suppression of specular reflection and enhancement of the first order of diffraction was $\lambda_\zeta \simeq 2s$. In a body-centred cubic metal the (110)-planes are the most densely packed ones; the distance between two consecutive planes is $a/\sqrt{2} \simeq 0{\cdot}707\, a$. λ_ζ now becomes $\simeq 1{\cdot}612\, a$ (see (1)). The ratio λ_ζ/s becomes approximately $1{\cdot}612/0{\cdot}707 \simeq 2{\cdot}28$ as compared to $1{\cdot}279/0{\cdot}577 \simeq 2{\cdot}22$ for the face-centred case, i.e., again close to the required value of about 2. The area of the basic cell (cf. (3)) becomes

$$F = \tfrac{1}{2} a^2 \sqrt{(h^2+k^2+l^2)},$$

if two of the (hkl) are odd and one even, otherwise

$$F = a^2 \sqrt{(h^2+k^2+l^2)}.$$

Apart from these minor differences and the fact that we have to consider the (110) instead of the (111)-planes, all the conclusions remain valid for the body-centred lattice.

ACKNOWLEDGMENTS

The author wishes to thank Professor N. F. Mott for permission to work in his department and for suggesting the problem; Professor Mott, Dr. F. C. Frank, and Mr. R. Wolfe of Bristol and Dr. A. B. Pippard and Dr. R. G. Chambers of Cambridge for stimulating discussions, and the British Council for granting the fellowship which enabled the author to carry out this work.

REFERENCES

PIPPARD, A. B., 1947, *Proc. Roy. Soc.* A, **191,** 385.

SOMMERFELD, A., 1950, *Vorlesungen über theoretische Physik*, vol. IV, Optik, pp. 203 and 233.

SONDHEIMER, E. H., 1952, *Advances in Physics*, **1,** 1.

VOIGT, W., 1911, *Nachr. Kgl. Ges. d. Wissensch. z. Göttingen*, Math.-Phys. Klasse 1911, p. 41.

CXL. *Turbulence in the Upper Ionosphere*

By A. MAXWELL
Jodrell Bank Experimental Station, University of Manchester *

[Received August 25, 1954]

ABSTRACT

From the experimental data at present available it is shown that the Reynolds number in the upper F region (300-400 km level) is of the order of 300. The region may therefore be turbulent. It is suggested that the high level diffracting screens which give rise to spread F echoes and to radio star fading are caused by non-laminar flow, and that their non-appearance during the daylight hours may be due to the inhibition of turbulence by large temperature gradients, by lower drift velocities, or by an increase in the kinematic viscosity.

§ 1. INTRODUCTION

RECENT observations by radio-echo, radio-astronomical and rocket methods have shown that in the F region of the ionosphere there are drift movements with exceedingly high velocities (Maxwell and Dagg 1954 a, Briggs and Spencer 1954). As most large-scale fluid motions in nature are turbulent it is interesting to enquire whether these movements in the uppermost ionosphere may also be turbulent, and whether the diffracting screens which constitute sporadic F phenomena (the screens which cause radio star fading, for example, and the ‘ cloudy ’ structure associated with spread F echoes on h′-f records) are the result of non-laminar flow.

Radio observations of movements in the ionosphere depend on the identification of irregularities in its structure and then on measurements of the rate at which they move. It is not yet certain whether the movements of these irregularities in the ionization represent true movements of the atmosphere, whether they are electrodynamic movements of the ionization alone, or even whether they should be interpreted simply as a redistribution of matter by progressive hydrodynamic waves. A complete investigation of the problem of turbulence in the ionosphere will not be possible until these questions are resolved. Rocket measurements of air movements in the E and F regions and photometric observations of the night sky glow suggest, however, that whatever relation may exist between the movements of irregularities in ionization and the neutral molecules of the atmosphere, the latter have systematic motions of comparable magnitude.

This paper is essentially concerned with (i) an examination of the turbulence criteria for levels of the ionosphere above the maximum of ionization in the F region, and with (ii) turbulence as a possible origin of the irregularities which diffract the radiation from the discrete sources of extra-terrestrial radio emission (radio stars); these irregularities are believed to be above the level of maximum ionization in the F region and are remarkable for their correlation with the appearance of spread F echoes on ionospheric sounding records, and for the fact that they appear mainly at night.

---

* Communicated by Professor A. C. B. Lovell.

§ 2. Criteria of Turbulence

(*a*) *Reynolds Number at the* 300–400 *km Level*

The main difficulty in applying the Reynolds criterion for turbulence to the F region is the selection of appropriate numerical values for the parameters from the imprecise data about the F region which are at present available. The Reynolds number, Re, is defined by

$$Re=\frac{\rho v l_0}{\mu},$$

where v=total velocity difference occurring over a depth l_0, μ=viscosity, ρ=density, $\mu/\rho=\zeta$=kinematic viscosity.* It may first be questioned whether the term 'viscosity' has any real meaning when referred to the uppermost ionosphere, because the mean free paths there are so large. Estimates of the mean free paths at the 300–400 km level vary considerably, as shown in table 1, but a probable value is 200 metres. The thickness of the region under consideration is some 500 times this path length and it may therefore be assumed that viscous effects will be evident.

Table 1. F Region Parameters (300–400 km Level)

Reference	Mean free path (cm)	Kinematic viscosity (cm^2 sec^{-1})
Gerson, N. C., 1952, *Advances in Geophysics I*, p. 165; 1951, *Rep. Phys. Soc. Progr. Phys.*, **14**, 316	2×10^4	10^9
de Jager, C., 1952, *Mém. Soc. Roy. Sci. Liège*, **12**, 223	6×10^3	4×10^8
Mitra, S. K., 1952, *The Upper Atmosphere*, 2nd Edition, p. 28		5×10^9
Yerg, D. G., 1952, *J. Geophys. Res.*, **57**, 217	6×10^5	$\begin{cases}2\times10^{10}\\10^8\end{cases}$
Yerg, D. G., 1951, *J. Met.*, **8**, 244	8×10^5	3×10^{10}

The present uncertainties in the temperature, pressure and density data for the F region lead to a similar diversity in the estimates of kinematic viscosity, ζ, but the values listed in table 1 suggest that it is of the order 10^9.

---

* To avoid confusing 'kinematic viscosity' with 'collision frequency', for both of which the symbol ν is widely used, it is suggested that the symbol ζ be used for kinematic viscosity in the ionosphere.

The length dimension l_0 appropriate to the Reynolds number might be taken as the thickness of the region, but this would imply that the drift direction throughout its vertical extent is the same; as this may not be the case, a value corresponding to half the thickness $=2\times$ scale height $=2\times70$ km will be assumed. Velocities in the region, estimated by visual and radio methods, have magnitudes of the order of 200 m/sec. These data lead to a value of $Re=300$.

There is no universally accepted critical value of the Reynolds number for shearing flow in a free atmosphere, but present evidence suggests that it is much lower than the classical value of 1000, estimated for the flow of liquids through tubes; for example, experiments with jet streams (Andrade 1939) give critical values of 30. It would therefore seem highly probable that in the absence of strong damping factors and at the Reynolds numbers observed in the upper F region turbulent flow will result.

(b) *Microscale of Turbulence at the* 300–400 *km Level*

The fluctuating velocity field in a turbulent medium may be regarded as the result of the superposition of periodic variations with all possible wavelengths. These constitute a hierarchy of 'turbulent eddies', the maximum wavelengths, l_0 (macroscale of turbulence) being limited by the dimensions of the medium under consideration, and the minimum wavelengths, η (microscale of turbulence) by viscous dissipation in the smallest eddies. In the case of the upper F region, where the Reynolds number is only of the order of 100–500, it is not permissible to apply the spectral laws (Kolmogoroff 1941, and others) which refer to fully developed turbulence, that is $Re\to\infty$, but it is possible to calculate the cut-off in the hierarchy of eddies due to viscous damping. This is given by the equation

$$\eta=\left(\frac{\zeta^3}{\epsilon}\right)^{1/4},$$

where ζ = kinematic viscosity and ϵ = rate of dissipation of energy $\div v^3/l_0$, that is,

$$\eta=\left(\frac{\zeta^3 l_0}{v^3}\right)^{1/4}$$

$$=l_0(Re)^{-3/4}.$$

For $l_0=140$ km and $Re=300$

$$\eta=2\text{ km}.$$

It is interesting to notice that the effective wavelength of the F region irregularities which diffract the radiation from extra-terrestrial radio sources is of the same order (Maxwell and Little 1952).

(c) *Turbulence at Lower Levels in the Ionosphere*

With decreasing height the kinematic viscosity (the parameter essentially controlling turbulence) decreases very considerably, so that turbulence should become increasingly evident in the lower levels of the ionosphere. In the lower half of the F region (200–300 km level) for example, $\zeta=10^7$, $l_0=100$ km, $v=100$ m/sec, whence the Reynolds number$=10^4$ and the microscale of turbulence$=100$ metres. In this connection it may be remarked that the diffracting screens used for radio-echo measurements of drift movements in the lower F region (Briggs and Spencer 1954, and others) are *always* observable—as distinct from the high level diffracting screens which in general occur only at night—and have wavelengths of the order of 100 metres.

In the E region (80–120 km level) $\zeta=10^5$, $v=50-100$ m/sec, $l_0=30$ km and the Reynolds number$=2\times10^5$. It is to be expected therefore that the E region will invariably be turbulent, and observations of the decay of meteor trails confirm this.* The microscale of turbulence in the E region$=10$ metres. Scattering of electromagnetic radiation by turbulent irregularities in the E region has been investigated by Villars and Weisskopf (1954).

§ 3. RADIO STAR FADING

It is now generally believed that the ionospheric diffracting screen which causes fading, or scintillation, in the signals from radio stars occurs above the level of maximum ionization in the F region (Little and Maxwell 1951, Hewish 1952), but its origin is not understood. The maximum of radio star fading occurs near 01^{h}, and from fig. 1 it will be seen that this coincides in time with a maximum in the occurrence of irregular ionization in the F region. Ryle and Hewish (1950) have sought an explanation of these phenomena in terms of some ionizing process which has a maximum shortly after midnight. They suggested that the additional agency might be corpuscular matter of interstellar origin moving under the gravitational attraction of the sun. The radial velocity of such particles when they intersect the earth's orbit is 42 km/sec, and as the orbital velocity of the earth is 30 km/sec their motion is normal to the surface of the earth at 02^{h} 20 local time. The mechanism should exhibit an onset at 20^{h} 20, a maximum at 02^{h} 20 and a cut off at 08^{h} 20, and Ryle and Hewish pointed out that this is in rough agreement with the known variations in the radio star scintillation amplitude and in the occurrence of irregularities

---

* It would appear that the Richardson criterion for turbulence, *Ri*, which was originally developed for tropospheric problems and which is defined by

$$Ri=\frac{g}{T}\left(\frac{dT}{dz}+\Gamma\right)\Big/\left(\frac{du}{dz}\right)^2,$$

is inapplicable to the ionosphere. In the case of the E region the velocity gradient $du/dz=3$ m sec^{-1} km^{-1} (Greenhow, J. S., 1954, *Phil. Mag.*, **45,** 371), the adiabatic lapse rate $\Gamma=1\cdot5\times10^{-4}$ deg. K cm^{-1}, the temperature gradient $dT/dz=3\cdot2$ deg. K km^{-1} (The Rocket Panel, 1952, *Phys. Rev.*, **88,** 1027), and the temperature $T\doteqdot250$ deg. K, whence the Richardson number$=10$. As this value is much greater than unity it requires that the E region should *not* be turbulent. This is in contradiction to the experimental evidence. It may therefore be concluded that, unlike the tropospheric case, turbulence in the E region is not chiefly maintained by heat convection and buoyancy processes; this further suggests that vertical movements in the E region may be restricted.

in the F region. Ginzburg (1952) has developed this theory in more detail and has considered not only the effect of incoming interstellar gas particles, diameter 10^{-8} cm, but also the possible effects of interstellar dust particles, diameter 10^{-3} cm; he concludes that the interstellar dust will pass unhindered through the F region and that it can therefore be ruled out entirely as a generator of sporadic ionization in that region.

The suggestion that interstellar gas is the ionizing mechanism must, however, withstand criticism on the following counts: (i) The interstellar gas attracted towards the sun comprises mainly protons, and their energy when moving at the maximum velocity relative to the earth, 52 km/sec, is only 14 ev, which is insufficient to ionize the particles of the upper atmosphere. Ginzburg has considered the possibility of ionization by the helium atoms of the interstellar gas; their energy is 57 ev, which is adequate for ionization, but it is questionable whether their density is sufficient for such a mechanism to be completely effective. (ii) It is difficult to understand why the diffracting screen should be formed for an average of only one night in three, since the interstellar matter impinges on the atmosphere every night. (iii) It is also difficult to understand why the interstellar matter should ionize in irregular patches. (iv) Radio star scintillations and sporadic F are often observed well before the predicted onset time, 20^h 20, and rarely after 06^h, even though the cut-off time is 08^h 20.

Observations of radio star fading during the recent eclipse, June 30, 1954 provide further evidence against an accretion mechanism. It has been mentioned above that the diffracting screens causing radio star scintillations and spread F echoes normally occur at night; during these hours there is a decrease in the F region critical frequency. At the time of the eclipse, 12^h 30 local time (=U.T.), the line of sight to the Cassiopeia radio star from Jodrell Bank intersected the F region at a point 100 km from the area of totality in the region, and the temporary simulation of night time conditions in this area caused the F region critical frequency to drop from 4·6 to 3·8 Mc/s.* On the equipment used at Jodrell Bank for continuous observations of the Cassiopeia radio star the records showed a sudden onset of scintillations at 13^h 10, that is 40 minutes after the maximum phase of the eclipse, and these continued for the following 90 minutes. This appearance of scintillations during an eclipse occurring at 12^h 30 could not be attributed to an accretion theory.

As an alternative mechanism, it may be suggested that the irregular distribution of ionization in the upper F region is caused by turbulence, and that the appearance of the diffracting screens represents a transition from laminar flow during the day to non-laminar flow at night. These irregularities may be distributed throughout the whole region, or they may be localized near an interface between different circulatory systems in the F region. The arguments advanced in § 2 show that the Reynolds number in the upper F region is, in all probability, above the critical value. It therefore becomes necessary to account for the disappearance of the smaller scale sporadic phenomena during daylight hours in terms of some process which decreases or inhibits turbulent flow during the daytime. This diurnal variation could be brought about by three mechanisms acting separately or in combination. (i) Repression of turbulence by large temperature gradients : if temperature gradients in the F region are much larger in the daytime than at night, there will be a greatly increased probability of turbulent flow occurring during the night hours. (ii) Increase in velocity : for example, measurements of drift movements by radio astronomical techniques show that drift speeds increase significantly at night, from an average of 60 m/sec at 19^h to 290 m/sec at 01^h decreasing again to 170 m/sec at 05^h (fig. 1). (iii) Decrease in kinematic viscosity : the night-time contraction of the ionosphere may lead to a decrease in kinematic viscosity but at present there is no experimental information about this. Finally it will be noted that turbulent flow will to some extent be continually damped by the terrestrial magnetic field.

---

* Inverness values. The mean value of the F region critical frequency at noon during June 1954 was 4·6 Mc/s, and it did not fall below 4·2 Mc/s on any other day during the month. It will further be noted that the eclipse day was geomagnetically quiet (K indices $\leqslant 3$) so that the decrease in F region critical frequency at the eclipse time could not be attributed to magnetic activity. The author is indebted to the Department of Scientific and Industrial Research for providing the ionospheric data in advance of publication.

The association of sporadic F with geomagnetically disturbed conditions, and the occurrence of radio-star scintillations in the day time during severe magnetic storms may be accounted for in a similar way. There is a fourfold increase in the drift speed of the F region irregularities during the most intense magnetic storms (Little and Maxwell 1952, Maxwell and Dagg 1954 b) and at the same time the ionosphere is irradiated by excess ultra-violet and x-ray emissions from active areas on the sun, or is penetrated by fast travelling auroral particles, so that violent changes in the kinematic viscosity and temperature gradients may also occur.

§ 4. FURTHER EXPERIMENTAL POINTS

The rapidity of the fading in radio star signals is proportional to the drift velocity of the ionospheric irregularities which diffracts the incident radiation (Maxwell and Dagg 1954 a). As turbulent effects become more pronounced with increasing velocity it would be expected that the *amplitude* of the fading should show some correlation with the fading *rate*. There is no one to one correlation between these two quantities, but there is some experimental evidence which qualitatively supports this prediction. Bolton, Slee and Stanley (1954) in an investigation of the fluctuating signals from the Cygnus source, found that variations of greater amplitude seemed to have shorter periods ; Ryle and Hewish (1950) occasionally observed sudden increases in both amplitude and fading rate which then gradually decreased during a subsequent period of 30 to 40 minutes. Mills and Thomas (1951) found a correlation of 0·6 between amplitude and the average fading rate for the case of fast fading ; at Jodrell Bank sudden and simultaneous increases in both amplitude and fading rate have often been observed, and it has been especially noticeable that the fading rate falls markedly as the fading amplitude decreases near dawn.

It is the nature of turbulent flow, that the eddies are constantly forming, disintegrating and reforming; this process goes on spontaneously and

Fig. 1

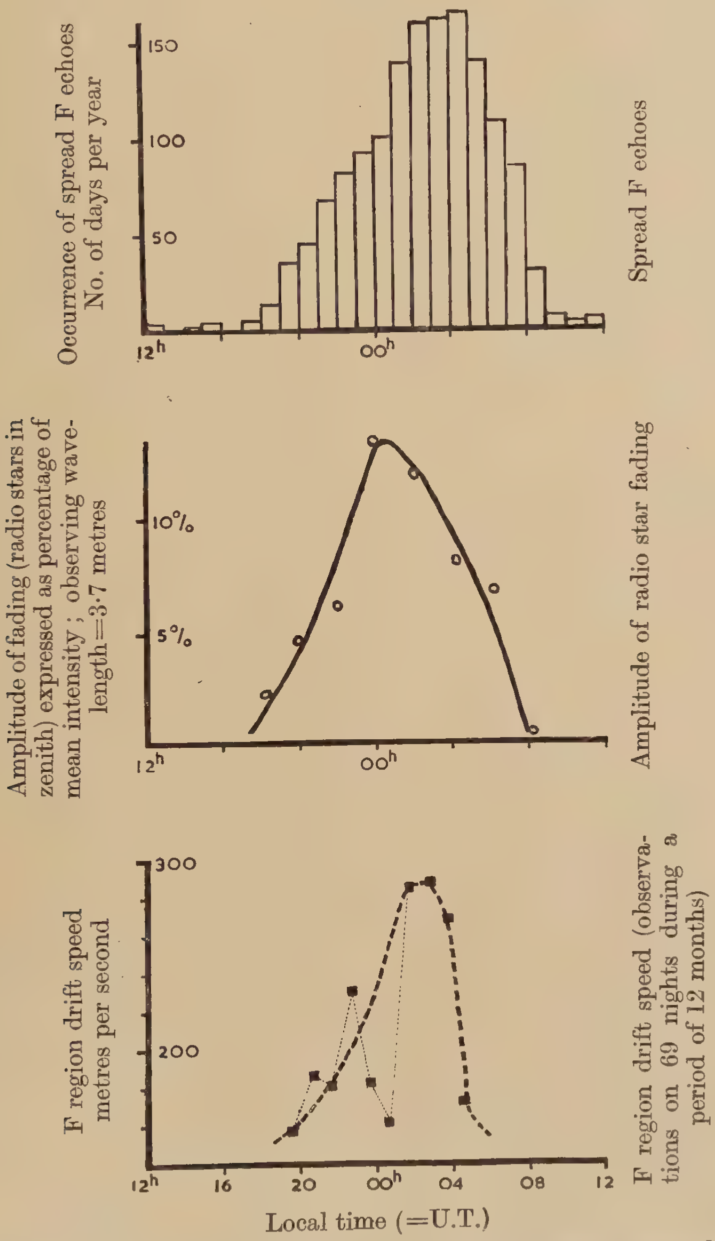

Diurnal variation of spread F echoes, radio star fading and F region drift speed.

continuously. The decay time τ of an eddy of wavelength, l, is given by

$$\tau=\frac{l}{u},$$

where u=the turbulent velocity. The contours of the radio star diffraction pattern have wavelengths of 3·5 km * and are moving at speeds of 200 m/sec. Assuming they are caused by turbulence, and that they have a turbulent velocity of 100–200 m/sec, these contours should have a decay time of 20 seconds and in consequence should be individually distinguishable only over paths of the order of their characteristic wavelength. Experimentally this is found to be so. Fading records taken with receiving equipments arranged at varying distances along the direction of motion show marked changes at spacings of 4 km (due allowance being made for the systematic time delays between the records) and no correlation at all at 7 km. It will also be noted that the decay time of an eddy is directly proportional to its characteristic wavelength. If the large-scale F region irregularities with fronts of the order of 200 km moving with velocities of 200 m/sec (observed by Munro 1948) represent a macroscale of turbulence in the region, they would be expected to retain their identity over paths of several hundred km. Experimentally this is again found to be the case.

ACKNOWLEDGMENTS

The author is indebted to Professor M. J. Lighthill of the Department of Mathematics, University of Manchester, and Mr. M. A. Johnson of the Cavendish Laboratory, Cambridge, for their valuable comments. The experimental work discussed in this paper forms part of a research programme financed by the Department of Scientific and Industrial Research. The author wishes to thank Mr. M. Dagg for assistance in taking the radio observations and Professor A. C. B. Lovell, director of the Jodrell Bank Experimental Station, for his helpful advice.

REFERENCES

ANDRADE, E. N. DA C., 1939, *Proc. Phys. Soc.*, **51**, 784.
BOLTON, J. G., SLEE, O. B., and STANLEY, G. J., 1953, *Aust. J. Physics*, **6**, 434.
BRIGGS, B. H., and SPENCER, M., 1954, *Rep. Phys. Soc. Progr. Phys.*, **17**, 245.
GINZBURG, V. L., 1952, *Dokl. Akad. Nauk. S.S.S.R.*, **84**, 245.
HEWISH, A., 1952, *Proc. Roy. Soc.* A, **214**, 494.
KOLMOGOROFF, A. N., 1941, *C. R. Acad. Sci., U.R.S.S.*, **30**, 301 ; **32**, 16.
LITTLE, C. G., and MAXWELL, A., 1951, *Phil. Mag.*, **42**, 267 ; 1952, *J. Atmos. Terr. Phys.*, **2**, 356.
MAXWELL, A., and LITTLE, C. G., 1952, *Nature, Lond.*, **169**, 746.
MAXWELL, A., and DAGG, M., 1954 a, *Phil. Mag.*, **45**, 551 ; 1954 b, in preparation.
MILLS, B. Y., and THOMAS, A. B., 1951, *Aust. J. Sci. Res.* A, **4**, 158.
MUNRO, G. H., 1948, *Nature, Lond.*, **162**, 886.
RYLE, M., and HEWISH, A., 1950, *Mon. Not. Roy. Astr. Soc.*, **110**, 381.
VILLARS, F., and WEISSKOPF, V. F., 1954, *Phys. Rev.*, **94**, 232.

---

* It is interesting to notice that the contours are anisotropic. Experiments made at Jodrell Bank with spaced receiving equipments show that in the North–South direction, that is, perpendicular to the direction of motion, the contours have diameters of approximately 7 km.

CXLI. *Self Trapped Electrons in a Fermi Gas*

By J. S. Plaskett*
H. H. Wills Physical Laboratory, University of Bristol†

[Received June 10, 1954]

Abstract

It is shown that Hartree's equations for the negative hydrogen ion have several solutions, the usual one of which does not minimize the energy. This non-uniqueness is also shown to exist for a Fermi gas where the usual plane waves of the Sommerfeld model do not even give a stationary value for the energy. The energy of the gas can be lowered, by describing some of the electrons by wave functions that decrease exponentially. The energy is lowered by about 1 ev per electron of this type. If the electron density is sufficiently low (band width $E<0{\cdot}5$ ev) all the electrons can be so trapped and the metal becomes an insulator; this provides an *a priori* reason for Mott's rejection of the Bloch wave functions for nickel oxide. For higher electron densities it is possible to trap a fraction of the electrons, so saving considerable energy; this is compared with Wigner's correlation energy. It is suggested that Friedel, in his explanation of the fine structure of an x-ray absorption edge, has used *several* solutions of Hartree's (or Fock's) equations that correspond to only *one* exact excited wave function, so invalidating his explanation of this effect.

§ 1. Introduction

The variation method, and *ipso facto* Hartree's and Fock's equations, have generally been used without regard to three important points: The variation method selects from a given set of wave functions that one which, on being varied, gives a zero first order variation in the energy; however:

(*a*) The minimum of the energy found need not be the only one. There may be several others.

(*b*) There is no *a priori* reason why the energy should be a minimum (as it must be for a ground state) for any given turning points; this depends on its second derivatives.

(*c*) There is no reason why the lowest energy should be attained at a turning point; it may be on the boundary of the set of wave functions.

These points are probably of no importance for the inner electrons of atoms, but the outer electrons, especially when these are loosely bound,

---

* Communicated by the Author.

† Now at the University of Virginia, Charlottesville, Virginia, U.S.A.

as in negative ions, may very well have several possible wave functions and the usual ones need not necessarily give the lowest energy. These three points are illustrated in the case of a two electron atom in § 2, where we show that for Z near to unity, e.g. for H^-, some or all of these points need attention.

In § 3 we consider the solution of Hartree's equations for the Sommerfeld model of a metal. In this model the electrons are supposed to move in the field of a uniform positive charge of density $|e|/\Omega$. The usual solutions of Hartree's equations for this problem are plane waves, but we shall show that there are other solutions in which electrons are trapped in a bound state, e.g. exponentially decreasing wave function from some centre. The free electrons decrease their density, $\Sigma|\psi|^2$, in the neighbourhood of the trapped electrons, so screening them. In consequence the Hartree field for a trapped electron is an attractive coulomb one, because an electron does not move in its own potential field. This immediately implies that it is possible to write down a solution with any number of electrons trapped self-consistently. That is to say Hartree's equations for this problem have a large number of solutions, all corresponding to the ground state (point (*a*) above). It now becomes essential to examine the energies of these solutions (point (*b*)) and in general the energy as a function of the bound wave functions (point (*c*)). This we do in § 3 taking only 1s states of the form $\exp(-\lambda r)$ for the bound electrons and using the Thomas–Fermi method to give the electron density and sum of the eigenvalues of the free electrons.

We find that, no matter what the electron density is, the energy is always lowered if one electron is trapped. We can now trap an electron at each one of a set of sites in the metal, but we must not put the trapped electrons too close together or they will overlap and the energy will rise. We suggest that this is a perfectly feasible explanation of correlation energy simply in terms of Hartree's equations and we compare it in § 4 with Wigner's (1934) calculation of the correlation energy using much more complicated wave functions. In our opinion the situation is exactly analogous to that considered by Chandrasekhar (1944) with H^-: that whereas it is possible to get a better value of the energy in the variation method by making the wave function much more complicated, as Wigner has done, it may also be possible by quite insignificant complications in the wave function to do just as well. The advantage of the latter process is not merely the mathematical simplicity of handling the problem but the greater physical insight which is possible for a simple wave function as compared with a conplicated one. Mott (1949) has proposed that NiO is an insulator, despite the fact that not all its bands are full or empty. He claims that the Bloch wave functions (plane waves in the Sommerfeld model) are not invariably the correct ones to use, but that in some cases NiO being one, Heitler–London wave functions should be used. We suggest in § 5 as an alternative description leading to the same result, that trapped electrons (corresponding to

Heitler–London wave functions) always exist but that provided the band is sufficiently narrow then all the electrons may be trapped (as was suggested by Wigner as early as 1934 and further amplified in his 1938 paper) so producing an insulator.

Friedel (1952 a) has suggested that the screening of impurities in metals may frequently be accomplished by trapping one or more electrons over the impurity. He has used this (Friedel 1952 a, b) to explain x-ray spectra, the atom of the metal which has lost a K-electron, say, being regarded as an impurity. He furthermore suggests that the wave function for the trapped electron is not uniquely fixed. Thus in lithium an atom minus a K-electron may be screened by a 2s, 2p, 3p . . . electron and each of these excited states have different energies. Friedel suggests that the fine structure near the absorption edge of x-ray spectra is caused by transitions between the ground state and these different excited states. We believe that these excited states are not really different states but are merely different approximations to one excited state (point (*a*)) and so Friedel's explanation of the fine structure breaks down. We discuss this further in § 6.

§ 2. Two Electron Atoms

The simplest possible choice of product wave function for a two electron atom is $\exp(-\lambda r_1)\exp(-\lambda r_2)$. Choosing a value of λ that gives a stationary value for the energy E, we find $E=-(Z-5/16)^2$ and $\lambda=Z-5/16$, in atomic units. We may compare this with the correct value of E by subtracting the energy of the corresponding one electron atom, to give the first ionization potential. Condon and Shortley (1951, p. 346) give a table showing the percentage error of these ionization potentials for $Z=2$, 3, and 4. The errors are 6·4, 2·1 and 1·0% respectively. For $Z=1$, i.e. H^-, the calculated value of the ionization potential is $-0{\cdot}027$ while the observed, or rather accurately calculated value is $+0{\cdot}028$ making an error of 200%. As Chandrasekhar (1944) has pointed out, while helium is a stable closed structure, the negative hydrogen ion is an open structure, which exists principally on account of incomplete screening and polarization. Chandrasekhar has therefore suggested that instead of starting with the above wave function we should try

$$\exp(-\lambda_1 r_1-\lambda_2 r_2)+\exp(-\lambda_1 r_2-\lambda_2 r_1)\,;$$

he then finds that $\lambda_1=1{\cdot}039$ and $\lambda_2=0{\cdot}283$ and that the first ionization potential is $+0{\cdot}013$ so reducing the error for H^- from 200% to 50%. Chandrasekhar's wave function is not of the Hartree product form, but this does suggest that we try for discussion the unsymmetrical wave function $\exp(-\lambda_1 r_1-\lambda_2 r_2)$. In other words we are not going to insist that electrons with the same quantum numbers n, l, and m, but opposite spin, should have the same space-like wave function. The energy of this wave function is easily computed; it is

$$E=\tfrac{1}{2}(\lambda_1^2+\lambda_2^2)-Z(\lambda_1+\lambda_2)+\lambda_1\lambda_2\frac{\lambda_1^2+3\lambda_1\lambda_2+\lambda_2^2}{(\lambda_1+\lambda_2)^3}\,.$$

For the turning points of this function we have the equations $\partial E/\partial\lambda_1=0$ and $\partial E/\partial\lambda_2=0$. We find that $\lambda_1=\lambda_2=Z-5/16$ is always a solution of these equations (for $Z>5/16$), but that for $Z<17/16$ ($=1{\cdot}062$) it is a saddle point and only for $Z>17/16$ is it a minimum (point (*b*) of § 1). Furthermore for $Z<1$ there are no other turning points, the lowest value of the energy being found on the boundary of admissible wave functions (point (*c*)), namely for $(Z, 0)$ or $(0, Z)$, the energy of which is $-Z^2/2$, which is less than $-(Z-5/16)^2$ for Z in the range $(2-\sqrt{2})5/16$ ($<5/16$) to $(2+\sqrt{2})5/16$ ($=1{\cdot}067$). We see that even when the solution $\lambda_1=\lambda_2$ is a minimum it does not necessarily give the lowest energy, namely when $1{\cdot}062<Z<1{\cdot}067$ (actually there is another minimum for these values of Z which is less than $-Z^2/2$). For $1<Z<13/12=1{\cdot}083$ the usual solution $\lambda_1=\lambda_2$ found above is not the only turning point (point (*a*)).

We now give a description of the motion of the turning points about the $\lambda_1\lambda_2$ plane as Z is increased; it will be followed more easily by reference to figs. 1 (*a*), (*b*), and (*c*). For $5/16<Z<1$ there is only one turning point (a saddle point) at the position $\lambda_1=\lambda_2=Z-5/16$. At $Z=1$ (fig. 1 (*a*) two minima appear at (1, 0) and (0, 1) and as Z increases they move in towards the line $\lambda_1=\lambda_2$. At $Z=17/16$ two new saddle points appear at $(17-5)/16$ and as Z increases they move away from the line $\lambda_1=\lambda_2$ leaving behind them a minimum at $\lambda_1=\lambda_2=Z-5/16$, where there was before a saddle point (fig. 1 (*b*)). At $Z=13/12$ the saddle points and minima coalesce leaving only the minimum at $\lambda_1=\lambda_2$ (fig. 1 (*c*)).

This simple example demonstrates very clearly the three points made in the introduction. It is true that we have not solved Hartree's equations exactly since we have limited our one-electron wave functions to the form $\exp(-\lambda r)$; there seems to be no reason however to suppose that the three points would not be confirmed by solving Hartree's equations exactly.

It may be objected that the solutions of Hartree's equations are not unique and do not give the minimum energy in only very narrow ranges of Z, and that no atoms exist with Z in these ranges (except for H^-), but that does not rob our results of physical significance. On the contrary we should say that when two or more electrons are very loosely bound, or as Chandrasekhar puts it: when incomplete screening and polarization are important effects, then their wave functions are not given uniquely by Hartree's equations. The same situation is probably implied when it is found difficult to obtain self-consistent solutions of Hartree's equations due to what Hartree would call 'over-stability' (Hartree 1933) a quite common occurrence for the outer electrons of atoms.

What we suggest in these cases is that the one-electron wave functions should not be assumed to be of the form (Hartree 1946)

$$\psi_i(\mathbf{r})=R(n_i\,l_i\,r)P_{l_i}^{|m_i|}(\cos\theta)\exp(im_i\phi)\,\chi_i(s)$$

but rather of the form

$$\psi_i(\mathbf{r})=R(n_i\,l_i\,m_i\,\sigma_i\,r)P_{l_i}^{|m}(\cos\theta)\exp(im_i\phi)\chi_i(s).$$

Fig. 1

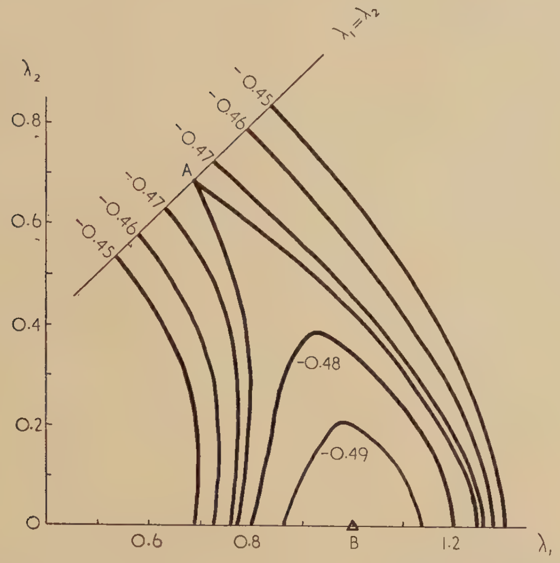

(*a*) $Z=1$. Energy at A is $-0{\cdot}4727$ and at B $-0{\cdot}5000$.

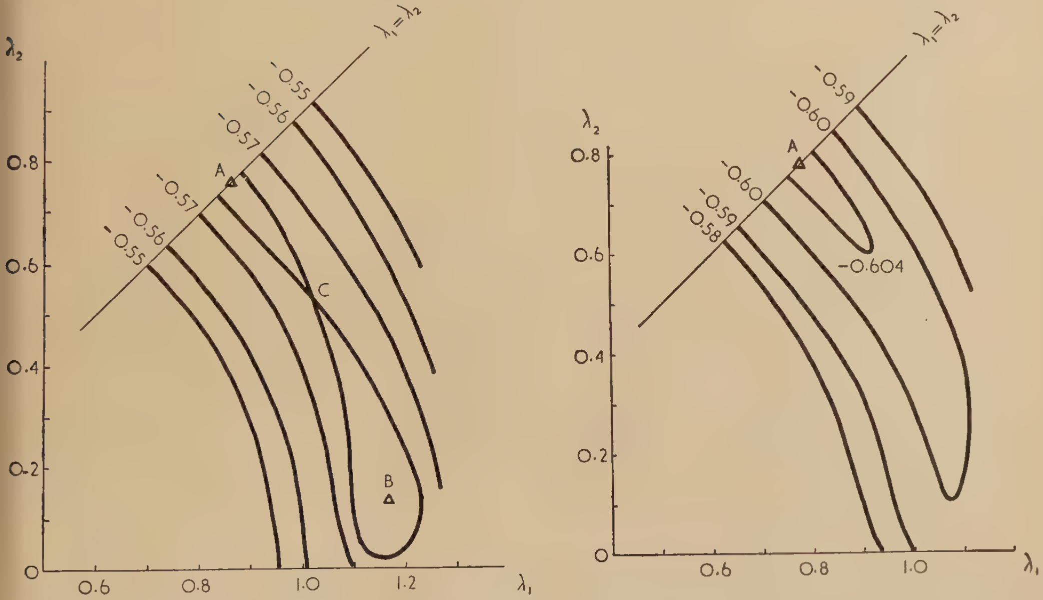

(*b*) $Z=1{\cdot}07$. Energy at A is $-0{\cdot}5738$, at B $-0{\cdot}5759$ and at C $-0{\cdot}5735$.

(*c*) $Z=1{\cdot}09$. Energy at A is $-0{\cdot}6045$.

Energy contours for a two-electron atom. Energies and λ's in atomic units. Minima are shown by Δ's and saddle points always have a contour crossing over at them. The contours are symmetrical about $\lambda_1=\lambda$

Condon and Shortley (1951) go some way towards this in working out Hartree's equations (eqn. $8^{14}4$) for the case where the radial function is assumed to depend on n_i, l_i, and m_i (cf. eqn. $8^{14}3$ where m_i has been mistakenly omitted).

All our remarks apply with equal force to Fock's equations, because Fock's and Hartree's equations are the same for a two-electron system when the electrons have opposite spin, and it is on such a system that we base our remarks. (The reason for this equivalence is that the exchange operator only operates on electrons of parallel spin.)

There does not seem to be nearly as much opportunity for this non-uniqueness in the case of Hartree's symmetrized equations (in which an electron moves in its own field): since with these equations the one-electron wave functions must be independent of the spin, and if there is spherical symmetry the radial parts of the wave functions can only depend on the quantum numbers n and l, not on m or σ.

§ 3. SELF-TRAPPED ELECTRONS IN A METAL

In § 2 we came to the conclusion that incomplete screening and polarization, if present in too great quantities, were liable to make the solutions of Hartree's or Fock's equations non-unique, and, of course, the usual wave function, which is always the simplest, would very likely not be the best to take account of these effects. Polarization must be very large in a solid, for in this case the electrons must be able to be found with equal probability throughout the solid, but at the same time they must avoid each other as well as possible. The usual wave functions for a metal are Bloch's, in which the electrons cannot avoid one another at all. This then is an ideal example to test whether Hartree's equations have a unique solution. (We have not examined Fock's equations.)

To simplify matters we consider the Sommerfeld model of a metal in which the metal ions are replaced by a smoothed out positive charge of density $|e|/\Omega$. The usual one-electron wave functions are just the Bloch waves $\exp(i\mathbf{k}\,.\,\mathbf{r})$. We have now to decide in what way to generalize these wave functions. We shall suppose that only one or two electrons cannot travel through the length of the metal and we shall take the wave function of these electrons to be of the form $\exp(-\lambda r)$. That is to say we take

$$\exp(-\lambda_1 r_1)\exp(-\lambda_2 r_2)\prod_i \psi_i(\mathbf{r}_i)$$

for our complete wave functions, where $\psi_i(\mathbf{r})$ extends throughout the metal. Using the variation method we find that the ψ_i must satisfy the Hartree equations

$$-\frac{\hbar^2}{2m}\nabla^2\psi_i+\left[-\frac{e^2}{\Omega}\int\frac{d\mathbf{r}'}{|\mathbf{r}-\mathbf{r}'|}+e^2\int\frac{\sum_{3\ldots}|\psi_j|^2+\psi_1{}^2+\psi_2{}^2}{|\mathbf{r}-\mathbf{r}'|}\,d\mathbf{r}'\right]\psi_i$$

$$=\epsilon_i\psi_i \qquad (i=34\ldots), \quad . \quad . \quad (1)$$

where $\psi_i=(\lambda_i^3/\pi)^{1/2}\exp(-\lambda_i r)$ ($i=1$ and 2). The energy is then given by

$$E(\lambda_1,\lambda_2)=-\frac{\hbar^2}{2m}\sum_{1\ldots}\int\psi_i^*\nabla^2\psi_i\,d\mathbf{r}-\sum_{1\ldots}\iint|\psi_i|^2\frac{1}{\Omega}\frac{e^2}{r_{12}}\,d\mathbf{r}_1\,d\mathbf{r}_2$$
$$+\frac{1}{2}\sum_{1\ldots}{}'\iint|\psi_i|^2|\psi_j|^2\frac{e^2}{r_{12}}\,d\mathbf{r}_1\,d\mathbf{r}_2,$$

where the $\psi_3\psi_4\ldots$ have been chosen to satisfy the eqn. (1). We have then to choose λ_1 and λ_2 so as to minimize $E(\lambda_1,\lambda_2)$; it may, of course, turn out that λ_1, and λ_2 are both zero; this would mean that our suggested wave function is worse than the plane waves. If we write $\sum_{3\ldots}|\psi_i|^2=\rho$ and call the potential for the free electrons occurring in (1) U, the energy is (using eqn. (1))

$$E(\lambda_1,\lambda_2)=-\frac{\hbar^2}{2m}\sum_{12}\int\psi_i\nabla^2\psi_i\,d\mathbf{r}+\sum_{3\ldots}\epsilon_i-\int\rho U\,d\mathbf{r}-\iint(\psi_1{}^2+\psi^2{}_2+\rho)$$
$$\times\frac{1}{\Omega}\frac{e^2}{r_{12}}\,d\mathbf{r}_1\,d\mathbf{r}_2+\frac{1}{2}\iint[2\psi_1{}^2\psi_2{}^2+2(\psi_1{}^2+\psi_2{}^2)\rho+\rho\rho]\frac{e^2}{r_{12}}\,d\mathbf{r}_1\,d\mathbf{r}_2. \qquad (2)$$

In other words we do not need to know the $\psi_i(i=34\ldots)$, but only $\sum_{3\ldots}\epsilon_i$, ρ, and U. All these can be obtained approximately by the Thomas–Fermi method

$$\rho=\frac{8\pi}{3h^3}[2m(E-U)]^{3/2},$$

and

$$\sum_{3\ldots}\epsilon_i=\int[\tfrac{3}{5}(E-U)\rho+U\rho]\,d\mathbf{r}+E(2,1,0), \qquad (3)$$

where E is chosen so that

$$\int\rho\,d\mathbf{r}=\int\frac{1}{\Omega}\,d\mathbf{r}-(2,1,0).$$

The expression (2, 1, 0) means either 2, 1, or 0, depending on whether there are 2, 1, or 0, bound states, i.e. λ_1 and $\lambda_2\neq0$, λ_1 or $\lambda_2=0$, or λ_1 and $\lambda_2=0$. The reason for adding the term $E(2,1,0)$ to the sum of the eigenvalues is that the Thomas–Fermi method sums over all the eigenvalues in the potential U including the 1s. (We are supposing that boundary conditions are applied on the surface of a sphere centred on the trapped electron, so that the quantum numbers of all the electrons bound or free are the usual n, l, and m.) However, if there are two bound 1s electrons, we must not fill the 1s free state with electrons in order to satisfy the Pauli principle. We must therefore add to the Thomas–Fermi expression for the sum of the eigenvalues the energy necessary to raise 2, 1, or 0, electrons to the top of the band. The corresponding change in ρ is, of course, insignificant. It turns out that E, the energy of the top of the band before the 1s electrons are put up there, is independent of the number of bound electrons, so this possible variation does not occur in the equations for ρ and $\Sigma\epsilon_i$.

In the usual way we take $U=\zeta/r$ (definition of ζ) as the dependent variable in the Thomas–Fermi equation for ρ and use the fact that

$$\nabla^2 U=\zeta''/r=-4\pi e^2\left[-\frac{1}{\Omega}+\rho+\psi_1{}^2+\psi_2{}^2\right]. \quad . \quad . \quad . \quad (4)$$

We then obtain the following differential equation for ζ

$$\frac{1}{4\pi e^2}\frac{\zeta''}{r}+A_1\exp(-2\lambda_1 r)+A_2\exp(-2\lambda_2 r)=-\frac{8\pi}{3h^3}(2m)^{3/2}[E-\zeta/r]^{3/2}+\frac{1}{\Omega} \quad . \quad . \quad . \quad (5)$$

where $A_i=\lambda_i{}^3/\pi$ is the normalization factor. One boundary condition is that $\zeta\rightarrow 0$ as $r\rightarrow\infty$, this is only possible if E is given by

$$\frac{8\pi}{3h^3}(2mE)^{3/2}=\frac{1}{\Omega} \quad . \quad . \quad . \quad . \quad . \quad . \quad . \quad . \quad (6)$$

irrespectively of whether λ_1 and λ_2 are zero or not, as we stated above.

If we did not have to take (2, 1, 0) electrons from the bottom of the band and put them at the top we could state the conclusion that the top of the band is unaltered by self-trapping, in agreement with Friedel's (1952 a) more general conclusion. When, however, we do have to raise electrons to the top of the band, it is clear that the whole band will be shifted upwards and narrowed. We consider this effect in greater detail in § 4.

The Thomas–Fermi eqn. (5) that we have obtained would have to be solved numerically; to avoid this we use the usual approximation (Mott 1936) of linearizing, that is to say we assume $\zeta/r\ll E$. This will be true, as we shall show, for λ_1 and λ_2 sufficiently small. Equation (5) now becomes

$$\zeta''-\kappa^2\zeta=-4\pi e^2[A_1\exp(-2\lambda_1 r)+A_2\exp(-2\lambda_2 r)], \quad . \quad . \quad (7)$$

where

$$\kappa^2=\frac{32\pi^2 e^2}{3h^3}(2m)^{3/2}\frac{3}{2}E^{1/2}. \quad . \quad . \quad . \quad . \quad . \quad . \quad . \quad (8)$$

Using the boundary conditions that $\zeta\rightarrow 0$ as $r\rightarrow 0$ and $r\rightarrow\infty$ we find the solution

$$\frac{1}{4\pi e^2}\zeta=\sum_{i=12}\left\{[\exp(-\kappa r)-\exp(-2\lambda_i r)]\frac{4\lambda_i A_i}{(\kappa^2-4\lambda_i{}^2)^2}+r\exp(-2\lambda_i r)\frac{A_i}{\kappa^2-4\lambda_i{}^2}\right\}. \quad . \quad . \quad . \quad . \quad . \quad (9)$$

If $2\lambda_i<\kappa$, which is always the case in our problem, ζ/r is a decreasing function of r with a maximum at the origin, where

$$\lim_{r\rightarrow 0}\frac{\zeta}{r}=\frac{4e^2\lambda_1{}^3}{(\kappa+2\lambda_1)^2}+\frac{4e^2\lambda_2{}^3}{(\kappa+2\lambda_2)^2} \quad . \quad . \quad . \quad . \quad . \quad (10)$$

so that for λ_i small enough this can be made as small as we like compared with E.

Now using the known relation between ρ and ζ'' (eqn. (4)), but not using the approximate eqn. (7) for ζ we find that eqn. (2) can be written

$$E(\lambda_1,\lambda_2)-E(0,0)=-\frac{\hbar^2}{2m}\sum_{12}\int\psi_i\nabla^2\psi_i\,d\mathbf{r}+\frac{2E}{5}(2,1,0)-\frac{1}{2}\int\int(\psi_1{}^2\psi_1{}^2+\psi_2{}^2\psi^2{}_2)$$
$$\times\frac{e^2}{r_{12}}d\mathbf{r}_1\,d\mathbf{r}_2+\frac{1}{10e^2}\int\zeta\zeta''\,dr+\frac{12\pi}{5}\int r\zeta\left(\psi_1{}^2+\psi_2{}^2-\frac{1}{\Omega}\right)dr. \quad . \quad (11)$$

The straightforward procedure would be to calculate the integrals involving ζ from the approximate ζ (eqn. (9)). This gives

$$E(\lambda_1,\lambda_2)-E(0,0)=\frac{\hbar^2}{2m}(\lambda_1{}^2+\lambda_2{}^2)-\frac{5e^2}{16}(\lambda_1+\lambda_2)+\frac{12e^2}{5}R(\lambda_1,\lambda_2)$$
$$-\frac{8e^2}{5}S(\lambda_1,\lambda_2), \quad . \quad . \quad . \quad . \quad . \quad . \quad . \quad . \quad (12)$$

where

$$R(\lambda_1,\lambda_2)=\sum_{ij}\lambda_i{}^3\lambda_j{}^3\frac{\kappa^2+4\kappa(\lambda_i+\lambda_j)+4\lambda_i{}^2+12\lambda_i\lambda_j+4\lambda_j{}^2}{(\kappa+2\lambda_i)^2(\kappa+2\lambda_j)^2(\lambda_i+\lambda_j)^3},$$

and

$$S(\lambda_1,\lambda_2)=\sum_{ij}\lambda_i{}^4\lambda_j{}^4\frac{\kappa^2+6\kappa(\lambda_i+\lambda_j)+4\lambda_i{}^2+12\lambda_i\lambda_j+4\lambda_j{}^2}{(\kappa+2\lambda_i)^3(\kappa+2\lambda_j)^3(\lambda_i+\lambda_j)^3}.$$

Another possible procedure would be to say that the second derivative of an approximately known function ζ is likely to be very poor, and that therefore we should get rid of the ζ'' in (11) by using the exact differential eqn. (5). In fact, one can show by using an extension of Milne's (1927) integrations by parts and eqn. (5) that

$$\frac{1}{4\pi e^2}\frac{7}{5}\int\zeta\zeta''\,dr=\frac{12E}{5}\int r^2(\psi_1{}^2+\psi_2{}^2)\,dr-\frac{2}{5}\int r\zeta\left(\psi_1{}^2+\psi_2{}^2-\frac{1}{\Omega}\right)dr$$
$$+2\int\zeta\frac{d}{dr}\left[r^2\left(\psi_1{}^2+\psi_2{}^2-\frac{1}{\Omega}\right)\right]dr,$$

using this in (11) we obtain from the approximate ζ (9)

$$E(\lambda_1,\lambda_2)-E(0,0)=\frac{\hbar^2}{2m}(\lambda_1{}^2+\lambda_2{}^2)-\frac{5e^2}{16}(\lambda_1+\lambda_2)$$
$$+\frac{24e^2}{7}R(\lambda_1,\lambda_2)-\frac{4e^2}{7}T(\lambda_1,\lambda_2),. \quad . \quad (13)$$

where $R(\lambda_1, \lambda_2)$ is the same as in eqn. (12) and $T(\lambda_1, \lambda_2)$ is

$$\sum_{ij}\lambda_i{}^3\lambda_j{}^4$$
$$\frac{3\kappa^3+6\kappa^2(2\lambda_i+3\lambda_j)+4\kappa(4\lambda_i{}^2+16\lambda_i\lambda_j+9\lambda_j{}^2)+8(2\lambda_i{}^3+8\lambda_i{}^2\lambda_j+12\lambda_i\lambda_j{}^2+3\lambda_j{}^3)}{(\kappa+2\lambda_i)^2(\kappa+2\lambda_j)^3(\lambda_i+\lambda_j)^4}.$$

The most striking conclusion that can be immediately drawn from eqn. (12) or (13) is that the energy, $E(\lambda_1, \lambda_2)-E(0, 0)$ is not stationary at $\lambda_1=\lambda_2=0$ due to the term $-5e^2(\lambda_1+\lambda_2)/16$, which is half the self-energy of the two bound electrons. That is to say the plane wave solution of Hartree's equations does not give even a stationary—let alone a minimum—value for the energy with respect to variations in the one-electron wave functions. At first sight this is very unexpected since Hartree's equations are deduced on the basis that variations in the wave functions produce no first order energy change. The explanation is that we have varied the plane waves by more than the first order in going from exp $(i\mathbf{k}\,.\,\mathbf{r})$ (or at least the corresponding 1s wave function containing the Bessel function $J_{1/2}$) to exp $(-\lambda r)$ no matter how small λ is. This shows that great caution must be exercized in using the variation principle when the wave functions have almost constant density over the whole system, cf. Coulson and Fischer's (1949) remarks on the molecular orbital method.

Fig. 2

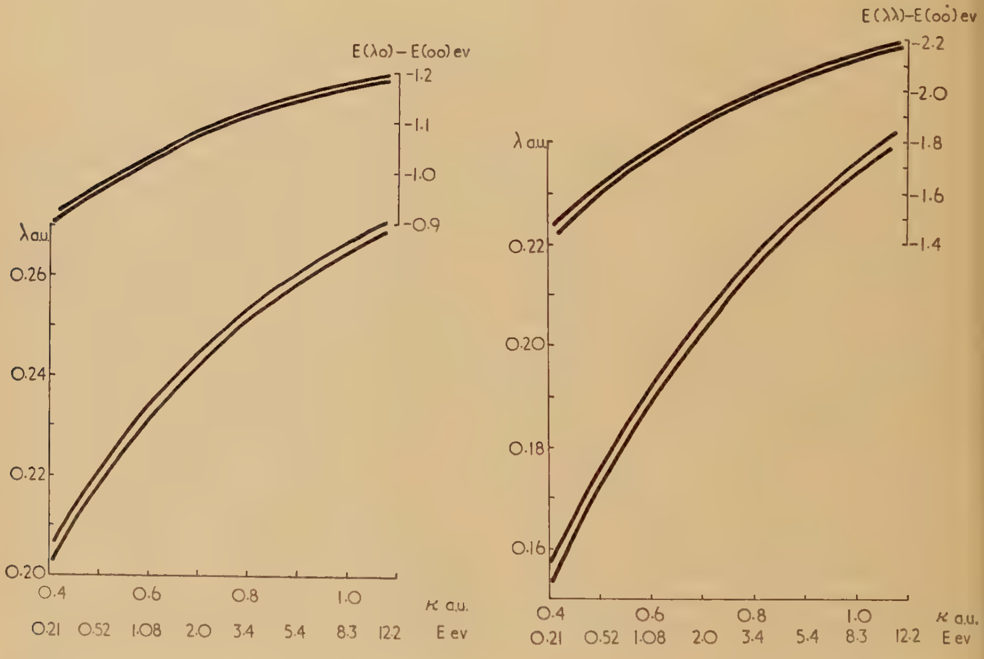

(*a*) (*b*)

The reciprocal of the radius of the orbit λ, and the energy saved (ev) when one (fig. 2 (*a*)) or two (fig. 2 (*b*)) electrons are trapped at a definite site. These are plotted as functions of the band width E (ev). The upper of each pair of curves corresponds to eqn. (12) and the lower to eqn. (13).

Consider now the variation of $E(\lambda_1, \lambda_2)-E(0, 0)$ along the lines $\lambda_2=0$, i.e. only one electron trapped, and $\lambda_1=\lambda_2$, i.e. two electrons of opposite spin trapped in the same wave function. In either case the energy has a minimum (notice that the discontinuities of the form (2, 1, 0) have dropped out of the expressions (12) and (13) for the energy), which is most easily found numerically by regarding κ/λ as the independent variable, when

$\partial E/\partial\lambda=0$ becomes a simple equation for λ as a function of κ/λ. The minimum is shown as a function of κ, and E the band width (eqn. (8)), in figs. 2 (*a*) and 2 (*b*) for $\lambda_2=0$ and $\lambda_1=\lambda_2$ respectively. The pair of curves in each case refer to the alternate formulae (12) and (13); it is seen that which formula is used makes little difference and this leads us to believe that our linearization eqn. (7) of the Thomas–Fermi eqn. (5) is quite accurate despite the fact that for band widths less than about 0·7 ev ζ/r at $r=0$ as given by eqn. (10) is bigger than E. In the same figures we show the energy saved, nearly 1 ev per electron trapped.

Now it may be asked: is the minimum along the line $\lambda_1=\lambda_2$ a minimum for variations off this line (cf. § 2)? The answer is easily seen to be yes, for the right-hand side of

$$\left[\frac{\partial^2E(\lambda_1,\lambda_2)}{\partial\lambda_1\partial\lambda_2}\right]^2 \gtrless \frac{\partial^2E}{\partial\lambda_1{}^2}\frac{\partial^2E}{\partial\lambda_2{}^2}$$

contains the dominant term $(\hbar^2/m)^2$. We can therefore say that if we are only interested in trapping electrons at one site we save most energy by trapping two in the wave function $\exp[-\lambda(r_1+r_2)]$, when only wave functions of the form $\exp(-\lambda_1r_1)\exp(-\lambda_2r_2)$ are allowed.

§ 4. CORRELATION ENERGY

So far we have only considered trapping one or two electrons at a definite position in the metal. In order to obtain an appreciable save of energy compared with the Fermi energy for plane waves we must trap a non-zero fraction of the electrons at different positions; for example, we might trap one electron on each lattice point of a body-centred lattice. It should be remembered that we are only considering a Sommerfeld model so this lattice has nothing to do with the position of the ions. For the relations between these lattices see § 5. However, if the trapped electrons are too close together compared with $1/\lambda$ we will loose energy due to the overlap. Let us put a Wigner–Seitz sphere around each lattice point, of which the radius is say, a/λ. Then the amplitude of the wave function of a trapped electron on the surface of the sphere is $\exp(-a)$ and with a equal to 2 or 3 this is 0·14 or 0·05; we may hope small enough. The corresponding fraction of electrons trapped is $f_1=\Omega 3\lambda^3/4\pi a^3$ (if we trap one per site) since Ω is the valume occupied by a charge e. So we have the following contribution to the energy saved $[E(\lambda, 0)-E(0, 0)]f_1N$, where N is the total number of electrons, but this is not the only term. It will be remembered from § 3 that for every electron we trapped we had to raise an electron from the bottom of the band and put it at the top because of the Pauli principle. The Pauli principle was there used in the simple form that there must not be two electrons with the same set of four quantum numbers. This is no longer of any use to us bcause the quantum numbers of the trapped electrons are n, l, m, and σ, while the quantum numbers of the free electrons, which are now Bloch waves, are k_x, k_y, k_z, and σ. We shall therefore suppose that f_1N electrons—the number that are trapped—have to be removed from wave functions at the bottom of the band and placed in wave functions at the top, remembering that as this is done the energies of the top and bottom of the band are shifting. We shall suppose that the energy of a wave function with quantum numbers $\mathbf{k}$ is $\hbar^2k^2/2m$. The original band width is E and so this transfer of electrons requires an energy

$$\frac{3}{5}\frac{\hbar^2}{2m}\left(\frac{3\pi^2}{\Omega}\right)^{2/3}N\left[(1+f_1)^{5/3}-f_1^{5/3}2^{2/3}-1\right],$$

where we have supposed that all the trapped electrons have the same spin, so that the f_1N electrons of lowest energy have the opposite spin. We must subtract from this

$$f_1NE=\frac{\hbar^2}{2m}f_1N\left(\frac{3\pi^2}{\Omega}\right)^{2/3}$$

(from eqn. (6)) the energy required to raise f_1N electrons to the top of a band that stays the same width E; this term has already been added in § 3, it was, in fact, the $(2E, E, 0)$ of eqn. (3).

If, on the other hand, we trap two electrons at each lattice site so that the fraction of electrons trapped is $f_2=2\Omega 3\lambda^3/4\pi a^3$ then we find for the total energy saved

$$\mathscr{E}_2=\frac{3}{5}\frac{\hbar^2}{2m}N\left(\frac{3\pi^2}{\Omega}\right)^{2/3}\left[(1+f_2)^{5/3}-f_2^{5/3}-1-\frac{5}{3}f_2\right]+\left[E(\lambda, \lambda)-E(0, 0)\right]f_2N. \quad . \quad . \quad . \quad . \quad (14)$$

This formula is not quite correct because the λ has been worked out for a certain band width E, whereas, in fact, the band width is less; in addition the free electrons that are doing the screening have a longer average wave length and this will also effect λ. We suppose these effects small as they certainly will be for big E, and plot the expression (14) divided by N in fig. 3, which therefore represents approximately the energy saved per electron when a certain fraction of electrons is trapped (it has been plotted for $a=2$, and 3). The corresponding energy saved, $\mathscr{E}_1$, when only one electron is trapped at each lattice site is also shown in fig. 3.

In the same figure the usual expression for this saving of energy on the Fermi energy is shown; it consists of the exchange energy—obtained by keeping electrons of parallel spin apart—and Wigner's expression for the 'correlation energy'—due to keeping apart electrons of opposite spin—that is to say

$$\mathscr{E}'=\frac{0{\cdot}46e^2}{r_s}+\frac{0{\cdot}29e^2}{r_s+5{\cdot}1a_H} \quad . \quad . \quad . \quad . \quad . \quad . \quad . \quad (15)$$

where $\Omega=4\pi r_s^3/3$ and $a_H=\hbar^2/me^2$. Our saving of energy is considerably less than this though it is comparable with Wigner's correlation term, presumably our expression could be increased considerably by introducing exchange.

Note that our curves in fig. 3 stop for sufficiently narrow band widths ; at these points all the electrons have become trapped (f_1 or $f_2=1$) and the Sommerfeld model (i.e. uniform positive charge) of a metal becomes insulating in this approximation. This situation has been envisaged by Wigner (1938) who calls such a system an ‘ inverted alkali metal ’ because “the positive charges are uniformly distributed while the negative electrons are localized because of their repulsive action”. Wigner has worked out the energy of such a set of localized electrons. He assumes that any given electron moves in the field (Wigner 1938, eqn. 10)

$$-3e^2/2r_s+r^2e^2/2r_s^3. \qquad \ldots\ldots\ldots \quad (16)$$

Fig. 3

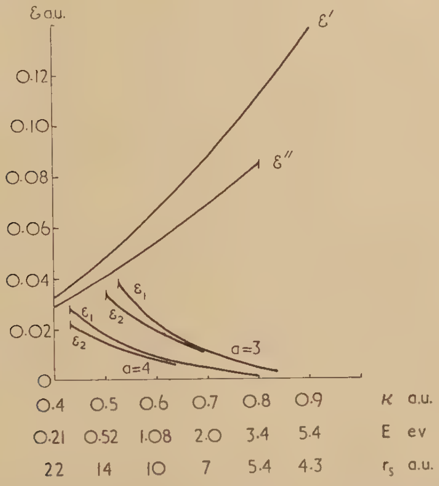

Energy saved in atomic units when a fraction of the electrons are trapped on a lattice, labelled $\mathscr{E}_1$ or $\mathscr{E}_2$ depending on whether one or two electrons are trapped per lattice site. $a=3$ and $a=4$ show how much overlap has been allowed between trapped electrons. $\mathscr{E}'$ is the ordinary exchange and Wigner correlation terms added together (eqn. (15)), $\mathscr{E}''$ is the energy saved by localizing all the electrons (eqn. (17)).

For $r\leqslant r_s$ this is the field due to a uniform positive charge distribution occupying the volume $4\pi/3r_s^3$; for $r\geqslant r_s$ the potential should be $-e^2/r$, but since the wave function is very nearly zero for these r's Wigner uses the potential (16) for all r. The wave function for a trapped electron is $\psi_i \propto \exp(-\alpha r^2/2)$ where $\alpha=r_s^{-3/2}a_H^{-1/2}$ and $a_H=\hbar^2/me^2$, and the eigenvalue of this wave function is (Wigner 1938, eqn. 11)

$$\epsilon_i=-3e^2/2r_s+3e^2a_H^{1/2}/2r_s^{3/2}.$$

The total energy of this system of electrons is

$$\mathscr{E}_{\text{ins}}=\sum_i \epsilon_i-\frac{1}{2}\sum_{ij}{}' \iint \psi_i^2\psi_j^2 \frac{e^2}{r_{12}}\,d\mathbf{r}_1\,d\mathbf{r}_2$$

whereas the energy of the free electron gas is

$$\mathscr{E}_{\rm con}=\Sigma\frac{\hbar^2}{2m}k^2-\frac{1}{2}\iint\frac{1}{\Omega^2}\frac{e^2}{r_{12}}\,d\mathbf{r}_1\,d\mathbf{r}_2.$$

Subtracting these to give the saving of energy when all the electrons are trapped we find

$$\mathscr{E}''=\mathscr{E}_{\rm ins}-\mathscr{E}_{\rm con}\doteqdot N\left[-\frac{3e^2}{2r_s}+\frac{3}{2}\frac{e^2a_H{}^{1/2}}{r_s{}^{3/2}}-\frac{\hbar^2}{2m}\frac{2\cdot21}{r_s{}^2}+\frac{3e^2}{5r_s}\right]. \qquad (17)$$

Wigner (1938) takes into account the exchange energy of the free electrons, namely $-0\cdot42e^2/r_s$. We must not do this since we wish to compare this calculation with our previous one in which only a fraction, f_1, of the electrons are localized and where we used Hartree's equations, not Fock's.

The saving of energy $\mathscr{E}_{\rm ins}-\mathscr{E}_{\rm con}$ given by eqn. (17) is plotted in fig. 3 (we have not made similar calculations for the case of two electrons trapped at each lattice site) as a function of the band width E for values of r_s greater than $6a_H$; Wigner does not believe the approximation is good below this. Note that the wave function has the value

$$\exp\left[-\sqrt{(r_s/4a_H)}\right],$$

on the Wigner–Seitz sphere, which is $0\cdot29$ for $r_s=6a_H$. This is bigger than our 0·14 or 0·05, but Wigner's wave function varies like $\exp(-r^2)$ whereas ours varies only like $\exp(-r)$.

Incidentally, the numerical comparison that Wigner makes between the correlation energy as obtained in his earlier paper (1934) (our eqn. (15)) and in the later paper (1938) (our eqn. (17)) where it is assumed that the electrons form a lattice appears to be wrong. He gives for the correlation energy using a lattice (footnote 25) $0\cdot15/r_s$ and $0\cdot21/r_s$ Rydbergs for $r_s=6$ and 8 atomic units, whereas it should be $0\cdot03/r_s$ and $0\cdot10/r_s$. This considerably reduces the agreement with the 1934 paper, which gives for the same values of r_s, $0\cdot32/r_s$ and $0\cdot36/r_s$.

§ 5. NICKEL OXIDE

We have seen in § 4 that if the electron density is below some critical value—corresponding to r_s between 6 and 15 atomic units—the Sommerfeld model gives an insulator. Before this result can be applied to any interesting case, say nickel oxide, we must, however, introduce the effect of the periodic potential. It should already be clear that our results in § 4 for the Sommerfeld model are not very reliable because of the *ad hoc* method we used to introduce the Pauli principle. Now that we introduce a periodic potential we cannot expect to get good quantitative results but only an idea of what a crystal lattice may do to self-trapped electrons.

The Hartree equations for the valence electrons in a periodic potential $V(\mathbf{r})$ are

$$-\frac{\hbar^2}{2m}\nabla^2\psi_i+\left[V(\mathbf{r})+e^2\int\frac{\Sigma'\,|\psi_j|^2}{|\mathbf{r}-\mathbf{r}'|}\,d\mathbf{r}'\right]\psi_i=\epsilon_i\psi_i. \quad . \quad . \quad (18)$$

A possible solution of these equations is Bloch's in which $|\psi_j|^2$ is periodic and so the total potential for the ith electron is periodic. Let us imagine, however, that a solution exists in which two wave functions ψ_1 and ψ_2, say, are localized, then the total potential is no longer periodic. However, we may write the potential in the form

$$\left(V(\mathbf{r})+\frac{e^2}{\Omega}\int\frac{d\mathbf{r}'}{|\mathbf{r}-\mathbf{r}'|}\right)+e^2\int\frac{\Sigma'|\psi_j|^2-1/\Omega}{|\mathbf{r}-\mathbf{r}'|}d\mathbf{r}',$$

the first part of which is periodic and gives a certain band structure—nearly the same as that obtained in a self-consistent Bloch solution of eqn. (18)—and the second term is (we hope) a slowly varying perturbation. We now use the Wannier–Slater approximation (Slater 1949) in which the eigenvalues of our problem are given by the eigenvalues of the equation

$$\left[E(\mathbf{p})+e^2\int\frac{\Sigma'|\psi_j|^2-1/\Omega}{|\mathbf{r}-\mathbf{r}'|}d\mathbf{r}'\right]\phi_i=\epsilon_i\phi_i,$$

where $E(\mathbf{p})$ is the energy of a wave function in the periodic lattice with momentum $\mathbf{p}=\hbar\mathbf{k}$ and $\mathbf{p}$ is replaced by the operator $-i\hbar\nabla$. We shall furthermore assume that the potential due to $\Sigma'|\psi_j|^2$ is about the same as that produced by $\Sigma'|\phi_j|^2$. If now we suppose that the energy of a Bloch wave in our crystal is simply $\hbar^2k^2/2m^*=p^2/2m^*=-\hbar^2\nabla^2/2m^*$ we have exactly reproduced eqn. (1) with m^* for m. In other words, all our graphs, and in particular figs. 3 (*a*) and 3 (*b*), remain the same and only the units of energy and distance are changed. Our new 'atomic unit' of length is $\hbar^2/m^*e^2=m/m^*$ times the usual unit ($0{\cdot}5\times10^{-8}$ cm) and our new 'atomic unit' of energy is $m^*e^4/\hbar^2=m^*/m$ times the usual unit (27 ev).

If in NiO we say that $r_s=2{\cdot}5\hbar^2/me^2$ (this is on the assumption that we need only trap two electrons per nickel atom) then we have to make $m^*>6m$ in order to have an insulator. Notice the peculiar result of the Wannier–Slater approximation: the trapped electrons have no preference in where they are localized; over the nickel ion, the oxygen ion, or in between, all are equally good in this approximation. In actual fact there will be definite preferred positions for the trapped electrons, and it seems likely that this will immobilize them.

A similar problem is the variation of the activation energy of semi-conductors with impurity concentration, which suggests that when the impurities are closer together than 100×10^{-8} cm they give a conduction band (see Mott 1951). If we replace the perfect crystal by a uniform dielectric, constant $K=13$ for silicon, then our previous results apply to the remaining 'crystal of impurities'. Wherever there is an e^2 in our previous expressions we must now put e^2/K and this makes our system insulating for r_s greater than some multiple of $\hbar^2K/m^*e^2=Km/m^*$ $0{\cdot}5\times10^{-8}$ cm, i.e. $r_s>39$ or $97m/m^*10^{-8}$ cm for the usual choices of multiple; 6 and 15. This would be in quite good agreement with experiment if m^* were equal to m, but for such an extended crystal the band width is bound to be very small so making m^*/m very big. We must agree then with Castillan and Seitz (1951) and Mott (1951) that this explanation, as it stands, is not adequate. Of course, if m^* is really about the size of m then, accepting this fact, there is no difficulty in the interaction of impurities up to 10^{-6} cm apart, but we have merely transferred the difficulty to understanding the low effective mass.

§ 6. FRIEDEL'S THEORY OF X-RAY SPECTRA

When an x-ray photon is absorbed by a metal an electron is knocked out of a low lying level in one of the atoms into a state of one of the conduction bands. The usual theory of the fine structure on the high frequency side of the edge is that it is due to the variation of the density of states in the bands and the variation of the transition probability. Friedel (1952 a) has pointed out, however, that when an electron is excited it leaves behind a positive ion that must be screened. For example, in lithium absorption Friedel suggests that the screening is due to a bound 2s electron. In addition, he supposes that it is possible to screen by a 2p, 3p, . . . bound state. Each one of these screenings gives a different absorption edge, and Friedel's explanation of the fine structure is that each edge produces a peak in the absorption. In a later paper (Friedel 1952 b) he goes further and supposes that the two possible spins of the bound electron, say, the 2s, will give two edges.

From our examples of the non-uniqueness of Hartree's equations, and especially from § 3 we believe that many, if not all of Friedel's solutions of Hartree's equations (or Fock's) in which he traps either a 2s, or 2p, or . . . electron, are merely different approximations to one exact excited state, just as our solutions of Hartree's equations in which we have all plane waves or one or two trapped 1s electrons are approximations to an exact ground state. We believe this will be the case if wave functions with all quantum numbers n, l, m, and σ, are occupied up to some energy E, the top of the band (except, of course, for the electron that has been excited). This may not be possible ; for example, if we bind a 2p electron there may be no 2s wave function in the band to fill ; in this event we clearly have a new excited state different from the one in which the 2s wave function is occupied. In other words, we say that approximate many electron wave functions are the same or different according as they have the same configuration or not.

When we screen the positive ion by a 2p bound electron and the 2s free wave functions exist, we may still produce a new state—different from the one in which we have a 2s bound electron—by merely removing one of the 2s free electrons and putting it at the top of the band. However, this does not resuscitate Friedel's theory because the new state has an energy greater than that expected by an amount equal to the band width.

Furthermore, if the system with a 2p bound electron really approximates to a different excited state then it must have been reached by a two (or more) electron transition, because we have had to remove one (or two) electrons from the 2s wave function in addition to the K electron. We are not convinced by Friedel's (1952 b) calculations of the high probability of such multiple electron transitions. True the transition probability may be high if the wave functions are taken to be plane waves, but it seems likely that if correlation is taken into account so that the electrons avoid each other, the probability might be much reduced.

ACKNOWLEDGMENTS

This paper has been inspired by discussions over the past three years at the H. H. Wills Physical Laboratory and, in particular, by Professor N. F. Mott and Dr. J. Friedel. During this time I have received both a grant and a senior award from the Department of Scientific and Industrial Research.

REFERENCES

CASTELLAN, G. W., and SEITZ, F., 1951, *Semi-Conducting Materials* (London : Butterworths), p. 8.
CHANDRASEKHAR, S., 1944, *Astrophys. J.*, **100,** 176.
CONDON, E. U., and SHORTLEY, G. H., 1951, *The Theory of Atomic Spectra* (Cambridge : University Press).
COULSON, C. A., and FISCHER, I., 1949, *Phil. Mag.*, **40,** 386.
FRIEDEL, J., 1952 a, *Phil. Mag.*, **43,** 153 ; 1952 b, *Ibid.*, **43,** 1115.
HARTREE, D. R., 1933, *Proc. Roy. Soc.* A, **141,** 282 ; 1946, *Rep. Prog. Phys.*, **11,** 113.
MILNE, E. A., 1927, *Proc. Camb. Phil. Soc.*, **23,** 794.
MOTT, N. F., 1936, *Proc. Camb. Phil. Soc.*, **32,** 281 ; 1949, *Proc. Phys. Soc.* A, **62,** 416 ; 1951, *Semi-Conducting Materials* (London : Butterworths), p. 1 ; 1952, *Progress in Metal Physics*, **3,** No. 3.
SLATER, J. C., 1949, *Phys. Rev.*, **76,** 1592.
WIGNER, E., 1934, *Phys. Rev.*, **46,** 1002 ; 1938, *Trans. Faraday Soc.*, **34,** 678.

CXLII. *Boundary Layer Growth in Three Dimensions*

By L. C. Squire
Department of Mathematics, University of Bristol*

[Received July 8, 1954]

Summary

The analysis of Goldstein and Rosenhead for the boundary layer growth on an impulsively started body has been extended to three dimensional bodies. The results are used to test various critera of three-dimensional separation.

§ 1. Introduction

Goldstein and Rosenhead† (1936) have studied the growth of the boundary layer on an impulsively started two-dimensional body. The initial motion may be assumed irrotational and without circulation. Thus initially the potential flow about the body will give a very close approximation to the flow outside the boundary layer. These conditions and assumptions cease to be valid as soon as the boundary layer separates from the body to form a wake. The analysis therefore gives an account of the initial motion of the boundary layer and the time and place of initial separation. In this note the method is extended to three-dimensional bodies; again the initial external flow may be assumed to be the potential flow about the body. The iterative form of solution employed in paper I may be extended without difficulty to include all three-dimensional effects; the successive approximations however increase rapidly in complexity. The complicated form for the skin-friction makes simple deductions of time and place of initial separation difficult; these may however be found easily, in any given case, by the data provided in this note.

This extension was carried out as part of work to investigate three-dimensional effects in boundary layers. Although valid for small time it seems probable that it will be the only solution in which it is possible to find curvature and cross-flow effects explicitly. Results of the solution are used to consider the conditions of three-dimensional boundary layer separation.

---

* Communicated by Professor L. Howarth, F.R.S.
† Referred to as paper I.

§ 2. BOUNDARY LAYER EQUATIONS

The three-dimensional boundary layer equations in their most general form may be written

$$\frac{\partial u}{\partial t}+\frac{u}{h_1}\frac{\partial u}{\partial x}+\frac{v}{h_2}\frac{\partial u}{\partial y}+w\frac{\partial u}{\partial z}-K_2uv+K_1v^2=-\frac{1}{\rho}\frac{1}{h_1}\frac{\partial p}{\partial x}+\nu\frac{\partial^2 u}{\partial z^2}, \quad . \quad (1)$$

$$\frac{\partial v}{\partial t}+\frac{u}{h_1}\frac{\partial v}{\partial x}+\frac{v}{h_2}\frac{\partial v}{\partial y}+w\frac{\partial v}{\partial z}+K_2u^2-K_1uv=-\frac{1}{\rho}\frac{1}{h_2}\frac{\partial p}{\partial y}+\nu\frac{\partial^2 v}{\partial z^2}, \quad . \quad (2)$$

$$\frac{1}{h_1}\frac{\partial u}{\partial x}+\frac{1}{h_2}\frac{\partial v}{\partial y}+\frac{\partial w}{\partial z}-K_1u-K_2v=0 \quad . \quad . \quad . \quad . \quad . \quad . \quad (3)$$

where
$$K_1=-\frac{1}{h_1h_2}\frac{\partial h_2}{\partial x} \quad \text{and} \quad K_2=-\frac{1}{h_1h_2}\frac{\partial h_1}{\partial y} \quad . \quad . \quad (4)$$

are the geodesic curvatures of the lines x=constant and y=constant, and U, V are the mainstream values. It is convenient to use the following abbreviated notation :—

$$\frac{1}{h_1}\frac{\partial(\ )}{\partial x}=(\ )'\,; \qquad \frac{1}{h_2}\frac{\partial(\ )}{\partial y}=\overline{(\ )}, \quad . \quad . \quad (5)$$

and similarly

$$\frac{1}{h_1}\frac{\partial}{\partial x}\left(\frac{1}{h_1}\frac{\partial(\ )}{\partial x}\right)=(\ )'', \qquad \frac{1}{h_1}\frac{\partial}{\partial x}\left(\frac{1}{h_2}\frac{\partial(\ )}{\partial y}\right)=\left(\overline{(\ )}\right)', \quad . \quad . \quad (6)$$

and to write
$$M=K_1U+K_2V, \qquad N=K_1U+K_2V-U'-\overline{V}, \quad . \quad . \quad (7)$$

since these latter combinations occur frequently.

First Approximation

Initially the boundary layer is of zero thickness and by a simple extension of Goldstein and Rosenhead's arguments the equations of the first approximation are found to be

$$\frac{\partial u_1}{\partial t}=\nu\frac{\partial^2 u_1}{\partial z^2}\,; \qquad \frac{\partial v_1}{\partial t}=\nu\frac{\partial^2 v_1}{\partial z^2}. \quad . \quad . \quad . \quad . \quad (8)$$

The boundary conditions on u and v are $u=v=0$ at $z=0$, u/U, v/V tend to 1 as $z\rightarrow\infty$, $u=U$, $v=V$ at $t=0$.

The solutions of eqn. (8) satisfying these conditions are

$$u_1=U\operatorname{erf}\eta, \qquad v_1=V\operatorname{erf}\eta\,; \qquad \operatorname{erf}\eta=\frac{2}{\pi^{1/2}}\int_0^\eta e^{-s^2}ds \quad . \quad (9)$$

where
$$\eta=\frac{z}{2(\nu t)^{1/2}}.$$

The first approximation to w_1 may be obtained from eqn. (3) and is

$$w_1=2(\nu t)^{1/2}N\left\{\eta\operatorname{erf}\eta-\frac{1}{\pi^{1/2}}(1-e^{-\eta^2})\right\}. \quad . \quad . \quad . \quad . \quad (10)$$

As noted by Goldstein and Rosenhead this value of w is not completely satisfactory, since it behaves like $2(\nu t)^{1/2}N\eta$ as $\eta\rightarrow\infty$, however they point out that u/U tends to 1 for moderate values of η so that within the boundary layer
$$w_1=NO(\nu t).$$

Second Approximation

The equations for the second approximation are found in the usual manner by substituting u_1, v_1, w_1 in the ignored terms of eqns. (1) and (2). In this way the equation for u_2 becomes

$$\nu\frac{\partial^2 u_2}{\partial z^2}-\frac{\partial u_2}{\partial t}=-UU'-VV'+\frac{u_1}{h_1}\frac{\partial u_1}{\partial x}+\frac{v_1}{h_2}\frac{\partial u_1}{\partial y}+w_1\frac{\partial u_1}{\partial z}$$
$$-K_2u_1v_1+K_1v_1^2. \quad . \quad . \quad . \quad . \quad . \quad . \quad . \quad . \quad . \quad . \quad (11)$$

When the values of u_1, v_1, w_1 are substituted into the r.h.s. of (11) and use made of the irrotational condition of the external flow the equation takes the form

$$\nu\frac{\partial^2 u_2}{\partial z^2}-\frac{\partial u_2}{\partial t}=-UN\left\{\operatorname{erf}^2\eta-1-\frac{2\eta}{(\pi)^{1/2}}\operatorname{erf}\eta e^{-\eta^2}+\frac{2}{\pi}(e^{-\eta^2}-e^{-2\eta^2})\right\}$$
$$+(VV'+UM-U\overline{V})(\operatorname{erf}^2\eta-1). \quad . \quad . \quad . \quad . \quad . \quad . \quad . \quad (12)$$

Putting

$$u_2=t\{-UNf_{21}(\eta)+(VV'+UM-U\overline{V})f_{22}(\eta)\}$$

the following equations for f_{21}, f_{22} are obtained :

$$f_{21}''+2\eta f_{21}'-4f_{21}=4\left\{\operatorname{erf}^2\eta-1-\frac{2}{\pi^{1/2}}\operatorname{erf}\eta e^{-\eta^2}+\frac{2}{\pi}\{e^{-\eta^2}+e^{-2\eta^2}\}\right\}, \quad (13)$$

$$f_{22}''+2\eta f_{22}'-4f_{22}=4\{\operatorname{erf}^2\eta-1\}, \quad . \quad . \quad . \quad . \quad . \quad . \quad . \quad . \quad . \quad . \quad (14)$$

where dashes now represent differentiation with respect to η. Equation (13) has been solved in paper I. This solution together with that of eqn. (14) may be written in the form

$$f_{2i}=f_{2ip}+\alpha_i(f_{2i})_{c1}+\beta_i(f_{2i})_{c2}$$

where f_{2ip} is a particular solution, $(f_{2i})_{c1}$, $(f_{2i})_{c2}$ are complementary functions and α_i, β_i constants which must be chosen to satisfy the boundary conditions $f_{2i}=0, \eta=0$; $f_{2i}\to 0, \eta\to\infty$. It may be shown that

$$(f_{21})_p=\tfrac{1}{2}(2\eta^2-1)\operatorname{erf}^2\eta+\frac{3}{\pi^{1/2}}\eta e^{-\eta^2}\operatorname{erf}\eta+1-\frac{4}{3\pi}e^{-\eta^2}+\frac{2}{\pi}e^{-2\eta^2}, \quad (15)$$

$$(f_{22})_p=2\eta^2\operatorname{erf}^2\eta+\frac{4}{\pi^{1/2}}\eta e^{-\eta^2}\operatorname{erf}\eta+\frac{2}{\pi}e^{-2\eta^2}+1, \quad . \quad . \quad . \quad . \quad . \quad . \quad (16)$$

$$(f_{2i})_{c1}=2\eta^2+1, \quad . \quad . \quad . \quad . \quad . \quad . \quad . \quad . \quad . \quad . \quad . \quad . \quad . \quad . \quad . \quad . \quad (17)$$

$$(f_{2i})_{c2}=\frac{2}{\pi^{1/2}}(2\eta^2+1)\operatorname{erf}\eta+\eta e^{-\eta^2}, \quad . \quad . \quad . \quad . \quad . \quad . \quad . \quad . \quad . \quad . \quad (18)$$

and that

$$\left.\begin{aligned}\alpha_1&=-\left(1+\frac{2}{3\pi}\right)=-1{\cdot}2122, & \beta_1&=\frac{1}{\pi^{1/2}}\left(1+\frac{4}{3\pi}\right)=0{\cdot}8036,\\ \alpha_2&=-\left(1+\frac{2}{\pi}\right)\;=-1{\cdot}6366, & \beta_2&=\frac{4}{\pi^{3/2}}\qquad\qquad\;\;=0{\cdot}7183.\end{aligned}\right\} \quad (19)$$

It is easily seen that the derivatives needed to find the skin-friction, are

$$\left.\frac{\partial f_{21}}{\partial\eta}\right)_0=\frac{2}{\pi^{1/2}}\left(1+\frac{4}{3\pi}\right)=1{\cdot}6073, \qquad \left.\frac{\partial f_{22}}{\partial\eta}\right)_0=\frac{8}{\pi^{3/2}}=1{\cdot}4367. \quad . \quad (20)$$

In a similar manner it may be shown that

$$V_2=t\{-VNf_{21}+(U\bar{U}+VM-VU')f_{22}\}. \quad . \quad . \quad . \quad (21)$$

Equation (3) then gives

$$w_2=2(\nu t^3)^{\frac{1}{2}}\left\{A\int_0^\eta f_{21}(s)\,ds+B\int_0^\eta f_{22}(s)\,ds\right\}, \quad . \quad . \quad . \quad . \quad (22)$$

where $A=-N^2-UU''-V\bar{\bar{V}}+UM'+V\bar{M}-U(\bar{V})'-V(\overline{U'})$

and

$$\begin{aligned}B=&M^2-M(U'+\bar{V})-VV''-U\bar{\bar{U}}-V\bar{M}-UM'+U(\bar{V})'\\&+V(\overline{U'})+K_1VV'+K_2U\bar{U}-V'^2-\bar{U}^2+2U'\bar{V}\\&-K_1U\bar{V}-K_2VU'.\end{aligned}$$

The integrals in eqn. (22) are given by

$$\begin{aligned}F_{21}=\int_0^\eta f_{21}(s)\,ds=&\tfrac{1}{6}(2\eta^3-3\eta)\operatorname{erf}^2\eta-\frac{1}{6\pi^{1/2}}\{4-(4\eta^2-11)\,e^{-\eta^2}\}\operatorname{erf}\eta\\&+\eta+\frac{1}{3\pi}\eta e^{-2\eta^2}+\frac{4(2)^{1/2}}{3\pi^{1/2}}\operatorname{erf}\sqrt{(2)}\eta+\alpha_1\{\tfrac{2}{3}\eta^3+\eta\}\\&+\beta_1\left\{\frac{\pi^{1/2}}{6}(2\eta^3+3\eta)\operatorname{erf}\eta+\tfrac{1}{3}(\eta^2+1)\,e^{-\eta^2}-\tfrac{1}{3}\right\}, \quad . \quad . \quad . \quad . \quad (23)\end{aligned}$$

and

$$\begin{aligned}F_{22}=\int_0^\eta f_{22}(s)\,ds=&\tfrac{2}{3}\eta^3\operatorname{erf}^2\eta+\eta+\frac{2^{3/2}}{3\pi^{1/2}}\operatorname{erf}(2)^{1/2}\eta\\&+\frac{2}{3\pi^{1/2}}(2\eta^2-1)\operatorname{erf}\eta e^{-\eta^2}+\frac{2}{3\pi}\eta e^{-2\eta^2}+\alpha_2(\tfrac{2}{3}\eta^3+\eta)\\&+\beta_2\left\{\frac{\pi^{1/2}}{6}(2\eta^3+3\eta)\operatorname{erf}\eta+\tfrac{1}{3}(\eta^2+1)e^{-\eta^2}-\tfrac{1}{3}\right\}. \quad . \quad . \quad . \quad . \quad (24)\end{aligned}$$

Third Approximation

The equation for u_3 is found in a similar way to that for u_2. The right hand side may be most conveniently collected together as follows :

$$\begin{aligned}\nu\frac{\partial^2u_3}{\partial z^2}-\frac{\partial u_3}{\partial t}=t\Bigg[&(Cf_{21}+Df_{22})\operatorname{erf}\eta+U(AF_{21}+BF_{22})\frac{2}{\pi^{1/2}}e^{-\eta^2}\\&+\left\{\eta\operatorname{erf}\eta-\frac{1}{\pi^{1/2}}(1-e^{-\eta^2})\right\}\left\{E\frac{\partial f_{21}}{\partial\eta}+F\frac{\partial f_{22}}{\partial\eta}\right\}\Bigg], \quad (25)\end{aligned}$$

where

$$\begin{aligned}C=&-2N\{K_1V^2-K_2UV+\bar{U}V+UU'\}+U^2\{U''-M'+(\bar{V})'\}\\&+UV\{\bar{\bar{V}}-\bar{M}+(\bar{U}')\},\\D=&\{U\bar{U}+VM-VU'\}\{2K_1V-K_2U+\bar{U}\}+UV\{V''-\bar{\bar{V}}\}\\&+\{VV'+UM-U\bar{V}\}\{U'-K_2V\}+UV'^2+V\bar{V}V'+M\{UU'+V\bar{U}\}\\&+U^2M'+UV\bar{M}-U\bar{V}U'-V\bar{U}\bar{V}-U^2(\bar{V})'+V^2(\bar{V}'),\\E=&-UN^2,\\F=&N\{VV'+UM-U\bar{V}\}.\end{aligned}$$

This grouping of similar terms in η rather than of terms similar in the external flow appears to be the best method, since this latter grouping produces 12–14 equations for solution.

A solution of (25) is obtained by writing

$$u_3=t^2\{Cf_{31}+Df_{32}+Ef_{33}+Ff_{34}+UAf_{35}+UBf_{36}\}, \quad . \quad . \quad (26)$$

where f_{3i} is a solution of the equation

$$f_{3i}''+2\eta f_{3i}'-8f_{3i}=4r_i, \quad . \quad . \quad . \quad . \quad . \quad . \quad (27)$$

with boundary conditions

$$f_{3i}=0, \qquad \eta=0\,; \qquad f_{3i}\rightarrow 0, \qquad \eta\rightarrow\infty,$$

and

$$r_1=f_{21}\,\mathrm{erf}\,\eta, \qquad r_2=f_{22}\,\mathrm{erf}\,\eta,$$

$$r_3=\left(\eta\,\mathrm{erf}\,\eta-\frac{1}{\pi^{1/2}}(1-\mathrm{e}^{-\eta^2})\right)\frac{\partial f_{21}}{\partial\eta}, \qquad r_4=\left(\eta\,\mathrm{erf}\,\eta-\frac{1}{\pi^{1/2}}(1-\mathrm{e}^{-\eta^2})\right)\frac{\partial f_{22}}{\partial\eta},$$

$$r_5=\frac{2}{\pi^{1/2}}\mathrm{e}^{-\eta^2}F_{21}, \qquad r_6=\frac{2}{\pi^{1/2}}\mathrm{e}^{-\eta^2}F_{22}.$$

Fig. 1

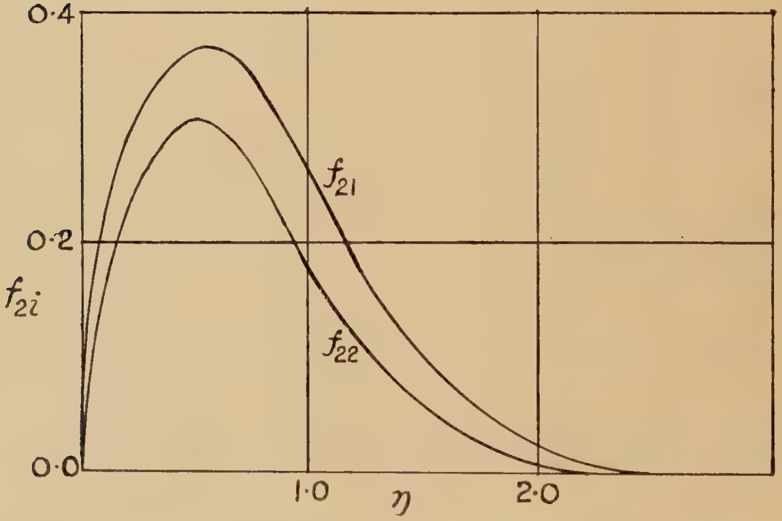

In paper I two equations of type (27) have been solved, these two solutions denoted in that paper by f_3 and F_3-f_3 are equal to $f_{31}-f_{35}$ and $f_{31}-f_{33}$ respectively in the present notation. Thus once $f_{31}, f_{32}, f_{34}, f_{36}$ have been obtained, f_{33}, f_{35} can be found from paper I.

As in paper I solutions of (27) are sought in the form

$$f_{3i}=X_i(\eta)\,\mathrm{erf}^3\,\eta+Y_i(\eta)\,\mathrm{erf}^2\,\eta+Z_i(\eta)\,\mathrm{erf}\,\eta+T_i(\eta)+\Delta_i m+\nabla_i n, \quad . \quad . \quad (28)$$

where m and n are the complementary functions

$$m=4\eta^4+12\eta^2+3, \qquad n=m\,\mathrm{erf}\,\eta+\frac{1}{\pi^{1/2}}(4\eta^3+10\eta)\,\mathrm{e}^{-\eta^2}. \qquad (29)$$

The solutions are shown graphically in fig. 2 and tabulated in table 1; for reference their analytic forms are expressed in the Appendix.

The derivatives needed to find the skin friction can be obtained by differentiating the expression (28) and evaluating at $\eta=0$. The derivative is then

$$\left.\frac{\partial f_{31}}{\partial \eta}\right)_{\eta=0}=\frac{2}{\pi^{1/2}}(Z_i)_0+(T_i)_0+\frac{16}{\pi^{1/2}}\nabla_i. \quad . \quad . \quad . \quad . \quad (30)$$

Fig. 2

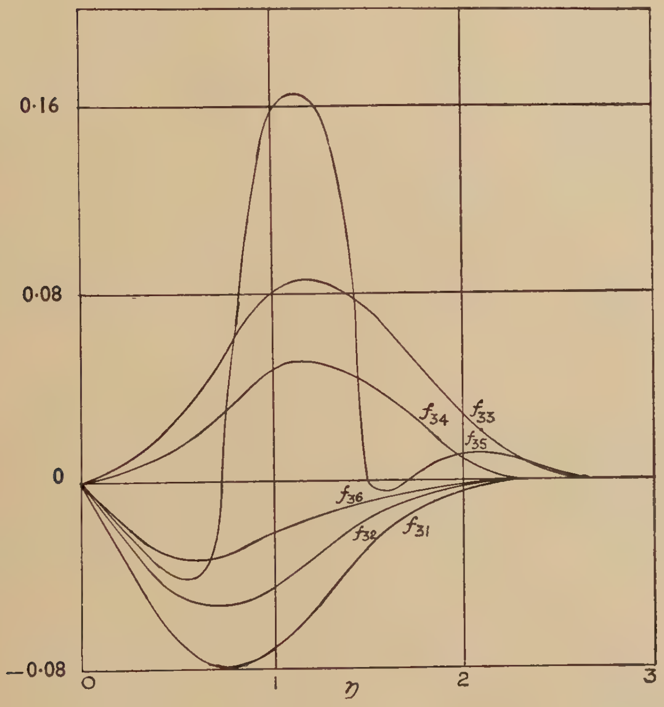

Table 1

η	f_{21}	f_{22}	f_{31}	f_{32}	f_{33}	f_{34}	f_{35}	f_{36}
0·0	0·0	0·0	0·0	0·0	0·0	0·0	0·0	0·0
0·5	0·381	0·307	—0·070	—0·049	0·026	0·021	—0·039	—0·033
1·0	0·269	0·173	—0·070	—0·044	0·079	0·047	+0·173	—0·020
1·5	0·098	0·051	—0·027	—0·015	0·074	0·044	—0·006	—0·008
2·0	0·020	0·002	—0·002	—0·002	0·029	0·011	+0·014	—0·003
2·5	0·000	0·000	0·000	0·000	0·003	0·000	+0·002	0·000

N.B.—f_{21} is taken from Goldstein and Rosenhead's paper and is given here for easy reference.

Substitution of the analytic forms now gives

$$\left.\frac{\partial f_{31}}{\partial \eta}\right)_0 = \pi^{-1/2} + \pi^{-3/2}\left\{\frac{48}{5} + 16\left\{\frac{32(2)^{1/2}}{45} - \frac{9(3)^{1/2}}{8}\right\}\right\} + \pi^{-5/2}\frac{128}{27} = -0{\cdot}1502, \quad (31)$$

$$\left.\frac{\partial f_{32}}{\partial \eta}\right)_0 = \frac{1}{9}\pi^{-1/2} + \pi^{-3/2}\left\{\frac{44}{9} - 6(3)^{1/2}\right\} + \pi^{-5/2}\frac{128}{9} = -0{\cdot}1127, \quad (32)$$

$$\left.\frac{\partial f_{33}}{\partial \eta}\right)_0 = -2\pi^{-1/2} + \pi^{-3/2}\left\{\frac{44}{15} + \frac{512}{45}(2)^{1/2} - 9(3)^{1/2}\right\} + \frac{256}{27}\pi^{-5/2} = 0{\cdot}0306, \quad (33)$$

$$\left.\frac{\partial f_{34}}{\partial \eta}\right)_0 = -\frac{10}{9}\pi^{-1/2} + \pi^{-3/2}\left\{\frac{16}{9}\left(\frac{64}{5}(2)^{1/2} - \frac{27}{4}(3)^{1/2}\right) - \frac{756}{45}\right\} + \frac{256}{9}\pi^{-5/2} = 0{\cdot}0286, \quad (34)$$

$$\left.\frac{\partial f_{35}}{\partial \eta}\right)_0 = \frac{13}{6}\pi^{-1/2} + \pi^{-3/2}\left\{\frac{93}{9} + 16\left(\frac{32}{45}(2)^{1/2} - \frac{99}{80}(3)^{1/2}\right\} + \frac{256}{135}\pi^{-5/2} = -0{\cdot}0827, \quad (35)$$

$$\left.\frac{\partial f_{36}}{\partial \eta}\right)_0 = \frac{19}{18}\pi^{-1/2} + \pi^{-3/2}\left\{\frac{407}{45} - \frac{42}{5}(3)^{1/2}\right\} + \frac{256}{45}\pi^{-5/2} = -0{\cdot}0679. \quad (36)$$

In a recent paper on a related problem, boundary layer growth on a spinning projectile, Illingworth (1954) has solved some other equations of type (27) by the method of variation of parameters. The resulting integral form has been found quite difficult to evaluate explicitly but gives a very simple form for the wall derivatives. This method applied to our equations leads to the result

$$\left.\frac{\partial f_{31}}{\partial \eta}\right)_0 = \frac{4}{3}\int_0^\infty (n-m)e^{s^2}\, r_i(s)\, ds.$$

These integrals have been evaluated numerically and used to check the values given by (31)–(36).

The third approximation for v_3 may be found in exactly the same way, the solution is

$$v_3 = t^2\{C^*f_{31} + D^*f_{32} + E^*f_{33} + F^*f_{34} + VAf_{35} + VBf_{36}\}, \quad . \quad . \quad (37)$$

where

$$\begin{aligned} C^* &= -2N\{K_2U^2 - K_1VU + V\bar{V} + UV'\} + UV\{U'' - M' - (\bar{V})'\} \\ &\quad + V^2\{\bar{\bar{V}} - \bar{M} + (\bar{U})'\}, \\ D^* &= \{VV' + UM - U\bar{V}\}\{2K_2U - K_1V + V'\} + UV\{\bar{\bar{U}} - U''\} \\ &\quad + \{U\bar{U} + VM - VU'\}\{\bar{V} - K_1U\} + V\bar{U}^2 + U\bar{U}U' \\ &\quad + M\{V\bar{V} + UV'\} + V^2\bar{M} + UVM' - V\bar{V}U' - UV'U' \\ &\quad - V^2(\bar{U}') + U(\bar{U})', \\ E^* &= -VN^2, \\ F^* &= N\{U\bar{U} + VM - VU'\}. \end{aligned}$$

The total results are now summarized in the skin-friction components which are given as

$$\left.\frac{\partial u}{\partial z}\right)_0 = \tfrac{1}{2}(\nu t)^{-1/2}[1{\cdot}1284U + t\{-1{\cdot}6073UN + 1{\cdot}4370(VV' + UM - U\overline{V})\} + t^2\{-0{\cdot}1501C - 0{\cdot}1127D + 0{\cdot}0306E + 0{\cdot}0286F - 0{\cdot}0827UA - 0{\cdot}0687UB\}], \qquad (38)$$

$$\left.\frac{\partial v}{\partial z}\right)_0 = \tfrac{1}{2}(\nu t)^{-1/2}[1{\cdot}1284V + t\{-1{\cdot}6073VN + 1{\cdot}4370(U\overline{U} + VM - VU')\} + t^2\{-0{\cdot}1501C^* - 0{\cdot}1127D^* + 0{\cdot}0306E^* + 0{\cdot}0286F^* - 0{\cdot}0827VA - 0{\cdot}0687VB\}]. \qquad (39)$$

§ 3. APPLICATION TO AN ELLIPSOID WITH A DISCUSSION OF THREE-DIMENSIONAL SEPARATION

The results of the last section have been used to study the boundary layer on an ellipsoid of axes in the ratio 30 : 6 : 1. The ellipsoid was considered moving parallel to its middle axis so that the external potential flow was known and the various functions needed to find the coefficients of the skin-friction in eqns. (38) and (39) had been tabulated in an earlier problem.

Fig 3

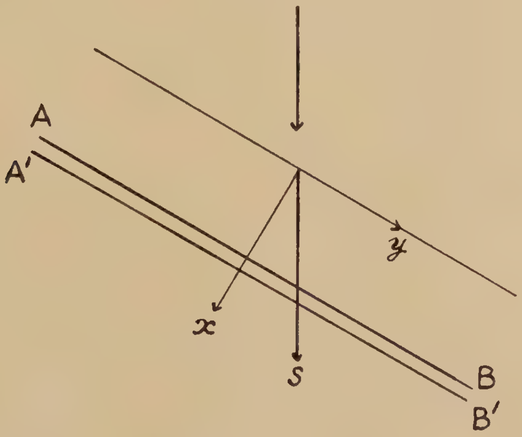

Before giving the results for this body, some possible definitions of separation in three-dimensional flows will be mentioned. These include separation as defined by the disappearance of the skin-friction in the external streamline direction on a general surface and by the disappearance of the chord-wise skin-friction component on a wing. Hayes (1951) points out that these criteria are not always consistent and suggests alternatively that one must expect regions of separated and unseparated flow to be divided by a skin-friction line.†

---

† A skin-friction line is defined as a line whose tangent is in the direction of the resultant skin-frictional force and as such it may be regarded as the limiting streamline direction as the surface is approached.

The definitions and their effects are now considered for the infinite wing of fig. 3. In this figure let x be measured normal, and y parallel to the leading edge and let s be in the external stream direction. Also let τ_x, τ_y, τ_z be the skin-friction components in these directions. Then the line of separation might be taken to be AB or A′B′ depending on whether $\tau_x=0$ or $\tau_s=0$ is chosen as the separation condition. Now consider Hayes's criterion applied to the same problem. Since the wing is infinite this criterion implies that separation is defined by a skin-friction line parallel to the leading edge, that is by a line on which there is no chordwise component of skin-friction. By definition AB is the only line with this property and so in this case Hayes's criterion gives two-dimensional separation.

Returning to the ellipsoid it will be seen that there are two lines where the external and surface streamlines coincide; these are the lines of symmetry joining the front and rear stagnation points, ACB and ADB in fig. 4. On these lines the first two definitions of separation lead to the same result; the point of separation being the point where the skin-friction component along the lines disappears. Also on this body Hayes's surface streamline would be expected to pass through these two points. This has been tested by the numerical method described below but the method is not accurate enough to give a completely conclusive result. The most that can be said is that a surface streamline starting from the separation point on ACB reaches ADB in the region of separation.

Fig. 4

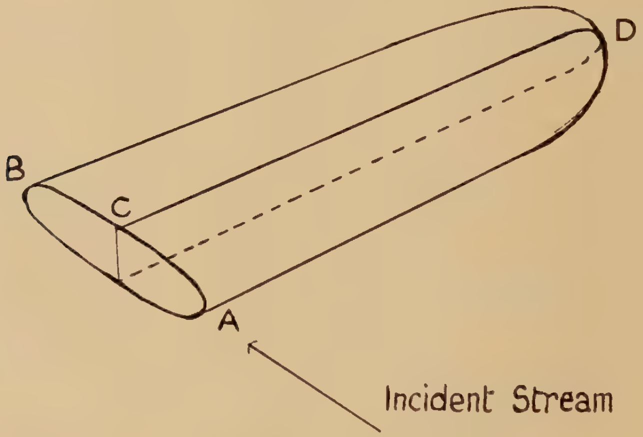

In the actual determination of the time and place of separation by eqns. (38) and (39) the second approximation was used first and the results checked by including the third approximation. This procedure showed that accurate results could be obtained for the inner half of the ellipsoid. On the outer region the influence of the third approximation was so large, often altering the initial time of separation by over 30%, that the results in these regions can only give a guide to the actual boundary-layer characteristics. Also potential flow is used throughout the investigation although it ceases to be accurate as soon as any part of the boundary layer separates. However, since the times used in this investigation are small the wake will be thin and so potential flow will be a reasonable approximation to the actual flow.

Subject to the restrictions of the last paragraph the growth of the boundary layer on the ellipsoid will now be described. The boundary layer first separated on the line ACB (fig. 4) at the rear stagnation point at time $UT/C=0{\cdot}0196$† by the second approximation and $UT/C=0{\cdot}0181$ by the third approximation. After this time the separation point on ACB moved forwards and separation began on neighbouring streamlines at points not coinciding with the rear stagnation point. Streamlines further along the wing remained unseparated right up to the rear stagnation point. At $TU/C=0{\cdot}04$ separation takes place on ACB at an eccentric angle of 6° from the rear stagnation point and streamlines over the centre half of the body were separated. Separation was complete at $TU/C=0{\cdot}05$ by which time separation took place on ADB on the trailing edge close to the wing tip. At this time the separation point on ACB has moved to 8° eccentric angle from the rear stagnation point.

In addition to the test described earlier the surface streamline given by Hayes's criterion was compared with the separation line defined by $\tau_s=0$ when $UT/C=0{\cdot}03$. The lines coincide on ACB by definition and a maximum divergence of 2° in eccentric angle was obtained. Hayes's line always gave earlier separation.

The results of this last comparison together with that of the yawed wing will now be used to state the following tentative separation criterion:

> The line of separation on a general surface is the last surface streamline on which the skin-friction in the external streamline direction does not become negative at any point.

Surface streamlines are chosen since they give no component of skin-friction normal to the separation line. This implies that the velocity profiles normal to separation are of similar form to the two-dimensional separation profile. The actual surface streamline chosen is based on the two examples above which show that Hayes's separation line τ_s is never negative.

ACKNOWLEDGMENTS

I would like to thank Professor L. Howarth for helpful discussion on this problem, also the Department of Scientific and Industrial Research for a maintenance grant.

REFERENCES

GOLDSTEIN, S., and ROSENHEAD, L., 1936, *Proc. Camb. Phil. Soc.*, 32.
HAYES, W. D., 1951, *NAVORD Report* 1313 (Nots 384).
ILLINGWORTH, C. R., 1954, *Phil. Mag.*, 45, 1.

---

† UT/C is a non-dimensional number based on time T and a standard velocity (U) and length (C).

APPENDIX.

f_{31}

$$X_1 = -\frac{1}{12}(4\eta^4+24\eta^2+3),$$

$$Y_1 = -\pi^{-1/2}\,e^{-\eta^2}\left(\eta^3+\frac{11}{2}\eta\right)+\tfrac{1}{3}\beta_1\pi^{1/2}(2\eta^4+3\eta^2),$$

$$Z_1 = -\pi^{-1}e^{-2\eta^2}(\eta^2+5)+e^{-\eta^2}\frac{1}{3}\left\{(4\eta^3+5\eta)\beta_1+\frac{8}{5}\pi^{-1}\right\}-\tfrac{1}{2}(4\alpha_1\eta^2+2\alpha_1+1),$$

$$T_1 = \pi^{-3/2}\frac{e^{-3\eta^2}}{2}\left(\frac{149}{6}\eta+9\eta^3\right)+\pi^{-1/2}\,e^{-2\eta^2}\left\{\frac{2}{3}(1+\eta^2)\beta_1\right.$$

$$\left.-\frac{1}{45}\pi^{-1}(352\eta+128\eta^3)\right\}-\frac{4}{3}\pi^{-1/2}\alpha_1\eta\,e^{-\eta^2}$$

$$+(4\eta^4+12\eta^2+3)\left\{\frac{9\sqrt{3}}{8\pi}\operatorname{erf}\sqrt{3}\eta-\frac{32\sqrt{2}}{45\pi}\operatorname{erf}\sqrt{2}\eta\right\},$$

$$\Delta_1 = -\frac{2}{9}\pi^{-1}\left(1+\frac{4}{3}\pi^{-1}\right),$$

$$\nabla_1 = \frac{8}{27}\pi^{-2}+\frac{32\sqrt{2}}{45}\pi^{-1}-\frac{9\sqrt{3}}{8}\pi^{-1}-\frac{1}{12}.$$

f_{32}

$$X_2 = \frac{1}{36}(20\eta^4-12\eta^2-3),$$

$$Y_2 = \tfrac{1}{6}\,e^{-\eta^2}\pi^{-1/2}(10\eta^3-7\eta)+\frac{\beta_2}{3}\pi^{-1/2}(2\eta^4+3\eta^2),$$

$$Z_2 = +\tfrac{1}{3}\,e^{-2\eta^2}\pi^{-1}(5\eta^2-4)+\tfrac{1}{3}e^{-\eta^2}\beta_2(4\eta^3+5\eta)-\tfrac{1}{2}(4\alpha_2\eta^2+2\alpha_2+1),$$

$$T_2 = \frac{1}{36}e^{-3\eta^2}\pi^{-3/2}(54\eta^3+173\eta)+\tfrac{2}{3}\beta_2\,e^{-2\eta^2}\pi^{-1/2}(\eta^2+1)-\frac{4}{3}\alpha_2\pi^{-1/2}e^{-\eta^2}\eta$$

$$+\frac{3}{8}\sqrt{(3)}\pi^{-1}\operatorname{erf}\sqrt{3}\eta[4\eta^4+12\eta^2+3],$$

$$\Delta_2 = -\frac{8}{9}\pi^{-2},$$

$$\nabla_2 = \frac{8}{9}\pi^{-2}-\left(\frac{3\sqrt{3}}{8}+\frac{2}{3}\right)\pi^{-1}-\frac{5}{36}.$$

f_{34}

$$X_4 = \frac{1}{9}\left(10\eta^4-6\eta^2-\frac{3}{2}\right),$$

$$Y_4 = \tfrac{1}{3}e^{-\eta^2}\pi^{-1/2}(10\eta^3-7\eta)+\frac{8}{3}\pi^{-1/2}\eta+\frac{1}{4}\beta_2\pi^{1/2}(4\eta^4+4\eta^2+1),$$

$$Z_4 = \tfrac{1}{3}e^{-2\eta^2}\pi^{-1}(10\eta^2-8)+e^{-\eta^2}\left(\frac{56}{15}\pi^{-1}+\beta_2(2\eta^3+\eta)\right)+\frac{4}{3}\beta_2\eta-(1+4\eta^2)\alpha_2,$$

$$T_4=\frac{1}{18}e^{-3\eta^2}\pi^{-3/2}(54\eta^3+173\eta)+e^{-2\eta^2}\pi^{-1/2}\left(\beta_2\eta^2-\frac{64}{45}\pi^{-1}(11\eta+4\eta^3)\right)$$

$$+\frac{4}{3}e^{-\eta^2}\pi^{-1/2}(\beta_2-3\alpha_2\eta)+\frac{8}{3}\pi^{-1/2}\alpha_2\eta$$

$$+\pi^{-1}\left[\frac{3}{4}\sqrt{3}\operatorname{erf}\sqrt{3}\eta-\frac{64}{45}\sqrt{2}\operatorname{erf}\sqrt{2}\eta\right][4\eta^4+12\eta^2+3],$$

$$\Delta_4=-\frac{16}{9}\pi^{-2},$$

$$\nabla_4=\frac{16}{9}\pi^{-2}-\left(1+\frac{3}{4}\sqrt{3}-\frac{64}{45}\sqrt{2}\right)\pi^{-1}-\frac{5}{18}.$$

f_{36}

$$X_6=-\frac{1}{18}[4\eta^4+12\eta^2+3],$$

$$Y_6=-\frac{1}{6}\pi^{-1/2}e^{-\eta^2}(6\eta^3+11\eta)+\frac{1}{24}\beta_2\pi^{+1/2}(4\eta^4+12\eta^2+3),$$

$$Z_6=-\frac{4}{3}\pi^{-1}e^{-2\eta^2}(\eta^2+1)+\frac{1}{12}\beta_2e^{-\eta^2}(2\eta^3+5\eta),$$

$$T_6=\frac{1}{180}\pi^{-3/2}e^{-3\eta^2}(378\eta^3+971\eta)+e^{-\eta^2}\pi^{-1/2}\left[\frac{4}{15}\beta_2-\frac{4+5\alpha_2}{6}\eta-\frac{\alpha_2}{3}\eta^3\right]$$

$$+\frac{21}{40}\sqrt{(3)}\pi^{-1}(4\eta^4+12\eta^2+3)\operatorname{erf}\sqrt{3}\eta-\frac{8}{15}\sqrt{(2)}\pi^{-1}e^{-\eta^2}\operatorname{erf}\sqrt{2}\eta,$$

$$\Delta_6=-\frac{16}{45}\pi^{-2},$$

$$\nabla_6=\frac{16}{45}\pi^{-2}-\pi^{-1}\left[\frac{1}{6}+\frac{21}{40}\sqrt{3}\right]+\frac{1}{18}.$$

CXLIII. *Delayed Disintegration of a Nuclear Fragment*

By A. Solheim and S. O. Sörensen
Fysisk Institutt, University of Oslo, Norway *

[Received August 20, 1954]

A number of reports on experiments with photographic plates exposed to cosmic radiation have recently described the observation of disintegrations produced by heavy fragments at the end of their range (Danysz and Pniewski 1953, Tidman *et al.* 1953, Freier *et al.* 1954, Cheston and Primakoff 1953, Hill *et al.* 1954, Bonetti *et al.* 1954 and Powell 1954). It is believed that the phenomenon is due to the existence within the fragment of a neutral hyperon Λ^0, and that the disintegration is caused by a transformation of the Λ^0 particle. This transformation may be either a 'mesonic' decay $\Lambda^0 \rightarrow \mathrm{P}+\pi^-+Q$ (37 MeV) in which a negative π-meson escapes from the disintegration, or it may be a 'non-mesonic' decay giving a neutron and ~178 MeV energy release leading to an excitation and subsequent break up of the fragment. An event bearing on this new type of nuclear excitation has recently been observed in our laboratory. It was recorded in a stack of stripped Ilford G5 emulsions, each $600\,\mu$ thick, exposed at high altitude by means of free balloons during the Sardinian Expedition 1953. A photo-micrograph of the event is shown in Plate 35.

From a nuclear disintegration A of type 12+4p in the nomenclature of Brown *et al.* (1949) is ejected a particle of range $243\,\mu$. An exact determination of the charge of the particle is not possible on account of the shortness of the track. But a comparison of the shape of the track with those of other charged particles stopped in the emulsion indicates that the track is very similar to that of particles with charge $2e$. In B, where the particle is brought to rest, or is moving with very low velocity, it disintegrates into two singly charged particles of approximately equal range $\sim 7300\,\mu$. We regard the equality of the two ranges as accidental. Both particles end in the stack of stripped emulsions, and show the characteristic appearance of tracks due to protons. In the following discussion the particles C and D will be assumed to be protons, each of kinetic energy ~44 MeV, although we cannot yet exclude the possibility of one or both of the tracks being due to deuterons or tritons. More exact mass determinations of the tracks by means of scattering and gap measurements are in progress. The angle between the two particles C and D is 71·5°.

---

* Communicated by the Authors.

Discussion

From reasons thoroughly discussed in previous reports we exclude the following three possible interpretations :

1. Chance coincidence of the end of the fragment's path with a two-pronged star.
2. Collision of the fragment with a nucleus in the emulsion.
3. Decay of an excited nucleus.

We are left with various alternative possibilities, and will first discuss the event considering it to be an example of a delayed disintegration of a helium fragment due to the presence within the nucleus of a Λ^0 particle. As neither of the tracks C and D is a π-meson we consider a ' non-mesonic ' decay of the Λ^0 particle with an energy release of $\sim$178 Mev. The energy and momentum balance in the disintegration process may then be used to determine which isotope of helium is emitted from star A. A certain ambiguity exists in calculating the energy release due to the unknown binding energies of the Λ^0 particle in various nuclear species. In the following, however, we take for the Λ^0 particle the same binding energy in the parent nucleus as for the neutron in the corresponding normal nucleus.

Alternative 1 : Assuming a single neutron to compensate for the momentum of the tracks C and D in the disintegration, i.e., the fragment being a ${}^3\mathrm{He}_2{}^*$ nucleus, we have the following energy release :

Sum of the kinetic energies of the two protons C and D :	88 Mev
Kinetic energy of the neutron :	116 Mev
Binding energy of ${}^3\mathrm{He}_2{}^*$:	8 Mev
Sum :	212 Mev

This energy is too high by an amount of $\sim$34 Mev to be provided for by a Q-value of $\sim$178 Mev. Even a strong reduction in the assumed value of the binding energy of the ${}^3\mathrm{He}_2{}^*$ nucleus cannot remove this discrepancy. We may therefore exclude the possibility of the fragment being a ${}^3\mathrm{He}_2{}^*$ nucleus.

Alternative 2 : Assuming two neutrons to compensate for the momentum in the disintegration, i.e., the fragment being a ${}^4\mathrm{He}_2{}^*$ nucleus, the minimum energy release in the process is obtained if the two neutrons recoil in the same direction with equal energy. We obtain the following energy release :

Sum of the kinetic energies of the two protons C and D :	88 Mev
Sum of the kinetic energies of the two neutrons :	58 Mev
Binding energy of ${}^4\mathrm{He}_2{}^*$:	28 Mev
Sum :	174 Mev

This energy is sufficiently low to correspond to a Q-value of $\sim$178 Mev. The minimum energy release may be even lower since the estimate of the binding energy is almost certainly too high. Hill *et al.* (1954) estimate the binding energy of a Λ^0 particle bound in a $^4He_2^*$ nucleus to be ~4 Mev, a value which has to be compared with the energy ~20 Mev required to remove a neutron from an alpha particle. The energy release in the disintegration is therefore consistent with the fragment being an alpha particle in which one of the neutrons is substituted by a Λ^0 particle.

The energy and momentum conservation laws do not exclude the fragment being a heavier isotope of helium. However, the instability of these nuclei in conjunction with the very low binding energy of the Λ^0 particles makes this very improbable.

Due to the short length of the track, and consequently the uncertainty in the charge determination, we can not definitely exclude the fragment being a nucleus of charge $3e$. This, however, would be very difficult to reconcile with the conservation of charge, as only two singly charged particles are ejected in the disintegration.

In the previously mentioned reports the ' mesonic ion '-hypothesis has been discussed, considering the fragment as ejected from the parent disintegration with a π-meson around it in a bound quantum orbit. The disintegration is then attributed to capture by the fragment of the π-meson with an energy release of $Q \sim 142$ Mev. In the present case the ' mesonic ion ' would consist of a lithium or beryllium nucleus with a negative π-meson rotating around it in a Bohr orbit. The evaluation of the energy release under this assumption, however, gives the energy of the disintegration to be too high for a π-meson star.

Assuming the emission of neutral particles of sufficiently high energy and momentum, the disintegration could be attributed to the nuclear capture of a negatively charged hyperon. We can, however, definitely exclude the fragment being of unit charge, and regard this possibility as very remote.

ACKNOWLEDGMENTS

The authors would like to express their gratitude to Professor J. Holtsmark and Professor R. Tangen of the University of Oslo for providing laboratory facilities. We are indebted to the Royal Norwegian Council for Scientific and Industrial Research for financial support.

REFERENCES

BONETTI, LEVI-SETTI, PANETTI, SCARSI, and TOMASINI, 1954, *Nuovo Cimento*, **11,** 210.
BROWN, CAMERINI, FOWLER, HEITLER, KING, and POWELL, 1949, *Phil. Mag.*, **40,** 862.
CHESTON, and PRIMAKOFF, 1953, *Phys. Rev.*, **92,** 1537.
DANYSZ, and PNIEWSKI, 1953, *Phil. Mag.*, **44,** 348.
FREIER, ANDERSON, and NAUGLE, 1953, *Phys. Rev.*, **94,** 677.
HILL, SALANT, WIDGOFF, OSBORNE, PEVSNER, RITSON, CRUSSARD, and WALKER, 1954, *Bull. Amer. Phys. Soc.*, **29,** 60.
POWELL, 1954, *Nature, Lond.*, **173,** 459.
TIDMAN, DAVIS, HERZ, and TENNENT, 1953, *Phil. Mag.*, **44,** 350.

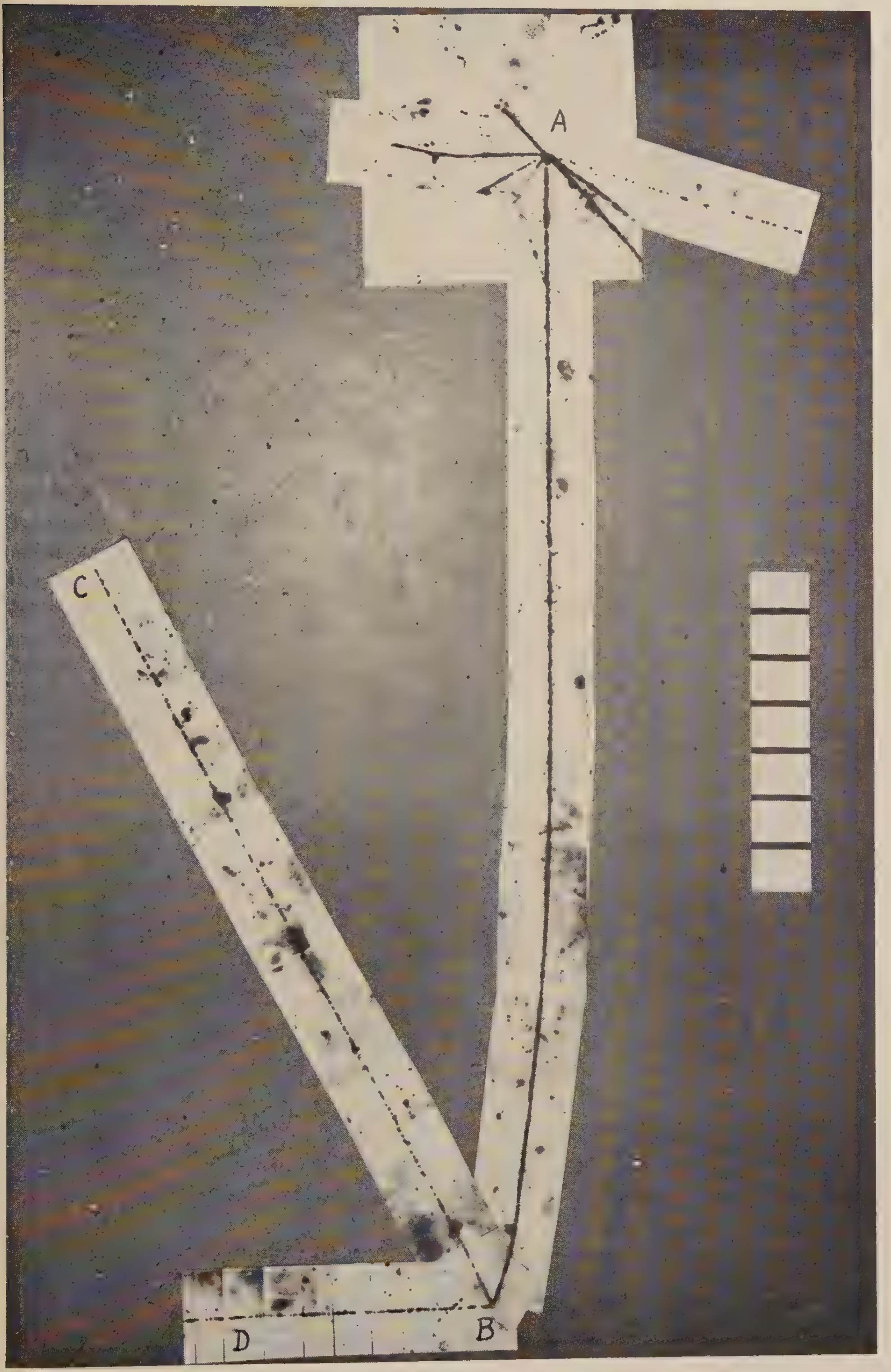

A nuclear fragment, ejected from the disintegration at A, produces a track of length 243 μ and comes to rest at B where it decays in two charged particles C and D.

Fig. 3

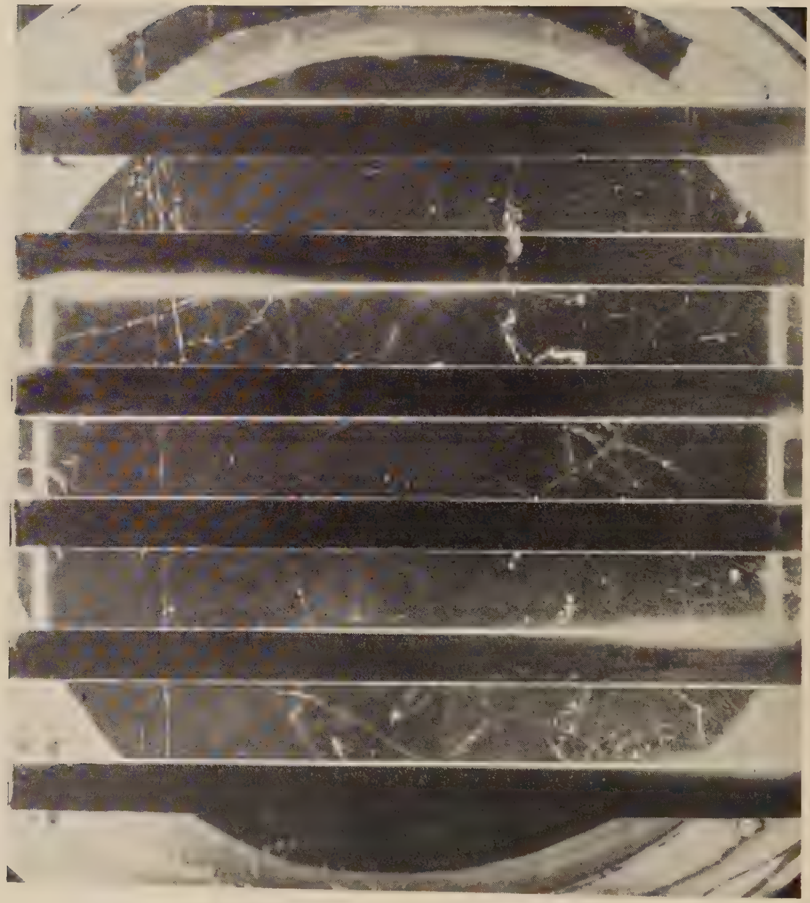

Example of nuclear interaction produced immediately above the chamber.

CXLIV. *A Cloud Chamber Study of Cosmic Ray Interactions Underground*

By H. J. J. BRADDICK and B. LEONTIC*
The Physical Laboratories, The University of Manchester †

[Received August 19, 1954]

ABSTRACT

A multiplate cloud chamber has been used to study the interactions of cosmic rays underground. The nature of events previously reported as pairs of associated penetrating particles (A.P.P.) is discussed and an upper limiting cross section for the formation of such particles is estimated as 2×10^{-30} cm^2 per nucleon. An explanation of the high cross section found previously is put forward. A cross section of $3 \cdot 2 \pm 1 \cdot 8 \times 10^{-30}$ cm^2 per nucleon for the nuclear interaction of cosmic rays underground has been obtained.

§ 1. INTRODUCTION

THE production of penetrating secondary particles by cosmic rays underground was first reported by Braddick and Hensby (1939), who used a cloud chamber at a depth equivalent to 60 m of water. The phenomenon was subsequently investigated by Braddick *et al.* (1951), George and Trent (1951) and more recently by Lovati *et al.* (1953), Deutschmann (1953), George *et al.* (1953), Appapillai *et al.* and others, all using cloud chambers.

In some of these experiments the cross section found for the production of single penetrating secondaries was an order of magnitude greater than that associated with the production of penetrating particles in stars produced by μ-mesons (George 1952); it was therefore suggested that a separate process was involved. The aim of the present work was to re-examine this phenomenon as well as other interactions of cosmic rays underground.

§ 2. EXPERIMENTAL ARRANGEMENT

A cloud chamber containing six lead plates, each 2 cm thick, was operated at a depth equivalent to 26 m of water. It was situated in a tunnel 80 cm below the rock roof. The lead plates were 30 cm wide, while the illuminated depth was about 14 cm. The chamber was of the conventional cylindrical type, 45 cm in diameter, illuminated by flash tubes. Two cameras were used for the photography; one was placed with its axis on the axis of the chamber, while the other made an angle of 15° with it.

---

* On leave from the University of Zagreb, Yugoslavia.

† Communicated by Professor P. M. S. Blackett, F.R.S.

The wide angle between the cameras enabled the reprojection of photographs to be done with great accuracy. The chamber was placed within a counter telescope which selected penetrating particles traversing the chamber plates and, in addition, a 10 cm lead block placed above the chamber. Later, the whole counter telescope was placed under the chamber to allow the observations of possible secondaries produced by neutral primaries.

Fig. 1

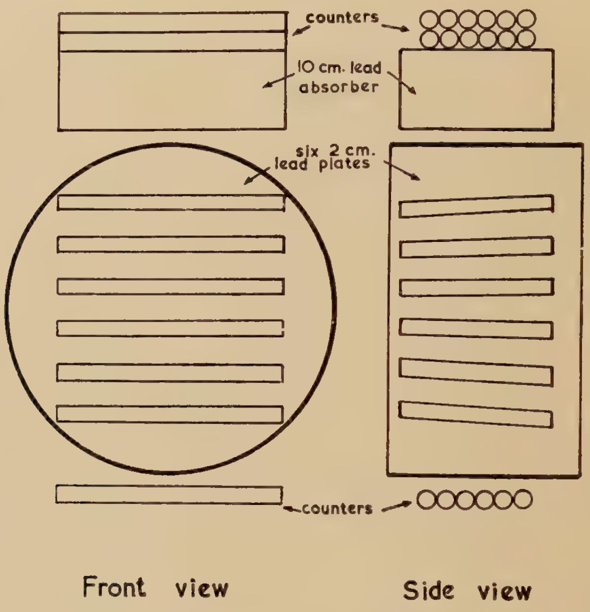

§ 3. Experimental Results

With the first arrangement (fig. 1) 6841 photographs were taken showing at least one ionizing particle traversing the lead plates inside and the absorber outside the chamber. In the search for single penetrating secondaries only events occurring inside the chamber and in the first four plates were considered. From 550 m of lead traversed by penetrating particles no certain cases of single penetrating secondaries were observed. The results of several other authors are shown in the table for comparison.

Since the production of penetrating particles found in the present experiment, and indeed in most of the recent work, is much less than that reported earlier, it is important to re-examine the former work for possible spurious effects simulating A.P.P. The present observations give data which assist this reinterpretation.

The main contributors to the high apparent cross sections are likely to be:

(1) Accidental coincidences between penetrating particles, and

(2) knock-on electrons not recognized as such.

We found that single secondary particles occasionally penetrated one lead plate without multiplication or conspicuous scattering. Fourteen cases were observed. The projected angle of scattering in the 2 cm lead plate was less than 5° in six of these, while there were five angles from 10° to 15°.

Authors	Experimental method	Metres of Pb of μ-meson track	No. of single penetrating secondaries
Braddick *et al.*	Single-plate cloud chamber	78	4
Braddick *et al.*	Multiplate cloud chamber	89	3
Lovati *et al.*	Multiplate cloud chamber	352	1
Deutschmann	Multiplate cloud chamber	422	0
George *et al.*	Two-plate cloud chamber	80	3
Appapillai *et al.*	Single-plate cloud chamber in magnetic field	690	<3
Braddick and Leontic	Multiplate cloud chamber	550	0

From the range and estimated ionization of these particles none of them could have been heavier than π-mesons. If they were π-mesons with the observed range, five of them should on the average have been recognizable by ionization greater than twice the minimum. The energy of these particles considered, as π- or μ-mesons, could not have been greater than 50–70 MeV and it seems unlikely that production would be confined to π-mesons of this energy range. The expected multiple scattering of mesons of this energy does not agree with that found in the experiment (fig. 2). It is therefore probable that all the particles were electrons.

Pairs of particles have formerly been considered to be associated if they were reasonably coplanar, contemporary, and appearing to come from a point in an absorber lying inside or outside the chamber. In the present experiment direct observation inside the chamber was used to estimate the number of cases in which chance coincidences could simulate A.P.P.'s coming from a point outside the chamber. This was done by selecting tracks of penetrating particles that appeared contemporary and crossed within 10 mm in a volume in the chamber corresponding in shape and size to 10 cm absorber above the chamber. This criterion wa made to correspond as closely as possible to that used previously in selecting A.P.P.'s. Nine cases satisfying it were found.

Fig. 2

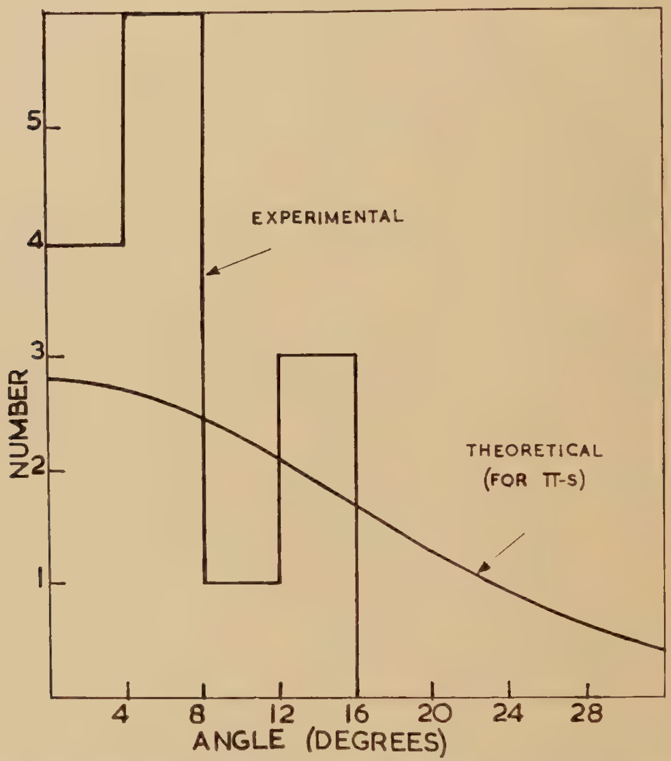

Distribution of scattering of secondary particles compared with multiple scattering calculated for mesons of mass 276.

The ' spurious pairs ' obtained in this way, and the ' electrons penetrating one lead plate ' were subjected to an analysis similar to that used by Braddick, Nash and Wolfendale (1951). They plotted the multiple scattering distribution of the more and less scattered members of their A.P.P. pairs and found that the two curves differed from those obtained from ' artificial pairs ' composed of single particles varied at random. This was used in support of the existence of A.P.P.'s. In the present experiment, the scattering distribution of the pairs of tracks considered as chance coincidences simulating A.P.P.'s did not differ from that of ' artificial pairs ', but when the electrons simulating A.P.P.'s were included, the distributions were altered to agree with those obtained by B.N.W. for A.P.P.'s.

If the results of the early work were in fact affected by the spurious events described above, then the cross section calculated by taking all these events as ‘ genuine cases ’ should be comparable to that obtained in those early experiments. If we therefore take the penetrating electrons and the chance coincidences together, the cross section so obtained is $4{\cdot}5\times10^{-29}$ cm^2/nucleon. Taking the chance coincidences only, this figure falls to $1{\cdot}9\times10^{-29}$ cm^2/nucleon. Both of these cross sections are fairly near the values obtained by Braddick and Hensby (1939), Braddick *et al.* (1951) and George and Trent (1951) and some others, and it seems that the results of the above authors can indeed be accounted for in terms of the spurious events described. If these are to be avoided, only those single penetrating secondaries that are formed inside the visible volume of the chamber and traverse at least two lead plates about 2 cm thick can be considered genuine.

According to the data of the present experiment the upper limit of the cross section for the production of single penetrating secondaries is about 2×10^{-30} cm^2/nucleon. Since the cross section for the production of energetic stars by μ-mesons is slightly higher than this, it is reasonable to assume that the production of single penetrating secondaries is analogous to this interaction.

Three cases of nuclear interactions initiated by ionizing primaries were found. In these interactions several secondaries were produced by an energetic primary, presumably a μ-meson. Some of these secondaries were heavily ionizing while others were minimum ionizing and penetrated several lead plates. Two of these events (fig. 3, Plate 36) occurred in the lead absorber above the chamber, while the other one occurred in the chamber. These interactions are considered to be analogous to energetic stars obtained in photographic emulsions underground by George and Evans (1950–51). The cross section found by us is also consistent with that obtained by these authors, being $3{\cdot}2\pm1{\cdot}8\times10^{-30}$ cm^2/nucleon. In calculating the cross section no geometrical corrections were applied, since it was considered unlikely that any event of this kind had escaped detection.

In order to investigate the possible interactions of neutral primaries inside the chamber, giving rise to ionizing secondaries, the counter telescope was placed under the chamber and about 2,000 photographs taken with this arrangement. No definite cases of interactions involving neutral primaries were observed.

§ 4. CONCLUSIONS AND DISCUSSION

Contrary to the results obtained by workers who used small cloud chambers equipped with only one or two plates, the data obtained in the course of the present investigation indicate that there is no justification for considering the formation of single penetrating secondaries by μ-mesons to be of a different mechanism from that responsible for production of energetic nuclear disintegration stars produced by these particles.

While this work was in progress, results of similar experiments were reported by Lovati *et al.* (1953) and Deutschmann (1953). The former worked at a depth equivalent to 55 m of water. Using a simple counter telescope as well as a split tray arrangement, they obtained several examples of nuclear interactions initiated presumably by μ-mesons. The latter obtained no events in which single penetrating secondaries were produced from 422 m of lead traversed by μ-mesons. Similar results were obtained by Walker (1953) who used a cloud chamber in a magnetic field.

From the arguments exposed above it is apparent that the results obtained lately with multiplate chambers and based on events occurring inside them are more reliable. Although they show that single penetrating secondaries may occasionally be formed by μ-mesons, this reaction is essentially the same as those in which more energetic nuclear events are initiated by μ-mesons and the adoption of a separate term for it seems therefore unjustified.

ACKNOWLEDGMENTS

The authors are grateful to Professor P. M. S. Blackett for his interest in the experiment. We wish to thank Mr. I. B. McDiarmid for his cooperation in the performing of the experiment and for many useful discussions. We also thank the Stockport Corporation for the permission to use the underground tunnel. One of us (B.L.) is indebted to the Institute of Physics, University of Zagreb for the provision of a maintenance grant.

REFERENCES

APPAPILLAI, V., MAILVAGANAM, A. W., and WOLFENDALE, A. W., *Phil. Mag.*, to be published.

BRADDICK, H. J. J., and HENSBY, G., 1939, *Nature, Lond.*, **144,** 1012.

BRADDICK, H. J. J., NASH, W. F., and WOLFENDALE, A. W., 1951, *Phil. Mag.*, **42,** 1277.

DEUTSCHMANN, M., 1953, *Z. Naturfor.*, **8a,** 308.

GEORGE, E. P., and EVANS, J., 1950, *Proc. Phys. Soc.* A, **63,** 1248 ; 1951, *Ibid.*, **64,** 193.

GEORGE, E. P., REDDING, J. L., and TRENT, P. T., 1953, *Proc. Phys. Soc.* A, **66,**, 533.

GEORGE, E. P., and TRENT, P. T., 1951, *Proc. Phys. Soc.* A, **64,** 1134.

GEORGE, E. P., 1952, *Progress in Cosmic Ray Physics* (Amsterdam : North Holland Publishing Co.).

LOVATI, A., MURA, A., SUCCI, C., and TAGLIAFERRI, G., 1953, *Nuovo Cimento*, **10,** 1201.

WALKER, W. D., 1953, *Phys. Rev.*, **90,** 234.

CXLV. *The Quasi-Cylindrical Shock Tube*

By W. Chester
Department of Mathematics, University of Bristol*

[Received July 16, 1954]

Summary

The disturbance produced behind a shock wave of arbitrary strength, travelling along a tube of varying cross section, is investigated. The shape of the cross section is arbitrary and the problem is linearized on the basis of small variations in area along the length of the tube.

It is found that if the initial cross sectional area is S, and there is a net change in area of amount $[\Delta S]$, then the consequent change in pressure behind the shock is

$$-K(p_1-p_0)[\Delta S]/S,$$

where (p_1-p_0) is the initial pressure discontinuity across the shock. The parameter K decreases monotonically with the shock strength and $0{\cdot}5 \geqslant K > 0{\cdot}394$.

More generally it is shown that the pressure is affected by two distinct perturbations superimposed on the initial flow, namely a permanent modification arising directly from the variations in cross section, and a transient disturbance reflected from the shock and propagated with sonic velocity relative to the main flow. Expressions for both these contributions are obtained.

§ 1. Introduction

In a recent paper (Chester 1953) the author investigated the flow behind a shock wave travelling along a two-dimensional channel of non-uniform width. In particular, when the variations in width took place within a finite length of the channel, the ultimate change in strength of the shock wave was calculated together with the form of the disturbance which is reflected back along the channel. A different approach is given here, and is applied to a tube whose cross section is quite arbitrary in shape, the perturbations on the flow behind the shock wave being produced by small variations in the cross sectional area. It is found that, ultimately, the disturbance depends only on the variations in the area of the tube and not on the actual shape of the cross section.

§ 2. Transition Relations across a Uniform Shock Wave

For future reference it is convenient to quote here the transition relations for a plane shock wave of uniform strength moving into a fluid at rest.

---

* Communicated by the Author.

Let the shock velocity be U_0 and let the fluid velocity, pressure, density and sonic velocity in the region of uniform flow behind the shock be q_1, p_1, ρ_1, a_1 respectively. The corresponding quantities ahead of the shock will be denoted by 0, p_0, ρ_0, a_0. It is also convenient to introduce the symbol $U_1=(U_0-q_1)$ for the velocity of the shock relative to the flow behind it.

If γ is the adiabatic index and $M_0=U_0/a_0$ is the Mach number of the shock, we then have the following relations (see, for example, Courant and Friedrichs 1948):

$$q_1=\frac{2U_0}{\gamma+1}\{1-M_0^{-2}\}, \quad . \quad . \quad . \quad . \quad . \quad . \quad . \quad . \quad (1)$$

$$U_1=U_0-q_1=\frac{U_0}{\gamma+1}\{\gamma-1+2M_0^{-2}\}, \quad . \quad . \quad . \quad . \quad (2)$$

$$p_1=\frac{2}{\gamma+1}\rho_0\left\{U_0^2-\frac{\gamma-1}{2\gamma}a_0^2\right\}=\frac{p_0}{\gamma+1}\{2\gamma M_0^2-\gamma+1\}, \quad . \quad . \quad (3)$$

$$M_1=\frac{U_1}{a_1}=\left[\frac{\gamma-1+2M_0^{-2}}{2\gamma-(\gamma-1)M_0^{-2}}\right]^{1/2}, \quad . \quad . \quad . \quad . \quad . \quad . \quad (4)$$

$$m=\frac{q_1}{a_1}=\frac{2}{\gamma+1}\frac{1-M_1^2}{M_1}. \quad . \quad . \quad . \quad . \quad . \quad . \quad . \quad . \quad . \quad . \quad (5)$$

§ 3. THE BOUNDARY CONDITIONS AT A NON-UNIFORM SHOCK

We next consider the effect of a small perturbation superimposed on the flow behind the otherwise uniform shock wave.

Let (x', r, θ) be cylindrical polar co-ordinates relative to a fixed origin with the x'-axis in the direction of propagation of the shock. Relative to these axes, let the fluid velocity and pressure behind the shock be respectively $\mathbf{V}_1=(q_1+u, v, w)$ and (p_1+p), and let the normal velocity of the shock be $\mathbf{V}_0$. Then the transition relations are

$$\mathbf{V}_1=\frac{2\mathbf{V}_0}{\gamma+1}\left\{1-\frac{a_0^2}{V_0^2}\right\}, \qquad p_1+p=\frac{2\rho_0}{\gamma+1}\left\{V_0^2-\frac{\gamma-1}{2\gamma}a_0^2\right\}, \quad (6)$$

and the equation of the shock may be written

$$x'-U_0t-f(r, \theta, t)=0, \quad . \quad . \quad . \quad . \quad . \quad . \quad . \quad . \quad (7)$$

where f is assumed to be uniformly small.

Correct to the first order of small quantities, $V_0=(U_0+f_t)$ and the unit normal at a point (r, θ) of the shock is $(1, -f_r, -f_{\theta/r})$. It follows that

$$\mathbf{V}_0=(U_0+f_t, -U_0f_r, -U_0f_{\theta/r}). \quad . \quad . \quad . \quad . \quad . \quad (8)$$

Substitution of relation (8) in (6) yields the following conditions to be satisfied at the shock front:

$$\left.\begin{aligned} u=\frac{2}{\gamma+1}(1+M_0^{-2})f_t, \qquad v=-q_1f_r, \qquad w=-q_1f_\theta/r, \\ p=\frac{4\rho_0U_0}{\gamma+1}f_t=\frac{4\rho_1U_1}{\gamma+1}f_t. \end{aligned}\right\} \quad . \quad (9)$$

Relations equivalent to these were first obtained by Ting and Ludloff (1952) and applied to a problem involving the diffraction of shock waves.

§ 4. THE EQUATIONS OF MOTION IN THE PERTURBED FLOW

It is more convenient to derive the equations of motion relative to axes which move with the mean flow behind the shock wave. The co-ordinates relative to these axes will be denoted by (x, r, θ). The velocity vector is now simply $(u, v, w)=\mathbf{V}$ (say) and the equations of conservation of mass, momentum and entropy, when linearized on the basis of small perturbations, are respectively

$$\frac{\partial\rho}{\partial t}+\rho_1\nabla\cdot\mathbf{V}=0, \qquad (10)$$

$$\frac{\partial\mathbf{V}}{\partial t}+\frac{1}{\rho_1}\nabla p=0, \qquad (11)$$

$$\frac{\partial S}{\partial t}=0. \qquad (12)$$

Here and elsewhere dependent variables without a suffix refer to the perturbed flow superimposed on the uniform flow denoted by suffix 1.

Equation (10) with the aid of eqn. (12) may be written

$$\frac{1}{a_1^2}\frac{\partial p}{\partial t}+\rho_1\nabla\cdot\mathbf{V}=0, \qquad (13)$$

where $a_1^2=(\partial p/\partial\rho)_S$ is the square of the velocity of sound in the uniform flow.

Between eqns. (11) and (13) the velocity $\mathbf{V}$ may be eliminated to yield the following equation for the pressure:

$$\nabla^2 p=\frac{1}{a_1^2}\frac{\partial^2 p}{\partial t^2}. \qquad (14)$$

Equation (14) implies that the propagation of small variations in pressure is still governed by the wave equation, notwithstanding the fact that there are entropy variations (and hence vorticity) present in the flow. It is not, however, true of the velocity components, as it would be in a genuine acoustical problem. This important fact was first realized and exploited by Lighthill (1949).

§ 5. APPLICATION TO FLOW IN A SHOCK TUBE

We now consider the application of the preceding results to the particular problem of flow in a quasi-cylinder. The boundary of the quasi-cylinder is defined by the equation

$$r=R(x', \theta)=R(x+q_1t, \theta), \qquad (15)$$

where R is arbitrary except for the restriction that R_x should be small.

Since the unit normal at the boundary has components

$$\{-R_x, -R_\theta/R, 1\}R/(R^2+R_\theta^2)^{\frac{1}{2}},$$

it follows that the condition to be satisfied there is

$$V_n = q_1 \frac{RR_x}{(R^2+R^{\;2})^{\frac{1}{2}}}, \quad \ldots \ldots \quad (16)$$

where V_n is the normal velocity. Since, by eqn. (11)

$$\frac{\partial V_n}{\partial t} = -\frac{1}{\rho_1}\frac{\partial p}{\partial n}, \quad \ldots \ldots \quad (17)$$

the corresponding condition for the pressure is that, at $r=R$,

$$\frac{\partial p}{\partial n} = -\frac{\rho_1 q_1^2}{(R^2+R_\theta^2)^{\frac{1}{2}}}\frac{\partial^2}{\partial x^2}(\tfrac{1}{2}R^2), \quad \ldots \ldots \quad (18)$$

correct to the first order.

Now ultimately we may expect the pressure to become uniform over the cross section of the tube, and restriction of the investigation to the average pressure leads to a significant simplification in the analysis. We make use of this simplification in the following way. The two-dimensional form of the divergence theorem is applied to ∇p over the cross section to get

$$\int \frac{\partial p}{\partial n}\, ds = \iint \left(\frac{\partial^2 p}{\partial r^2} + \frac{1}{r}\frac{\partial p}{\partial r} + \frac{1}{r^2}\frac{\partial^2 p}{\partial \theta^2}\right) dS. \quad \ldots \quad (19)$$

Since, on a linear theory, it is permissible to apply the boundary condition (18) in the plane of the cross section, the left-hand side of eqn. (19) may be written

$$-\rho_1 q_1^2 \int \frac{\partial^2}{\partial x^2}(\tfrac{1}{2}R^2)\, d\theta = -\rho_1 q_1^2 \Delta S''(x+q_1 t), \quad \ldots \quad (20)$$

where ΔS has been written for the variation in cross section relative to some reference cross section.*

Furthermore, since p satisfies the wave equation,

$$\iint \left(\frac{\partial^2 p}{\partial r^2} + \frac{1}{r}\frac{\partial p}{\partial r} + \frac{1}{r^2}\frac{\partial^2 p}{\partial \theta^2}\right) dS = \iint \left(\frac{1}{a_1^2}\frac{\partial^2 p}{\partial t^2} - \frac{\partial^2 p}{\partial x^2}\right) dS. \quad (21)$$

Hence, if

$$P = \iint p\, dS,$$

where the integral is taken over the cross section, it follows that

$$\frac{\partial^2 P}{\partial x^2} - \frac{1}{a_1^2}\frac{\partial^2 P}{\partial t^2} = \rho_1 q_1^2 \Delta S''(x+q_1 t). \quad \ldots \quad (22)$$

The solution may be written in the form

$$P = A\rho_1 q_1^2 [F(x+a_1 t) + \Delta S(x+q_1 t)], \quad \ldots \quad (23)$$

---

* The entropy, for which the symbol S was also used, does not appear in the subsequent analysis.

where

$$A=\frac{a_1^2}{a_1^2-q_1^2}=\frac{1}{1-m^2}, \quad . \quad . \quad . \quad . \quad . \quad . \quad . \quad (24)$$

and F is some function to be determined. The contribution to P from the term involving ΔS is the variation in pressure due directly to the change in cross section. This disturbance is reflected at the shock and gives rise to the term involving $F(x+a_1t)$. No contribution of the form $G(x-a_1t)$ is included since there is no mechanism for reflection upstream of the shock which could give rise to such a term.

To obtain F we require the boundary condition to be satisfied at the shock wave, where eqns. (9) must be satisfied and from which a condition can be derived to be satisfied by P.

We note first that, as a consequence of (9),

$$\frac{\partial p}{\partial n}=-\frac{4\rho_1U_1}{q_1(\gamma+1)}\frac{dV_n}{dt}, \quad . \quad . \quad . \quad . \quad . \quad . \quad . \quad (25)$$

at $x=U_1t$ and $r=R$.

With the help of eqn. (16), this gives

$$\frac{\partial p}{\partial n}=-\frac{4\rho_1U_1}{(\gamma+1)\ (R^2+R_\theta^2)^{\frac{1}{2}}}\frac{d}{dt}(RR_x), \quad . \quad . \quad . \quad (26)$$

when $x=U_1t$.

If now we apply eqn. (19) *in the plane of the shock*, the left hand side will be

$$-\frac{4\rho_1U_1U_0}{\gamma+1}\Delta S''(U_0t), \quad . \quad . \quad . \quad . \quad . \quad . \quad . \quad . \quad (27)$$

where (U_1+q_1) has been replaced by U_0. To evaluate the integrand on the right of (19) we have, from (9) and (13),

$$\frac{1}{r}\frac{\partial}{\partial r}\{rq_1f_r\}+\frac{1}{r^2}\frac{\partial}{\partial\theta}\{q_1f_\theta\}=\left\{u_x+\frac{1}{\rho_1a_1^2}p_t\right\}, \quad . \quad . \quad . \quad (28)$$

at $x=U_1t$. Hence, by differentiation,

$$\frac{1}{r}\frac{\partial}{\partial r}\left\{\frac{rq_1(\gamma+1)}{4\rho_1U_1}p_r\right\}+\frac{1}{r^2}\frac{q_1(\gamma+1)}{4\rho_1U_1}\Big\}p_{0\theta}=\frac{d}{dt}\left\{u_x+\frac{1}{\rho_1a_1^2}p_t\right\}. \quad (29)$$

But, by (9) and (11),

$$\begin{aligned}\frac{du}{dt}=u_t+U_1u_x=-\frac{1}{\rho_1}p_x+U_1u_x=\frac{(1+M_0^{-2})}{2\rho_1U_1}\frac{dp}{dt}\\ =\frac{(1+M_0^{-2})}{2\rho_1U_1}(p_t+U_1p_x). \quad . \quad . \quad . \quad . \quad . \quad . \quad . \quad . \quad (30)\end{aligned}$$

Hence

$$u_x=\frac{(1+M_0^{-2})}{2\rho_1U_1^2}\{p_t+U_1p_x\}+\frac{1}{\rho_1U_1}p_x, \quad . \quad . \quad . \quad . \quad (31)$$

and (29) becomes

$$\begin{aligned}\frac{1}{r}\frac{\partial}{\partial r}(rp_r)+\frac{1}{r^2}p_{\theta\theta}=\frac{4}{(\gamma+1)q_1U_1}\left\{\frac{\partial}{\partial t}+U_1\frac{\partial}{\partial x}\right\}\\ \times\left\{\frac{(1+M_0^{-2}}{2}(p_t+U_1p_x)+M_1^2\left(p_t+\frac{a_1^2}{U_1}p_x\right)\right\}, \quad (32)\end{aligned}$$

at $x=U_1t$.

This relation may now be used as the integrand on the right of (19). When combined with (27) the following boundary condition is obtained, to be satisfied at $x=U_1t$:

$$\left\{\frac{\partial}{\partial t}+U_1\frac{\partial}{\partial x}\right\}\left\{\frac{1+M_0^{-2}}{2}(P_t+U_1P_x)+M_1^2\left(P_t+\frac{a_1^2}{U_1}P_x\right)\right\}$$
$$=-\frac{U_0U_1^2}{q_1}\rho_1q_1^2\Delta S''(U_0t). \quad . \quad . \quad . \quad . \quad . \quad (33)$$

The function $F(x+a_1t)$ is now found from the fact that the relation (23) for P should satisfy (33). It follows at once that F is of the form

$$-B\Delta S\{\tau(x+a_1t)\},$$

where

$$\tau=\frac{U_0}{U_1+a_1}=\frac{M_1+m}{M_1+1}, \quad . \quad . \quad . \quad . \quad . \quad . \quad . \quad (34)$$

so that

$$P=A\rho_1q_1^2[-B\Delta S\{\tau(x+a_1t)\}+\Delta S(x+q_1t)], \quad . \quad . \quad . \quad (35)$$
$$=-A\rho_1q_1^2[B\Delta S\{\tau(x'+(a_1-q_1)t)\}\tau-\Delta S(x')]. \quad . \quad . \quad (36)$$

Substitution of (35) in (33) now gives

$$B=\frac{1+M_0^{-2}+2M_1m^{-1}}{1+M_0^{-2}+2M_1} \quad . \quad . \quad . \quad . \quad . \quad . \quad . \quad . \quad . \quad (37)$$

Equation (36) illustrates clearly the two distinct perturbations superimposed on the initial flow, namely a permanent modification from the term $A\rho_1q_1^2\Delta S(x')$ arising from the variations in cross section, and a transient disturbance, $-AB\rho_1q_1^2\Delta S\{\tau(x'+(a_1-q_1)t)\}$. The latter is propagated with sonic velocity relative to the fluid and is due to reflection from the shock of the perturbations in the flow caused directly by the variations in cross section.

When the tube consists of two cylinders connected by a transition section, and the uniform flow denoted by suffix 1 refers to the upstream section, the ultimate pressure change behind the shock will be given by

$$\left.\begin{aligned}p_2-p_1&=-A[B-1]\rho_1q_1^2[\Delta S]/S\\&=-K(p_1-p_0)[\Delta S]/S\end{aligned}\right\} \quad . \quad . \quad . \quad . \quad (38)$$

(say), where S is the cross sectional area in the upstream section, $[\Delta S]$ is the net change in area and

$$K=\frac{2}{(1+m)(1+M_0^{-2}+2M_1)}, \quad . \quad . \quad . \quad . \quad (39)$$

use being made of the relation

$$p_1-p_0=\rho_1q_1U_1.$$

The parameters m, M_0 and M_1 are all functions of p_1/p_0 through eqns. (3), (4) and (5), and the variation of K with this parameter is shown in fig. 1. It is a monotonic decreasing function with upper and lower limits respectively 0·5 and 0·394.... It is interesting that the pressure increment has the same sign for both subsonic and supersonic flow behind the shock ($m \gtrless 1$) even though the contribution arising directly from the variations in cross section is of different sign for the two regimes (for there is a change of sign in the parameter A). This implies that to increase the Mach number behind the shock, even in supersonic flow, requires a contraction, as opposed to the expansion necessary in steady supersonic flow in a duct.

Fig. 1

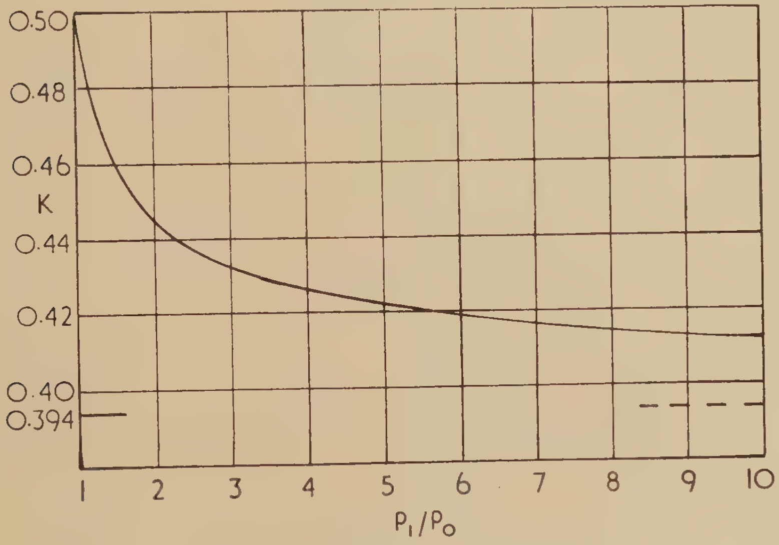

Variation of K with p_1/p_0. ($\gamma=1{\cdot}4$)

For subsonic flow behind the shock a disturbance will be reflected into the upstream section of the tube, and the pressure variation in the pulse will ultimately be given by

$$p_2-p_1=-AB\rho_1 q_1^2 \Delta S\{\tau(x'+(a_1-q_1)t)\}/S$$
$$=-N(p_1-p_0)\Delta S\{\tau(x'+(a_1-q_1)t)\}/S \quad . \quad . \quad (40)$$

(say), where

$$N=-\frac{ABm}{M_1}=-\frac{m(1+M_0^{-2})+2M_1}{M_1(1-m^2)(1+M_0^{-2}+2M_1)} . \quad . \quad . \quad (41)$$

But, when the flow behind the shock is supersonic, this pulse will be convected into the downstream section of the tube and the whole of eqn. (36) is required to obtain the average pressure increment, since $\Delta S(x')$ is non-zero in the downstream section. Furthermore the assumption that the pressure will ultimately be uniform over a cross section is no longer true in the supersonic case (except in so far as neglected effects, such as the action of viscosity, will tend to produce such a state), for the full solution contains a fluctuating contribution which does not die out even at distances remote from the origin of the disturbance. However, the average pressure is a reasonable guide to an understanding of the state of the fluid and, in any case, the fluctuations do not penetrate downstream as far as the shock, so that this criticism applies only to the rearward pulse (for further details see Chester 1953).

The values of τ and N for various shock strengths are shown in figs. 2 and 3 respectively. The parameter τ is monotonic decreasing and takes the values 2, 1 and 0·6076... respectively when the incident shock has zero strength, when the flow behind the shock is sonic and when the shock strength becomes infinite.

Fig. 2

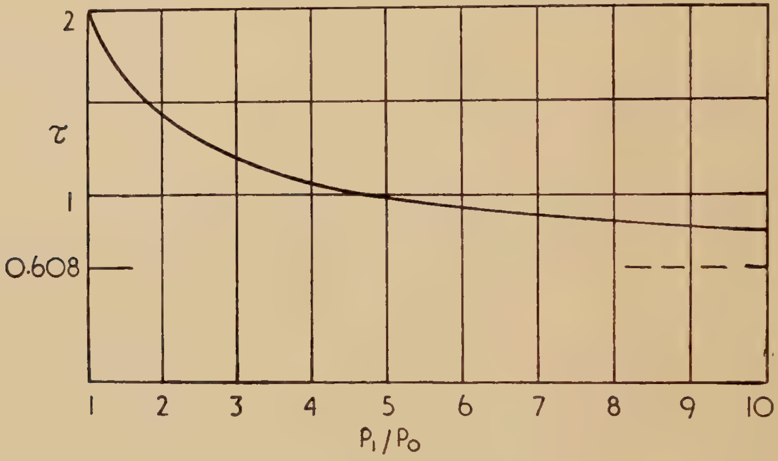

Variation of τ with p_1/p_0. $(\gamma=1{\cdot}4)$

For subsonic flow behind the shock N increases rapidly from a value of 0·5 for a shock of zero strength, and becomes singular when the flow behind the shock is sonic. For supersonic flow N becomes negative (and singular at $m=1$) and increases monotonically to an asymptotic value of $-0{\cdot}1550....$

The singularity in N at $m=1$ (which arises from the singularity in A) does not imply a similar behaviour in the solution for the pressure. For, by (37), $B=1$ when $m=1$ and hence, in eqn. (36), the term in square brackets is zero. More precisely, if $m=1+\delta$, then $A=0(\delta^{-1})$ and the term in square brackets is $0(\delta)$, at least for moderate values of the time. But the tendency for A to become large for transonic flow can have an appreciable effect on the pressure when t is so large that

$$\Delta S\{\tau(x'+(a_1-q_1)t)\}$$

differs appreciably from $\Delta S(x')$. For subsonic flow $(q_1<a_1)$ this can only

occur in and upstream of the transition section, for (36) is equivalent to (38) in the downstream section. On the other hand, if $q_1 > a_1$, these large disturbances are excluded from the upstream section. This tendency of the disturbances to accumulate will undoubtedly give rise to non-linear phenomena such as shock waves and in practice becomes manifest as the familiar process of 'choking'. These remarks, of course, apply only to the rearward pulse and not to the region immediately behind the main shock wave where eqn. (38) is always valid.

Fig. 3

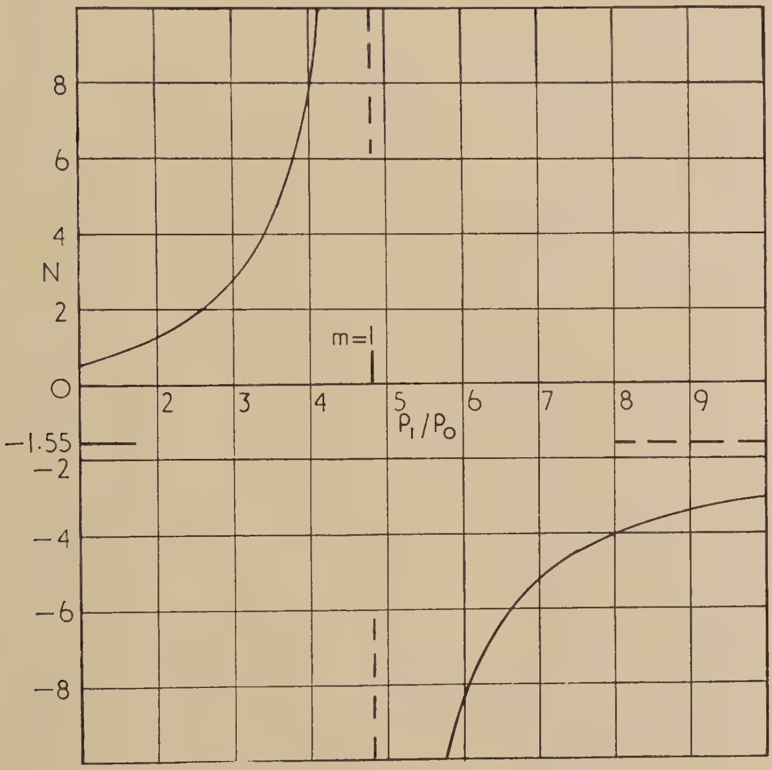

Variation of $\bar{N}$ with p_1/p_0. (γ=1·4)

REFERENCES

CHESTER, W., 1953, *Q.J.M.A.M.*, **6**, 440.

COURANT, R., and FRIEDRICHS, K. O., 1948, *Supersonic Flow and Shock Waves* (Interscience Publishers).

LIGHTHILL, M. J., 1949, *Proc. Roy. Soc.* A, **198**, 455.

TING, L., and LUDLOFF, H. F., 1952, *J. Aero. Sci.*, **19**, 317.

CXLVI. *Multiple Beam Investigation of Liquid Helium in Narrow Gaps*

By N. G. McCrum*
Clarendon Laboratory, Oxford†

[Received July 1, 1954]

Abstract

A multiple beam interferometer used for detecting liquid helium in thin gaps is described. Experiments performed with this apparatus have led to the conclusion that helium II will enter a narrow gap maintained above the liquid surface, providing the gap is bridged at a point below the surface tension height. A plausible mechanism is proposed and the bearing of the conclusions on experiments with liquid helium II discussed.

§ 1. Introduction

Experiments have recently been reported by Lane and Dyba (1953) concerning the rising of liquid helium II into narrow gaps by an extraordinary capillary action. Two parallel plates held in close juxtaposition separated by spacers were maintained above the liquid surface and in contact with it by means of the helium II film. These authors observed liquid to fill the gap between the plates up to the surface tension equilibrium height, and found further evidence to support the hypothesis that the film was the agent transmitting hydrostatic pressure. This is reasonable, yet the mechanism by which liquid transported through the film is first established in an empty gap is very difficult to understand.

Perhaps the simplest interpretation would be to assume that the appearance of liquid was in some way connected with the spacers which directly bridged the gap. However, experiments performed some time ago in this laboratory (Hatton and Rollin, unpublished‡) seemed to indicate that the phenomenon occurred even when the gap was not directly bridged by spacers. The experiments described in this paper using an optical method especially adapted to conditions in liquid helium, were therefore made in an effort to clarify the situation.

§ 2. Method

Liquid helium has a very low refractive index and a small absorption coefficient in the optical region. This means that observation of the meniscus between liquid and vapour in small apertures is particularly

---

* Now at the State University of Pennsylvania.

† Communicated by K. Mendelssohn, F.R.S.

‡ I am grateful to Dr. Rollin and to Dr. Hatton for a description of their experiment.

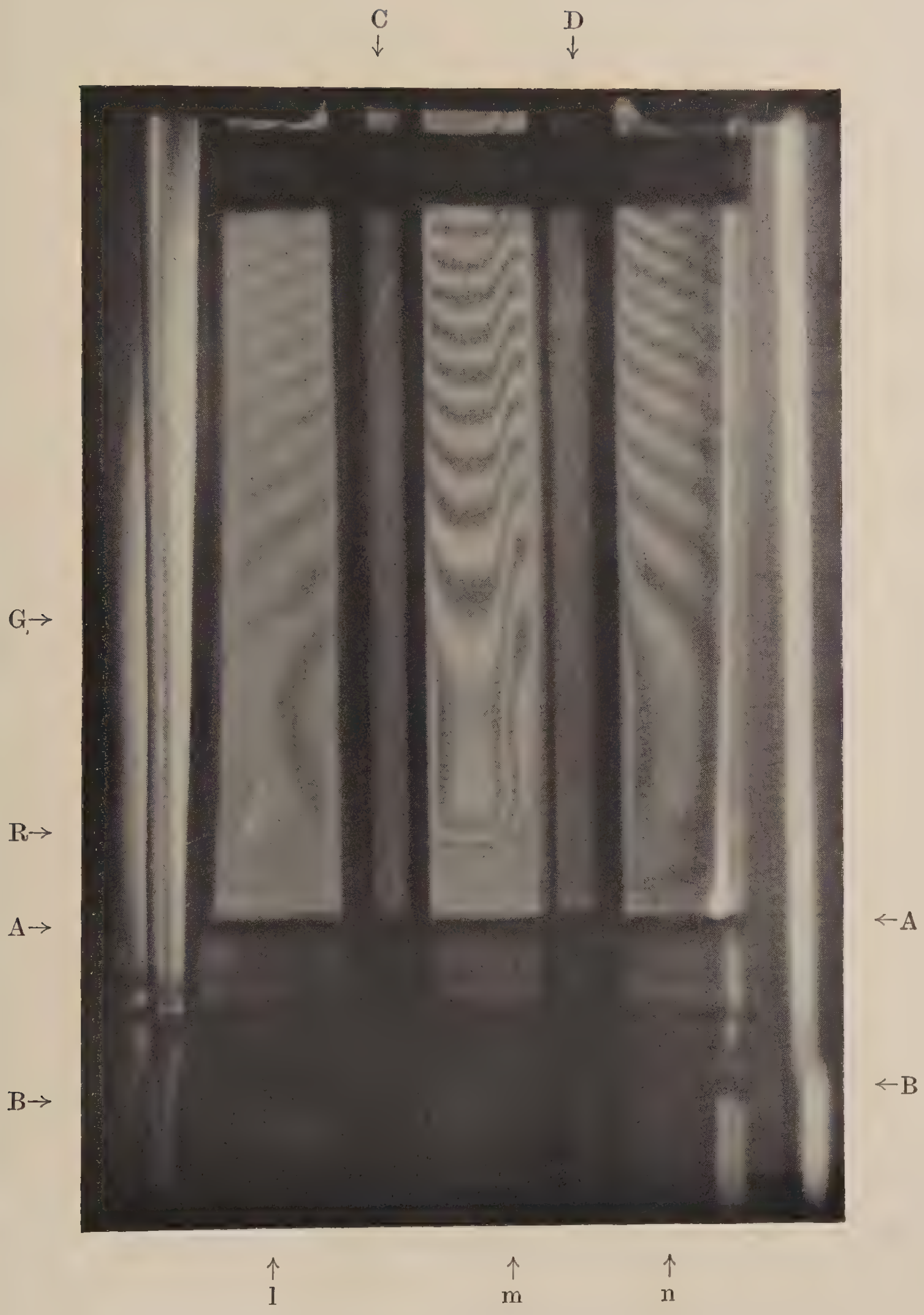

The interferometer illuminated with green mercury light. The letters refer to the parts indicated in fig. 1. The gap l has been filled through the film ; the meniscus is at G. The other two gaps m and n are empty. The wire bridging the gap is indicated by R. The transmission in this region has been increased by the removal of several small flakes of silver from the glass owing to the wire moving as the interferometer was assembled. The small variations of the gap width indicated by the fringes were caused by the rubbing down of the edges with jewellers' rouge.

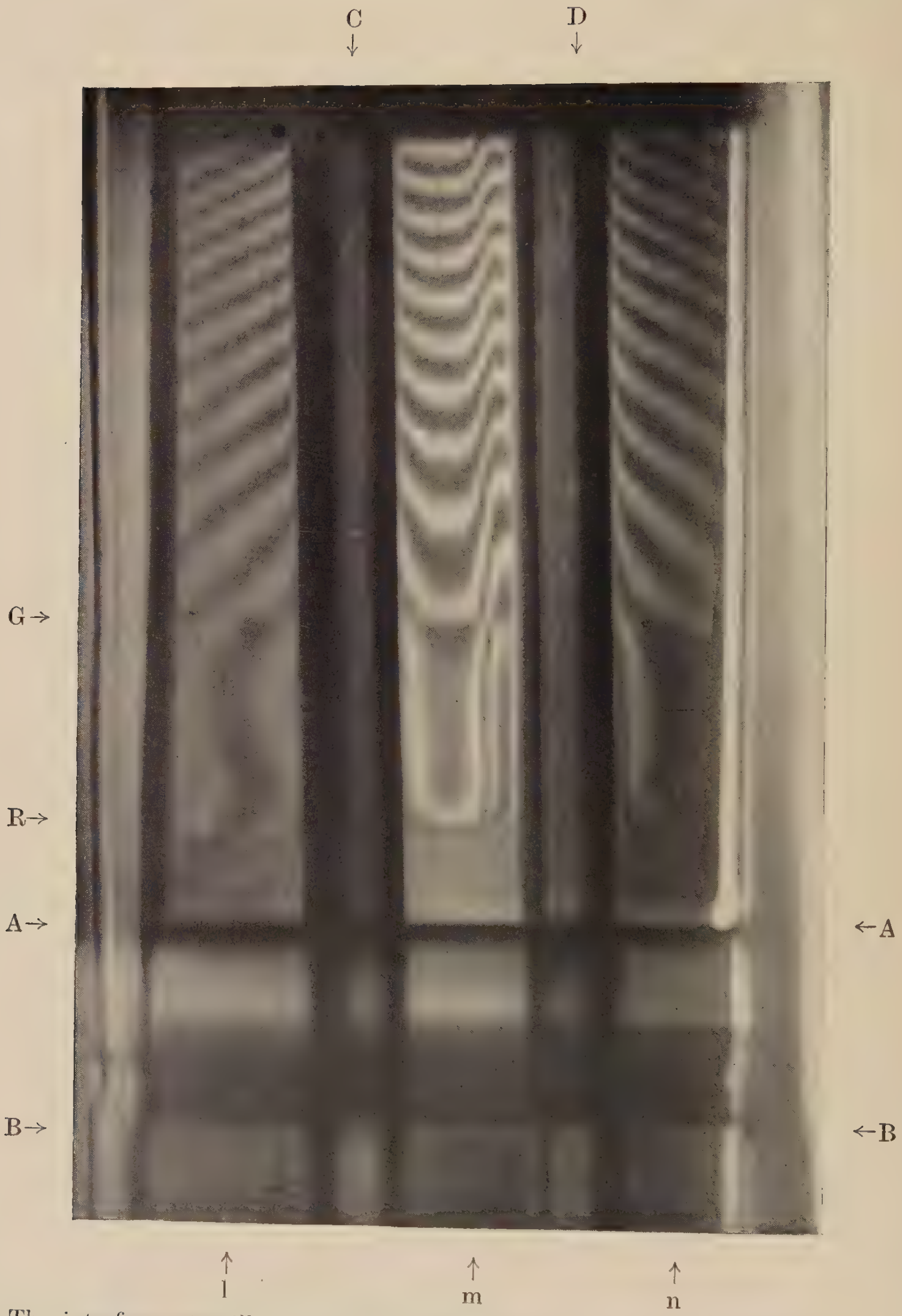

The interferometer illuminated with green mercury light. All three gaps l, m and n are filled with helium, the menisci being at G. To fill the gaps m and n it was necessary to lower the interferometer until the edge AA touched the surface of the bath liquid.

difficult. As it was expected that minute transient volumes of helium were to be detected, an interferometric method was devised capable of doing this.

Fig. 1

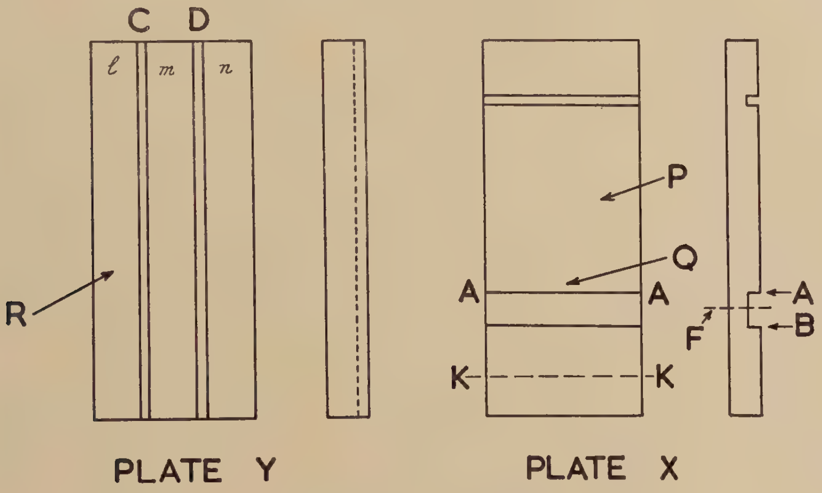

The interferometer plates.

Fig. 2

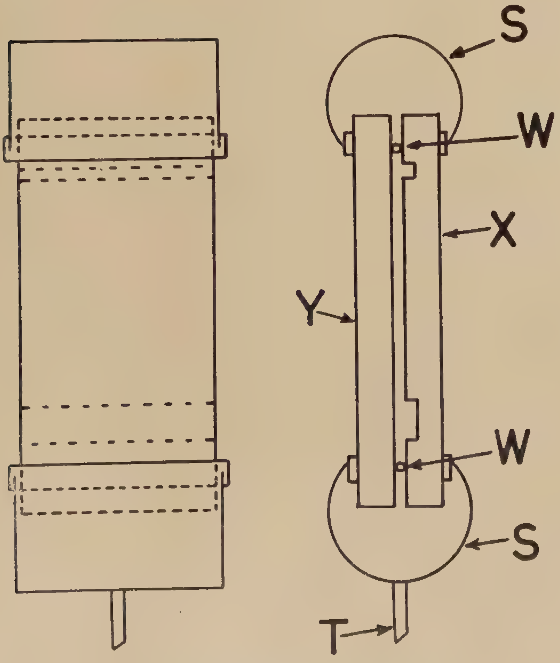

The interferometer assembly.

The apparatus consisted of two optically polished glass plates X and Y, held together with springs S and separated by wire spacers W, as shown in figs. 1 and 2. In order to eliminate edge effects, horizontal grooves were cut into X so as to separate the area under observation from the spacers and to prevent liquid reaching the gap by ordinary capillary action. The edges of the grooves after the initial rough cutting were rubbed down with jewellers' rouge to remove small chip marks and abrasive scratches. The lower spring bore a brass strut T as shown in fig. 2 which supported the apparatus vertically in the cryostat. The strut was bolted to a cylindrical wire cage which could be moved up and down inside the cryostat through the liquid helium, by means of a waxed hemp line and a windlass operated by turning a glass cone in a ground joint. Thus, the mechanical support for the glass plates passed through the helium bath. This method of support ensured that the heat leak into the glass plates was extremely small, thereby simplifying the interpretation of the results.

By depositing a thin film of silver on each of the plates, the assembly was turned into a multiple beam interferometer. With silvering of the order of 90% reflection and with the springing carefully adjusted three or four well resolved interference fringes per cm were observed. Very small droplets of helium were usually detected with unfiltered mercury light, changes of optical path then producing very clearly defined variations of tint. When using monochromatic light, liquid was distinguished from vapour by means of a break in the interference fringes. The green mercury line or the sodium doublet was used depending on which wavelength gave the better fringe separation. The actual fringe separation was visually estimated and the interferometer spacing calculated, a rough knowledge of the spacer width resolving the ambiguity in the order of interference. Defects in the surface, plate distortion caused by the springs or thermal contraction and small foreign particles were all easily observed.

An optical bench consisting of a monochromatic source, a collimating lens, several layers of Chances 'ON 20' glass and, when necessary, suitable Wratten filters, was mounted on one side of the cryostat so as to introduce light normally on to one of the faces of the interferometer. General features of the formation of liquid between the plates were conveniently observed with the naked eye held close to the opposite side of the apparatus, but small detail was detected by means of a low-powered microscope with ×8 magnification.

§ 3. EXPERIMENTS

The first experiments were made with an interferometer formed from plates similar to X and Y (fig. 1). The horizontal groove AB in X, was in this case 1·3 mm deep and 3·5 mm high, having a roughly triangular cross section. The other plate was identical to Y except that it did not contain the vertical grooves C and D. It was then found that the empty interferometer could be filled with helium II but not with helium I, when the liquid surface was below the edge AA. The filling was done either by varying the height of the interferometer isothermally or by lowering the temperature to below the λ-point with the edge AA above the surface yet below the equilibrium surface tension height appropriate to the gap width. The interferometer was emptied by raising it clear of the liquid. The maximum height of the edge AA above the free surface when on lowering the interferometer, the helium entered the empty gap, the entry height was less than the height of AA above the surface, the exit height, when on raising, the last liquid left the gap. In this experiment the heights were 0·65 cm and 1·6 cm and the gap 36 μ. The exit height was equal to the surface tension equilibrium height (Allen and Misener 1938) appropriate to the gap width.

The shape and proportions of the cross section of the triangular groove AB were not considered satisfactory and it was therefore cut with a rectangular cross section, being 5 mm high and 2 mm deep. The plates were then resilvered, assembled and placed in the cryostat. In the first experiment, on cooling to helium temperatures, the plate X cracked horizontally at F forming two independently sprung segments. The upper segment formed a small angled wedge with the plate Y. The fringes were horizontal and closely spaced and on counting it appeared that the gap varied from approximately 30 μ at the top to 50 μ at the edge AA. The exit height was approximately 1 cm and the entry height zero; the empty interferometer could now only be filled by lowering it until the surface touched the edge AA.

For the next experiment a new plate was cut similar to X. It was mounted with plate Y in the interferometer, the gap being throughout 30 μ wide. The entry height was approximately half the exit height which was 14 mm. The liquid on entering the slit appeared first as a very small droplet just above the edge AA. Its initial growth was slow but increased as the perimeter increased, as would be expected if helium were being transported to it through the film. The time taken from the first appearance of the initial droplet to the final equilibrium position was of the order of seconds, being shorter the lower the temperature.

The next experiment was conducted with the same assembly as the last one, but the gap reduced to 12 μ by using a finer tungsten wire spacer. A short length of this wire, U, was also placed horizontally across the gap as indicated in fig. 3. No precautions were taken to exclude dust particles and a careful examination of the surfaces revealed that the silvering, which was that of the previous experiment, had deteriorated. Small areas of silver were detached from the glass and lay as minute flakes between the two surfaces. In this experiment detailed observations were made of the formation of helium II in the gap.

On lowering the empty interferometer until the helium II surface was in the region of KK (fig. 1) the first sign of liquid was seen between the plates as shown in fig. 3 (A). This droplet then grew slowly out towards the edges. Subsequently a small drop appeared in the region L. The silvering appeared badly flaked in this region. This drop although of a circular section initially, grew into a pear shape and then moved down as indicated. The two volumes of helium then joined as shown in (3 C+D). At the same time small droplets were appearing higher up in the gap, growing and then moving down either to the rising meniscus or to the wire (3 E, F+G). The final equilibrium position is shown

Fig. 3

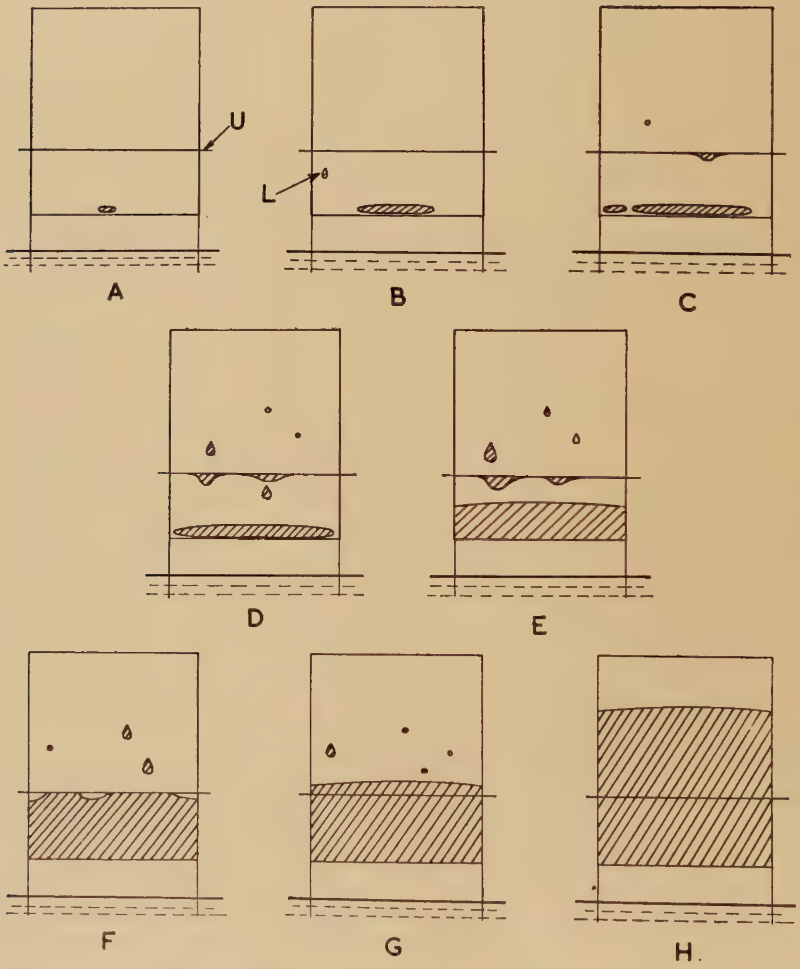

Successive stages in the establishment of liquid helium II in an empty gap which contains small quantities of bridging material. The time taken from the initial stage A, to the final stage H was of the order of seconds.

in fig. 3 (H). The distance from the meniscus at this position to the bath surface was now equal to the appropriate surface tension height. It was noted that droplets apparently grew where the silvering was badly flaked or at the wire and that no droplets ever occurred above the equilibrium height. The inference was that liquid would not enter an empty gap unless there was a nucleation centre below the appropriate surface tension height.

The next experiment was designed to test this hypothesis. Plates X and Y were assembled freshly silvered with a $30\,\mu$ spacing. A close inspection of the surface after liquefaction revealed a very small particle of dust at the point P (fig. 1). Isothermal variations of the height of the empty interferometer showed that after filling at the maximum entry height the meniscus in the gap, when finally in equilibrium, passed through the enclosed particle at P. If the empty interferometer was raised a small distance of the order of a millimetre above this entry height the empty gap could be filled by tapping the apparatus, thus causing the bath surface to oscillate. It would not fill at this height unless tapped and at greater heights would not fill under any circumstance. Further evidence was obtained by carefully stripping the interferometer so as not to injure the silvering and placing a small piece of wire about 2 millimetres long and of the same cross section as the spacer at the point Q (fig. 1). The plates were then replaced and the assembly placed in the liquefier. Great care was taken to prevent dust particles fouling the surfaces in order that the experimental conditions should be identical with those of the preceding experiment with the exception of the small piece of wire at Q. As was to be expected the maximum entry height was now larger than in the former experiments. The final equilibrium position of the meniscus in the interferometer when filled at this height coincided with the wire at Q.

For the concluding experiment a plate similar to Y as shown in fig. 1 was constructed. Two vertical grooves C and D, 2 mm wide and 2 mm deep were cut and the edges polished with jewellers' rouge. This plate was then assembled in the interferometer with plate X and separated by $30\,\mu$ wire spacers. This method of mounting provided three identical, independent gaps l, m and n. Gaps m and n were kept free of any bridging material but a small piece of wire was placed at R in slit l just above the edge AA. It was found that liquid helium II would not enter the empty gaps m and n unless the bath surface was brought into direct contact with the edge AA. Gap l on the other hand, could be filled through the film. If gap l was filled so that the entry height was a maximum, the meniscus of the liquid in the gap when finally in equilibrium coincided with the wire. Photographs of the appearance of the interferometer under these conditions illuminated with green mercury light are shown in Plates 37 and 38.

Since in these more detailed experiments a bridge at or below the surface tension height was found to have caused the appearance of liquid between the plates it must be assumed that the formation of the droplets in the first and third experiments was due to the presence of unobserved bridging material. The positions of these bridges were evidently at 1·6 cm and 1·4 cm above the bath surface when the empty interferometer was filled at the maximum entry height.

§ 4. DISCUSSION

Kelvin has discussed a hypothetical experiment bearing a marked resemblance to that just described (Thomson 1871). He considers a closed system containing two detached volumes of the same liquid, one with a large meniscus and the other in a small capillary, in communication with each other only through the vapour phase. The capillary contains insufficient liquid to raise the meniscus to the height that would be attained if it were in direct hydrostatic communication with the large volume of liquid. It is argued that given sufficient time and some thermal contact between the two volumes of liquid, equilibrium would finally be achieved by the condensation of vapour into the capillary. The experiments reported in the previous section indicate that if the liquid were helium below the λ-point, equilibrium would certainly be established quickly since the mass transfer would take place through the film acting as a hydrostatic link. The permanence of equilibrium between detached volumes of liquid implies the maintenance of equilibrium between the vapour and all the various liquid menisci.

In common with other liquids, a concave liquid helium surface is in equilibrium with a vapour at a pressure lower than the equilibrium pressure for a plane meniscus maintained at the same temperature. The relation between p, the equilibrium pressure over the curved surface of radius r, p_0 the equilibrium pressure for a flat surface, σ the surface tension and V the molar volume of the liquid at temperature T is given by the Kelvin equation,

$$\ln\frac{p}{p_0}=-\frac{2\sigma V}{rRT}. \qquad (1)$$

At a height H above the meniscus of the bulk liquid the pressure will be given

$$p=p_0\exp\left(-MgH/RT\right), \qquad (2)$$

where M is the molecular weight, assuming the vapour obeys the ideal gas laws. Let us assume that there are a set of small irregularities of varying radii on an object projecting through the surface of a liquid in a closed vessel. If the object is lowered into the bulk liquid the height of any one of these irregularities above the surface is decreased. Consequently the pressure p and therefore the potential for capillary condensation are increased (eqns. (1) and (2)). Shown in fig. 4 is a schematic diagram illustrating the proposed mechanism by which a drop of liquid helium II is first established in an empty gap between two parallel plates. Bridging material is enclosed in the gap at B. As the plates are lowered into the liquid helium the height of B above the surface S is varied from H_1 to H_2 to H_3. The corresponding liquid radii of curvature R_1 R_2 R_3 respectively are in equilibrium at these heights. Once the radius R_3 is established then liquid from the film bridges the whole gap, the drop falls to the lower part of the gap at C and then proceeds to expand. As this case corresponds to filling at the maximum entry height, the meniscus, when finally in equilibrium, will coincide with B and H_3 will be the surface tension height appropriate to the gap width. It must be presumed that similar equilibrium conditions are never attained above the λ-point owing to the immobility of the helium I film and the relative inefficiency of mass transport through the gas phase. For under the experimental conditions previously described, the gap, when filled with helium II, could be emptied by raising the temperature above

Fig. 4

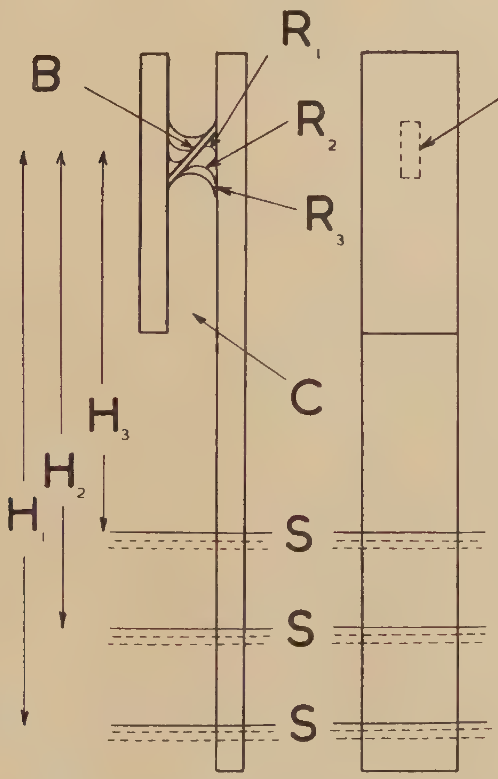

A schematic diagram illustrating the formation of liquid helium II in a gap containing bridging material, B.

the λ-point; the helium I would slowly evaporate away owing to the absorption of radiant energy. Presumably the isothermal conditions existing in the helium II region due to the mobile film are destroyed at the λ-point.

The van der Waals interaction of helium atoms with an ideally flat substrate has been estimated to permit a film of the order of 400 Å to exist above the liquid meniscus (Frenkel 1940, Schiff 1941). This liquid will be known as the film liquid. However, since it is very difficult to get a truly flat surface (Thomson 1953) it must be assumed that on any surface other than perhaps a cleavage plane, the total volume of adsorbed liquid will exceed the film liquid. This additional liquid will be known as the capillary liquid. The volume of capillary liquid will be a function of the microstate of the surface and will be temperature dependent. The experiments previously described indicate that the volume of capillary liquid will probably change discontinuously at the λ-point, owing to non-equilibrium conditions in the helium I range. Schiff (*loc. cit.*) suggests that the volume of film liquid will change discontinuously for similar reasons. These experiments emphasize the significance of the microstate of the surface of vessels used in film flow experiments (Chandrasekhar and Mendelssohn 1952). It is possible that the wide divergence in measurements of the He II film thickness (Kikoin and Lazarew 1938, Daunt and Mendelssohn 1939, Burge and Jackson 1950, Bowers 1953, McCrum and Mendelssohn 1954) may be, in part, due to the use of different substrate.

Most probably in the experiments of Hatton and Rollin small particles were trapped in the gap thus forming suitable nucleation centres for the formation of the initial droplet. The foil spacers used by Lane and Dyba (*loc. cit.*) would presumably also initiate the entry of liquid. Bowers (1953) has described difficulties encountered in using a loosely wound foil to measure the thickness of the helium II film. It appeared that at saturation the formation and retention of liquid between the folds rendered a precise determination of the thickness impossible. This was probably due to the surface tension rise of liquid into gaps lying between the foils. The nucleation centres would be provided either by direct touches of two foil surfaces or by bridging material.

Lane and Dyba (*loc. cit.*) have already pointed out that the curious tendency of helium to form in narrow gaps above the liquid level, will have to be considered in experiments below the λ-point. The present work must certainly serve to emphasize this caution. In addition however, these observations have now elucidated the mechanism by which this undesired formation of liquid takes place. The safest way to avoid such formation will be to see that the experimental arrangements used in future work do not contain constrictions in which capillary condensation may occur. If gaps of constrictions below the surface tension height have to be employed they will only stay free of liquid if bridging material such as dust or condensed gases are rigorously excluded.

ACKNOWLEDGMENTS

I would like to thank Dr. Mendelssohn for the interest he has shown in this work. I am grateful to Dr. D. F. Brewer for several valuable discussions and Mr. D. O. Edwards for assistance with the experiments.

REFERENCES

ALLEN, J. F., and MISENER, A. D., 1938, *Proc. Camb. Phil. Soc.*, **34,** 299.
BOWERS, R., 1953, *Phil. Mag.*, **44,** 1309.
BURGE, E. J., and JACKSON, L. C., 1949, *Proc. Roy. Soc.* A, **205,** 270.
DAUNT, J. G., and MENDELSSOHN, K., 1939, *Proc. Roy. Soc.* A, **170,** 423.
CHANDRASEKHAR, B. S., and MENDELSSOHN, K., 1952, *Proc. Phys. Soc.* A, **65,** 226.
FRENKEL, J., 1940, *J. Phys. U.S.S.R.*, **2,** 365.
KIKOIN, A. K., and LAZAREW, B. G., 1938, *Nature, Lond.*, **141,** 912 ; **142,** 289.
LANE, C. T., and DYBA, R. V., 1953, *Phys. Rev.*, **92,** 829.
McCRUM, N. G., and MENDELSSOHN, K., 1954, *Phil. Mag.*, **45,** 102.
SCHIFF, L. I., 1941, *Phys. Rev.*, **59,** 839.
THOMSON, W., 1871, *Phil. Mag.*, [4] **42,** 448.
THOMSON, G. P., 1953, *Structure and Properties of Solid Surfaces* (Chicago Gomer and Smith).

CXLVII. *The Alpha-Particle Component of the Cosmic Radiation*

By C. J. Waddington
H. H. Wills Physical Laboratory, University of Bristol *

[Received July 14, 1954]

Summary

In an investigation of the primary α-particle component of the cosmic radiation a nuclear emulsion technique has been employed. A value of 60 ± 17 g/cm^2 was found for the collision mean free path of α-particles in emulsion. The justification for using this value to obtain values for the mean free paths in other media is discussed.

A value of 320 ± 36 α-particles per m^2 per steradian per sec was found for the primary flux at a geomagnetic latitude of 55°N. This was in agreement with previous values. The energy distribution found was in agreement with that for the heavy primaries ($Z \geqslant 3$) given by Dainton *et al.* (1952) and Gottstein (1954).

§ 1. Introduction

The presence of multiply charged particles in the primary cosmic radiation was first reported by Freier *et al.* (1948), who showed that there were highly energetic nuclei of elements with atomic number as high as 20 incident on the earth's atmosphere. Since then, mainly by the use of nuclear emulsion techniques, a number of investigations have been made of the various properties of these ' heavy primaries '. In particular, attention has been directed towards the problems of determining their fluxes, energy distribution, charge distributions, and mean free paths. These properties have been shown to be of fundamental importance in any consideration of the possible origins of the cosmic radiation (Bradt and Peters 1950 a, b, Dainton *et al.* 1952). Some of the results obtained have, however, been conflicting, in particular those concerning the energy and charge distributions.

In an attempt to clarify some of these problems an investigation has been undertaken of the primary α-particle component of the cosmic radiation. Values have been found for the mean free path in emulsion, for the primary flux at a geomagnetic latitude of 55°N, and for the energy distribution up to 3 Bev per nucleon. These results have been compared with those found previously (for the heavy primaries), and they have been shown to be consistent with those obtained by other workers using the same emulsions but different techniques (Dainton *et al.* 1952, and Gottstein 1954).

---

* Communicated by the Author.

§ 2. Experimental Procedure

A stack of glass-backed 400μ Ilford G5 emulsions was flown for four hours at an altitude of 98 000 feet at a geomagnetic latitude of 55°N (corresponding for α-particles to a geomagnetic cut-off of 0·33 BEV per nucleon). This stack was the same as that used by Dainton *et al.* and Gottstein in their investigations of the heavy primaries. It was arranged in such a manner that half the emulsions faced each other, with air gaps of approximately 1 mm between them.

(a) *Track Selection*

A number of these 'facing' plates, which were particularly selected for their lack of distortion, were scanned for tracks satisfying the following criteria :

(i) That the track should have a length in the emulsion greater than 8 mm. This eliminated from consideration all the slow singly charged particles, and ensured that there was sufficient length of track to allow an attempt to be made to determine the scattering parameter $\bar{\alpha}$.

(ii) That the track should have a grain density greater than three times the plateau value. This criterion eliminated all the fast singly charged particles, while including all those with multiple charge.

The plates were scanned along horizontal lines parallel to the top edges. These scanning lines were separated from each other by a distance of 10 mm, and from the edges of the plates by a distance of at least 10 mm. When allowance was made for tracks crossing two or more scans, each scan could be considered as being independent. Thus the scanning was along a line rather than over an area, and the expected length distribution was of the form dl/l^2 rather than dl/l^3.

Using these selection criteria in the scanning, there were a number of possible ways in which a track could have been missed due to inefficient scanning. Because of this possibility various checks were made on the experimental data to ensure that no systematic errors had been introduced.

(i) Tracks with ranges only just in excess of the minimum length accepted (8 mm) could have been missed. Whether this had in fact occurred was checked by plotting the length distribution of all the tracks found. This showed that, to within the statistical limits, few tracks had been missed due to this effect.

(ii) Tracks with grain densities only just in excess of the minimum accepted could have been missed due to an underestimate of their grain densities. This possibility was checked by comparing the grain density distribution of the singly charged particles with that found by Camerini *et al.* (1950) for the singly charged particles ejected from stars. There were no apparent differences between these distributions which could be attributed to the missing of tracks. The statistical fluctuations were large however, because of the limited number of events, and the possibility could not be eliminated that a proportion of those particles with the minimum acceptable grain density had in fact been missed. However, since the α-particle minimum grain density was 1·3 times the minimum accepted grain density, the possibility that any α-particles had been missed due to this effect was certainly small.

(iii) There could have been a systematic missing of tracks, of all grain densities and all ranges, but of the fifty-four cases where a track was observed in one scan and was expected to be observed in another, only one was missed in a manner which could not be explained, indicating that any effect of systematic missing was negligible.

(iv) Tracks which appeared in the scan to be steeply dipping and which were therefore neglected by the scanner, could have been scattered into the plane of the emulsion elsewhere along their paths, and have had a range greater than the minimum accepted. Calculation shows that this effect would only be of importance for those particles having a large scattering parameter, and hence, although it is probable that a certain number of the slow singly charged particles were missed due to this effect, the number of α-particles missed was extremely small. In addition, tracks with high grain densities and thus probably high scattering parameters were examined, even if they appeared to be quite steeply dipping. In fact one track, not that of an α-particle, was missed on a second scan due to this effect.

From the above considerations it was assumed that the effects of bad scanning were small, and could be neglected in any analysis of the results.

(*b*) *Track Measurement*

A determination was made of the scattering parameter, $\bar{\alpha}$, and of the grain density, g, on each of the 345 tracks found in a scanning length of 50 cm. The scattering parameter was determined by the coordinate method of Fowler (1950) using a $4\bar{D}$ block cut-off, while the grain density was determined using an arbitrary counting convention. In those cases where the grain density was greater than about eight times plateau and the particles were identified as being of charge two or greater, the delta ray density per 100 μ was also determined, using the same counting conventions as those employed by Dainton *et al.*

Due to the difficulty of making accurate and reproducible grain counts on tracks having densities greater than about 50 grains per 50 μ, this parameter could not be considered to be as reliable as the scattering parameter. While it was possible to resolve the doubly charged from the singly charged particles (fig. 1), it was not possible to draw any conclusions concerning the existence, or otherwise, of a ‘ trough ’ in the grain density of the relativistic α-particles, analogous to that occurring for the fast singly charged particles (Morrish 1952). This is in agreement with the results of Zorn (1953) who found that even when more refined grain counting techniques are used, there is no evidence for such a trough. Moreover, the question of whether there are any He^3 particles among the primary α-particles must await better measurements.

Since it was possible in nearly every case to distinguish by inspection between particles with charge one, and those with charge two or greater, the measurements on the singly charged particles were made with less accuracy than those on the multiply charged particles. In those few cases where this immediate identification was not possible the parameters $\bar{\alpha}$ and g were measured as accurately as were those for an α-particle. As a result of this simplification, little reliance should be placed on the individual measurements of any of the singly charged particles.

Fig. 1

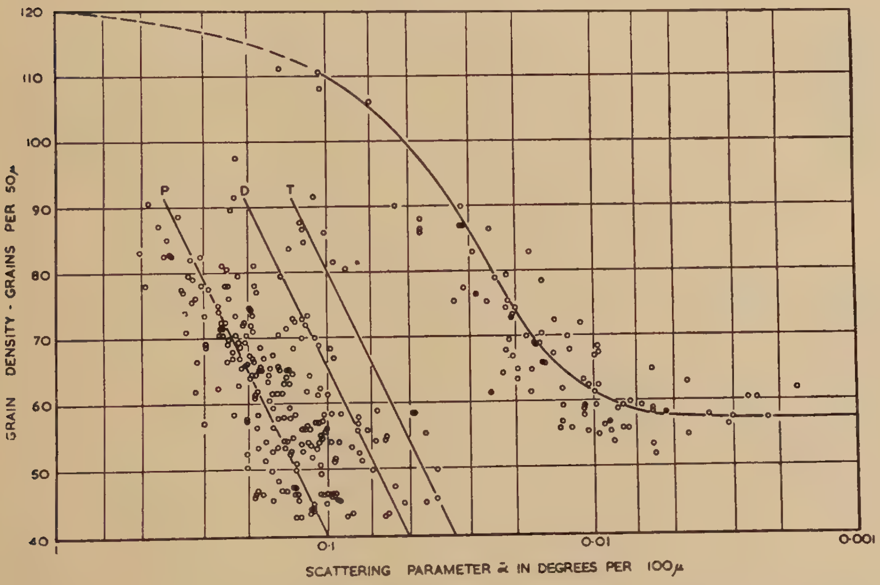

Relation between the grain density—in grains per 50 μ—and the scattering parameter $\bar{\alpha}$—in degrees per 100 μ. Star producing α-particles are represented by the symbol ●, all other particles by ○. The proton (P) curve was calculated from the range–energy relation, and from comparison grain counts made on π-mesons ending in the emulsions. The deuteron (D) and triton (T) curves are constructed from the proton curve.

§ 3. The Mean Free Path

In calculating the flux at the top of the atmosphere it is necessary to know the value of the collision mean free path of α-particles in air (λ_{air}) and glass (λ_{gl}). Unfortunately a direct experimental determination of λ_{air} does not appear to have been made, and as a result it is necessary to obtain this quantity either by extrapolation from the values found in other media (Bradt and Peters 1950), or from the variation in star density with depth in the atmosphere (Segre 1952). The results obtained by these methods do not agree, and both are open to criticism. The extrapolation of Bradt and Peters is empirical, while the results of Segre could be strongly influenced by the difficulties of detecting α-particle produced stars.

In an attempt to distinguish between these various conflicting results, a direct determination has been made of the collision mean free path of α-particles in emulsion (λ_{em}). In making this determination it has been necessary to neglect any variation of λ_{em} with energy, due to the limited experimental material available. The average energy may be taken as being of the order of 1 Bev per nucleon.

In the various emulsions scanned a total length of 165·3 cm of α-particle track was observed, but due to the scanning criteria used, this length had to be corrected before the mean free path could be calculated. From the track length of each α-particle it was necessary to subtract a quantity ϕ which was either (i) the track length traversed before reaching the scan (δ) or (ii) 8 mm if δ was less than 8 mm, the minimum length of α-particle accepted. Because of this correction the track length of α-particles which were capable, under the scanning conditions, of producing an observable nuclear disintegration was reduced to 80·1 cm. Since all the plates scanned were exposed with another plate facing them, it was in certain cases possible to follow the α-particle tracks found in one plate into the facing one. This resulted in a further 21·4 cm of track. Altogether six nuclear disintegrations were observed, four in the scanned plates, and two in the facing ones.

Due to the poor statistical weight of this result, a supplementary investigation was undertaken to increase the significance of the value found experimentally for λ_{em}.

Using scanning criteria similar to those employed previously, the tracks of α-particles were found near the top edges of various plates of a stack of 600 μ Ilford G5 stripped emulsions, which had been flown at an altitude of about 80000 feet, at a geomagnetic latitude of 55°N. These tracks were identified by scattering and grain density measurements as being those of α-particles, and were followed through the stack until they either caused a disintegration or left it. A similar correction was applied to the lengths of the tracks as before. In addition a number of high energy heavy primary disintegrations were found from which relativistic α-particles were emitted. These were also followed through the stack.

Altogether, in a total effective path length of 199·2 cm, thirteen disintegrations were observed, which gave a final value for λ_{em} of

$$\lambda_{em}{}^{*}=60\pm17\ \mathrm{g/cm^2}$$
$$=15{\cdot}3\pm4{\cdot}3\ \text{cm of emulsion,}$$

which does not agree with the experimental value of 120 g/cm² found by Segre.

In order to convert this experimental value for the mean free path in emulsion to a value for the mean free path in air, it is necessary to find a relation between the mean free path and the type of absorber

---

[*] It is interesting to note here that Zorn (1953), using a monoenergetic beam of α-particles of total energy 380 Mev, finds a collision mean free path of 80±10 g/cm².

through which the particle is passing. An empirical relation of this kind has been found by Bradt and Peters (1950 b) from a consideration of the mean free paths of particles with $Z \geqslant 2$ in brass and glass. In this the cross section σ_B is represented by the relation

$$\sigma_B = \pi(r_1 + r_2 - 2\Delta r)^2,$$

where the subscripts refer to the two colliding nuclei,

$$r = 1{\cdot}45 \times 10^{-13} \times A^{1/3} \text{ cm}$$

and

$$\Delta r = 0{\cdot}85 \times 10^{-13} \text{ cm}.$$

Using this relation, $\lambda_{\rm em}$ is found to have a value of 72 g/cm², which is in good agreement with the experimental value found in this investigation. As a result of this agreement the values for $\lambda_{\rm air}$ (44 g/cm²) and $\lambda_{\rm gl}$ (53 g/cm²) used in the calculation of the flux have been those determined by Bradt and Peters.

§ 4. THE PRIMARY α-PARTICLE FLUX

In order to obtain the flux at the top of the atmosphere it was necessary to correct the directly observed flux for the effects produced by the matter above the plates. To reduce the uncertainties introduced by these corrections as far as possible without unduly increasing the statistical errors, particles entering the plates at zenith angles greater than 60° were excluded from the analysis. Calculation showed that for the remaining α-particles the number brought to rest due to the loss of energy by ionization was small and could be neglected.

The flux at the top of the atmosphere (I) in particles per m² per steradian per sec was then given by the expression

$$I = \left\{ N\left(\sum_i \sec\theta_i\right)\left(\frac{30}{2\pi}\right)\left(\frac{1}{h}\right)\left(\frac{1}{a}\right) - z \right\} \exp\left(\frac{x_1}{\lambda_{\rm air}} + \frac{x_2}{\lambda_{\rm gl}} + \frac{\bar{\phi}}{\lambda_{\rm em}}\right),$$

where N=the total number of α-particle tracks crossing a scan (104. cf. 82 individual α-particle tracks), θ_i=the zenith angle of incidence of the ith track, $30/2\pi$=a geometrical factor, h=the time of exposure (4 hours) in seconds, a=the area of emulsion scanned (2 cm²) in m², x_1=the average grammage traversed by an α-particle in air passing from the top of the atmosphere to the stack (18·5 g/cm²), x_2=the average grammage traversed by an α-particle in glass in the stack before being detected in a scan (2·23 g/cm²), $\bar{\phi}$=the average value of ϕ as defined in § 3 (4·10 g/cm²) and z=the number of secondary α-particles per m² per steradian per sec entering the plates due to nuclear disintegrations produced by heavy nuclei.

In order to calculate z it was necessary to assume values for the flux and mean free paths of the heavy primaries, and for the frequency of production of α-particles in nuclear disintegrations initiated by heavy primaries. The values used were those of Dainton *et al.* for the flux, those of Gottstein for the frequency of production of α-particles, and those of Bradt and Peters for the mean free paths. The effect of re-absorption of these secondary α-particles was calculated making the simplifying assumption that on the average they were created mid-way between the top of the atmosphere and the plates. This factor was so small that a more refined calculation appeared unjustified.

The influence of any secondary α-particles due to disintegrations initiated by singly charged particles was neglected. That this was justifiable could be seen from the data of Sörensen (1951) on the frequency of ejection and distribution in energy of the helium nuclei emitted in disintegrations of this type. Even if the extreme assumptions were made that the probability of ejection of helium nuclei in air was the same as in emulsion, and the ionization loss above the plates could be neglected, it appeared that secondary α-particles of this type would not make up more than 5% of the total number of secondaries entering the plates. Since z was only about 8% of I, the influence of the charge one initiated α-particles could be neglected.

The value found for the flux was

$$I=320\pm36\ \alpha\text{-particles per m}^2\text{ per steradian per sec.}$$

The error quoted in this value is purely statistical and does not include the uncertainties introduced by the mean free path corrections, which will however be relatively small as the value of I is not very sensitive to small changes in the mean free paths.

This value should be compared with the value of 280 ± 8 α-particles per m^2 per steradian per sec, found by Ney and Thon (1951) at the same geomagnetic latitude and an altitude of 105000 feet using a scintillation counter inserted into a counter telescope.

Four tracks were found of particles having charges greater than two, all of the Li, Be, B group, but due to the very limited statistics it did not seem profitable to give a value for the flux.

§ 5. THE ENERGY SPECTRUM

(*a*) *Introduction*

Kaplon *et al.* (1952) have obtained integral energy spectra for the various groups of nuclei composing the heavy ($Z\geqslant2$) component of the primary cosmic radiation. They were able to relate these spectra to an empirical expression of the form

$$N(E)=\frac{C}{(1+E)^n},$$

where $N(E)$ was the number of α-particles having an energy greater than E, E was the kinetic energy in BEV per nucleon, n was a constant having the value of 1·35, and C was another constant whose value depended on the group of nuclei being considered. For the α-particles C was given as 400 particles per m^2 per steradian per sec.

Dainton *et al.* and Gottstein in their work on the heavy primaries ($Z\geqslant3$) have reported energy spectra which fall off with increasing energy more rapidly than that of Kaplon *et al.* but which like that of Kaplon *et al.* appear to have a constant value of n when related to a similar empirical expression.

Fig. 2

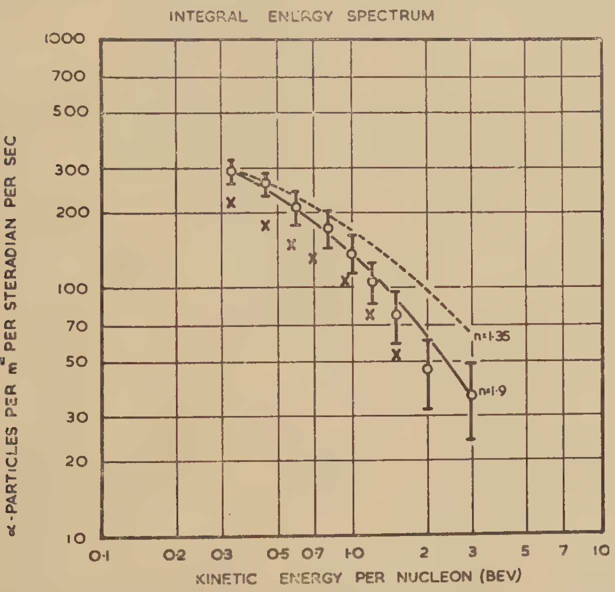

(*a*) The integral energy spectrum for the primary α-particles together with the statistical fluctuations for each point. For comparison the spectrum of Be, B, C, N, O, F, nuclei (×10) found by Dainton *et al.* is shown marked by X. Curves with $n=1{\cdot}9$ and $n=1{\cdot}35$ are also shown.

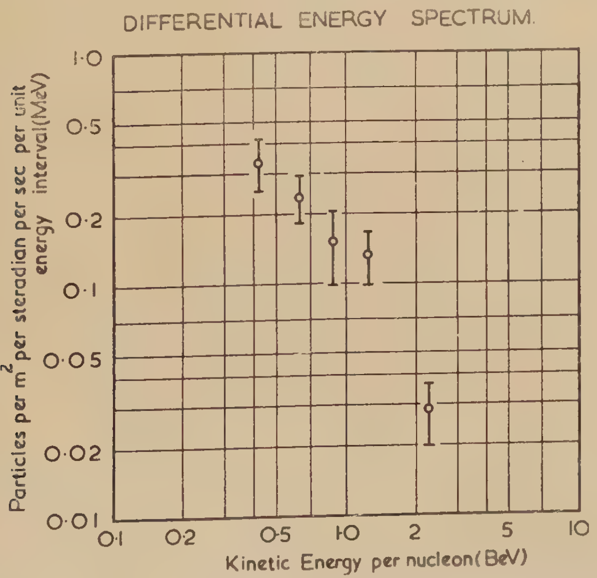

(*b*) The differential energy spectrum for the primary α-particles together with the statistical fluctuations for each point.

In view of the disagreement concerning the form of the energy spectrum, and the generally accepted constancy of the form for the various components of the heavy primaries, the energy spectrum of the α-particles is of considerable interest, since a determination of it should help to decide between these two conflicting reports.

(*b*) *Determination*

The values of the scattering parameters obtained gave the energies in the plates up to about 3 Bev per nucleon. At higher energies than this the measurements became unreliable as the determinations of the scattering parameters could only represent upper limits. In order to find the primary energy distribution it was necessary to extrapolate these individual energies to the top of the atmosphere. To reduce the uncertainties involved in this extrapolation, particles with zenith angles greater than 60° were excluded from the analysis.

The energy loss due to ionization as the particle moved from the top of the atmosphere to the detector was evaluated for each individual particle, the assumption being made that each particle was a primary one. Thus it was possible to obtain the energy distribution at the top of the atmosphere, and the resulting integral and differential energy spectra are shown in fig. 2.

On the integral energy spectrum are shown curves given by the empirical expression of Kaplon *et al.* with a value for C of 505 particles per m² per steradian per sec, and with $n=1{\cdot}35$ and $1{\cdot}9$. Although the curves are not very sensitive, particularly at low energies, to the precise value of n, it appears that the experimentally obtained spectrum is best fitted when $n=1{\cdot}9$. While Dainton *et al.* and Gottstein have not expressed their energy spectra in this form it would appear that they are in good agreement with this result, as is shown in fig. 2, where the results of Dainton *et al.* for the heavy nuclei ($4\leqslant Z\leqslant 9$) are compared with those obtained here.

It would thus appear that, provided it is justifiable to assume that n is a constant from $Z=2$ to higher values of Z, the energy distributions obtained in the present experiment are in agreement with some other workers. However it does not appear possible to reconcile these with those of Kaplon *et al.* Further investigations into the form of the energy spectrum at low energies are required in order to resolve this discrepancy.

Acknowledgements

The author wishes to express his gratitude to Professor C. F. Powell, F.R.S., for the hospitality and facilities of his laboratory. He is deeply grateful to Mr. P. H. Fowler, for introducing him to nuclear emulsion techniques, and for many valuable discussions. He also wishes to thank the Department of Scientific and Industrial Research for a maintenance grant.

References

Bradt, and Peters, 1950 a, *Phys. Rev.*, **77,** 54 ; 1950 b, *Ibid.*, **80,** 943.
Camerini, Fowler, Lock, and Muirhead, 1950, *Phil. Mag.*, **41,** 413.
Dainton, Fowler, and Kent, 1952, *Phil. Mag.*, **43,** 729.
Fowler, 1950, *Phil. Mag.*, **41,** 169.
Freier, Lofgren, Oppenheimer, Bradt, and Peters, 1948, *Phys. Rev.*, **74,** 213.
Gottstein, 1954, *Phil. Mag.*, **45,** 347.
Gottstein, Menon, Mulvey, O'Ceallaigh, and Rochat, 1951, *Phil. Mag.*, **42,** 708.
Kaplon, Peters, Reynolds, and Ritson, 1952, *Phys. Rev.*, **85,** 292.
Morrish, 1952, *Phil. Mag.*, **43,** 533.
Ney, and Thon, 1951, *Phys. Rev.*, **81,** 1068.
Segre, 1952, *Nuovo Cim.*, **9,** 116.
Sörensen, 1951, *Phil. Mag.*, **42,** 188.
Zorn, 1953, private communication.

CXLVIII. *Neutron-Widths and the Density of Nuclear Levels*

By J. M. C. Scott
Cavendish Laboratory *

[Received July 7, 1954]

Summary

The theoretical relation between the level width and the mean spacing D of the levels is investigated, using a model with strong configuration-mixing, not strong enough however to destroy the size resonance effect. Rough numerical values of Γ/D are obtained using a previous analysis of the size resonance effect in the thermal-neutron cross sections. The lack of sharpness of the surface of the nucleus has been taken into account, and is responsible for a factor of two or three in the calculated level widths.

§ 1. Introduction

In the present state of nuclear theory, the quantitative interpretation of resonance reactions can be reduced to the problem of explaining or predicting the partial widths of the energy levels of the compound nucleus. Although in favourable cases, with light nuclei, it may be possible to make a theoretical estimate of the width of an individual level for nucleon emission, it seems that usually we can only hope to predict the average width in a statistical sense.

In view of the extensive data on level widths which it is hoped will soon emerge from experiments with fast choppers of the Brookhaven type, it seems desirable to consider what should be expected theoretically, taking into account the size-resonance in nuclei, in order that we may make the best use of the new observations in testing theories of nuclear structure. The model developed here, which may perhaps be called the medium interaction model, involves no new adjustable parameters, so that a comparison with observed level-widths ought to furnish quite a severe test.

§ 2. Widths and Mean Spacing of Levels

There is certainly a rough proportionality between the mean level-spacing, D, and the mean reduced level-width (when barrier-penetrability has been allowed for). The method of deriving this relation from thermodynamic reasoning (the evaporation theory of Weisskopf (1937), N. Bohr and Frenkel) does not seem capable of much further refinement. A more promising line of attack is suggested by the refraction picture (Feshbach, Peaslee and Weisskopf 1947, Blatt and Weisskopf 1952,

---

* Communicated by the Author.

Kapur and Peierls 1938). In Weisskopf's later treatment it is supposed that one can write a wave function for an incident neutron, just inside the surface of the nucleus, in the form

$$\psi(r)=(C/r)\cos[Kr+\zeta(E)], \quad . \; . \; . \; . \; . \; . \; . \quad (1)$$

and its logarithmic derivative at the surface is then expressed in the form

$$f(E)=R[(r\psi)'/r\psi]_{r=R}=-KR\tan[KR+\zeta(E)]=-KR\tan z(E). \quad (2)$$

The angle $z(E)$ which is thus introduced is monotonic and is equal to a multiple of π at each resonance.

If we are prepared to assume that the average value of dz/dE at the resonances is equal to its general average, π/D, then the usual formula for the average neutron-width of the levels follows, namely

$$\Gamma=2kD/\pi K. \quad . \; . \; . \; . \; . \; . \; . \quad (3)$$

This assumption is sometimes described by saying that the behaviour of $z(E)$ for an actual nucleus resembles the smooth behaviour that would be expected for a simple refracting sphere, but with a much longer optical path-length inside.

In order to get a more precise relation one needs a more detailed hypothesis about nuclear structure. It is not difficult to show that with some models (3) can be quite misleading. For example, consider for a moment the most extreme weak-interaction models, which are used in the theory of atomic spectra. In such a model the wave function of a state of the compound nucleus is supposed to be quite well described by a zero-order approximation constructed out of single-particle wave functions, or else out of a one-particle wave function and a wave function for the target or core. Most of the levels will only be able to emit a neutron by virtue of configuration mixing, and will have widths much smaller than (3). These are the ‘ compound levels ’ of Bohr and Mottelson (1953) or the ‘ Auger levels ’ of Scott (1954 a). If such a model were correct, the behaviour of Weisskopf's phase angle $z(E)$ would deviate greatly from the smooth behaviour originally suggested, in a way depending on the optical path length to the centre and back.

In such a weak-interaction model, the perturbation term in the Hamiltonian must be so small that it shifts the levels of a configuration by an amount small compared with the distance of the next configuration with which it can mix. This criterion is practically never satisfied in nuclei. The level spacing revealed in neutron transmission experiments is often of the order of 1 kev or less, whereas the perturbing term is certainly far larger than would be needed to displace the levels from their zero-order positions by 1 kev. A statistical theory of perturbations is developed below, for the case in which the level density is great but the perturbing term not large enough to destroy the influence of the ‘ optical path ’ $2KR$ on the behaviour of $z(E)$, producing deviations from (3) corresponding to systematic fluctuations in dz/dE.

§ 3. WAVE-FUNCTIONS OF COMPOUND STATES IN A MEDIUM-INTERACTION MODEL

In order to avoid complication, the following assumptions and simplifications will be made. A neutron with energy E is incident on the target nucleus. The compound system can only break up in one way, by re-emission of a neutron with $l=0$; thus radiative capture is neglected, and inelastic scattering is only possible at higher energies. All angular momenta are taken to be zero.

All co-ordinates describing the internal motions of the target nucleus are denoted by the single symbol $\mathbf{r}_i$, and the relative position of the incident neutron by (r, θ, ϕ). Antisymmetry requirements are ignored for simplicity. Following current usage, that part of configuration space where the system can be regarded as completely separated, and where the wave function can be decomposed

$$\Psi(\mathbf{r}_i, \mathbf{r})=\chi_0(\mathbf{r}_i) \cdot (4\pi)^{-1/2} r^{-1} u(r) \quad . \quad . \quad . \quad . \quad (4)$$

is called a channel.

The Hamiltonian

$$H=H^{(i)}+H^{(V)}+H'=H^{(0)}+H' \quad . \quad . \quad . \quad . \quad (5)$$

is split up into that of the target nucleus $(H^{(i)})$, that of a neutron in a suitably chosen central field $V(r)$, and a perturbation term.

The equation

$$H\Phi_s(\mathbf{r}_i, \mathbf{r})=E_s\Phi_s, \quad . \quad . \quad . \quad . \quad . \quad . \quad . \quad (6)$$

taken with the boundary condition

$$(\partial/\partial r)r\Phi_s=0 \quad \text{at} \quad r=R, \quad . \quad . \quad . \quad . \quad . \quad . \quad (7)$$

possesses a complete ortho-normal set of eigenfunctions Φ_s and resonance energies E_s for the internal region $r \leqslant R$ (the compound nucleus). There is another complete ortho-normal set of eigenfunctions $\Phi_m^{(0)}$ associated with the unperturbed zero-order Hamiltonian, and satisfying

$$H^{(0)}\Phi_m^{(0)} \equiv (H^{(i)}+H^{(V)})\Phi_m^{(0)}=E_m^{(0)}\Phi_m^{(0)}. \quad . \quad . \quad (8)$$

These two sets are connected with each other by a unitary matrix $\{c_{ms}\}$, the elements of which determine the level widths of the compound nucleus (as indicated in § 5 (ii)). We therefore wish to estimate the order of magnitude of c_{ms}.

Now one can easily deduce from the definitions (6) (8) that

$$\int \Phi_s{}^*H'\Phi_m^{(0)}\, d\tau=(E_s-E_m^{(0)}) \int \Phi_s{}^*\Phi_m^{(0)} d\tau,$$

that is to say,

$$c_{ms}=\frac{1}{E_s-E_m^{(0)}} \int \Phi_s{}^*H'\Phi_m^{(0)}\, d\tau. \quad . \quad . \quad . \quad . \quad (9)$$

This resembles the formula for first-order wave functions in perturbation theory, but is exact. If the perturbation is very weak and we can assign a small upper bound U to the factor on the right, (9) may give the order of magnitude of c_{ms}. But the plausible conclusion that

$$|c_{ms}| \sim U/|E_s-E_m^{(0)}| \quad . \quad . \quad . \quad . \quad . \quad (10)$$

cannot be right when this upper bound U is large compared with the level spacing D. For the completeness relation

$$\sum_m |c_{ms}|^2 = 1, \quad \dots \dots \dots \quad (11)$$

would then give

$$1 = \int |c_{ms}|^2 (1/D)\, dE \sim U^2/D^2 \gg 1.$$

We should instead expect the following: whereas for $U \gg D$ each perturbed state can be related to a unique unperturbed state ($c_{ms} \simeq \delta_{ms}$), for $U \gg D$ any perturbed state Φ_s consists largely of a mixture of unperturbed states from the range $(E_s - D, E_s + D)$ in roughly equal proportions, so that $|c_{ms}|^2$ is at most of the order of $1/D$. A more definite result of this kind will now be obtained (§ 4).

§ 4. A THEORY OF STRONG PERTURBATIONS ('MEDIUM INTERACTION')

The term strong perturbations is perhaps paradoxical, for an effect that can be treated as a perturbation must be small compared with *something*: what is assumed here is that the levels are very closely spaced (e.g. $D = 100$ ev), and that, whereas the perturbation is much too strong merely to displace the levels by an amount $\ll D$ and instead mixes up many adjacent levels, it is nevertheless weak enough for the contamination by *distant* levels to be slight. Thus, if the perturbation is gradually increased from zero to its full value, a perturbed level Φ_s (energy E_s) retains hardly anything of the individual characteristics of $\Phi_s^{(0)}$ except of course its serial number s which is preserved in consequence of the non-crossing rule of v. Neumann and Wigner.

The result we need is not an exact algebraic theorem about the unitary matrix $\{c_{ms}\}$ connecting the eigenstates of two Hermitian operators which differ slightly, but rather involves probability theory in a way which makes a physical argument more appropriate. As a convenient starting point we may take the analysis given by Weisskopf and Wigner for the problem of line-broadening by radiation damping. Just as with the radiation field in a large enclosure, $H^{(0)}$ has many closely spaced eigenvalues, and only certain average properties of the eigenfunctions are required.

We analyse the system $H^{(0)} + H'$ first in terms of the eigenfunctions $\Phi^{(0)}$ of $H^{(0)}$, and then in terms of those of $H^{(0)} + H'$.

Starting from the equation

$$i\hbar\, \partial\psi/\partial t = (H^{(0)} + H')\psi, \quad \dots \dots \dots \quad (12)$$

and seeking a solution of the form

$$\psi = \sum_m a_m(t) \Phi_m^{(0)} \exp(-iE_m^{(0)} t/\hbar), \quad \dots \dots \quad (13)$$

one obtains the equations

$$\dot{a}_k = (1/i\hbar) H'_{k0} a_0 \exp[i(E_k^{(0)} - E_0^{(0)})t/\hbar], \quad \dots \dots \quad (14\,a)$$

$$\dot{a}_0 = (1/i\hbar) \Sigma H_{0m}' a_m \exp[i(E_0^{(0)} - E_m^{(0)})t/\hbar]. \quad \dots \dots \quad (14\,b)$$

The initial conditions are $a_0(0) = 1$, with all the other $a_m(0) = 0$. The usual text-book procedure is to put $a_0(t) = 1$ in (14 a) and to ignore (14 b), which is good enough for small t. Weisskopf and Wigner (1930), however, showed how to extend the solution to larger values of t. Their procedure is to try putting

$$a_0=\exp(-\tfrac{1}{2}gt/\hbar). \qquad (15)$$

Then by integrating (14 *a*),

$$a_k(t)=H_{k0}'\,\frac{1-\exp(iE_k-iE_0-\frac{1}{2}g)t/\hbar}{E_k-E_0+\frac{1}{2}ig}. \qquad (16)$$

This satisfies (14 *b*) too, provided that $\frac{1}{2}ig$ is equal to

$$\sum_m |H_{0m}'|^2\,\frac{1-\exp(iE_0-iE_m+\frac{1}{2}g)t/\hbar}{E_m-E_0+\frac{1}{2}ig}=i\pi\,|H_{0m}'|^2/D,$$

which is assumed to be independent of m, or at any rate constant when averaged over any small range of energies. We therefore define g by

$$g=2\pi\,\mathrm{Av}\,|H_{0m}'|^2/D. \qquad (17)$$

The distribution of the probability of occupation of the states when $t\gg\hbar/g$ follows from (16)

$$|a_m(t)|^2\rightarrow\frac{|H_{m0}'|^2}{(E_m-E_0)^2+\frac{1}{4}g^2}, \quad (t\rightarrow\infty)$$

and one can check that

$$\Sigma\,|a_m(\infty)|^2=\int\frac{g/2\pi}{(E-E_0)^2+\frac{1}{4}g^2}\,dE=1, \qquad (18)$$

as it should be.

In the original application to the emission of light, g gives the natural breadth of the emitting state. The expression under the integral sign in (18) gives the probability distribution of the energy of the system.

Now let ψ be analysed instead into eigenfunctions of H, i.e. the truly stationary states of the system. Since the initial condition of the system is

$$\Phi_0^{(0)}=\sum_s c_{0s}\Phi_s, \qquad (19)$$

our solution (13) must be

$$\psi=\Sigma c_{0s}\Phi_s\exp(-iE_st/\hbar). \qquad (20)$$

The probability distribution of the energy of the system can thus be expressed alternatively in terms of the local average of $|c_{0s}|^2/D$. Hence

$$\mathrm{Av}\,|c_{ms}|^2=\frac{gD}{2\pi}\,\frac{1}{(E_m-E_s)^2+\frac{1}{4}g^2}. \qquad (21)$$

This relation (21) supersedes (10), and in fact (21) yields (10) as a limiting case ; (21) is of course now consistent with (11), which (10) was not.

§ 5. APPLICATION OF THE PERTURBATION THEORY TO ELASTIC SCATTERING

(i) *The General Nuclear Dispersion Formula*

For the sake of convenience a derivation of the nuclear dispersion formula will be given here with the simplifying assumptions of § 3 (elastic scattering of neutrons, $l=0$, etc). Detailed discussions can be found in the literature.

The actual wave function Ψ at any chosen energy E can be decomposed according to (4) in the external region or channel, and it satisfies

$$H\Psi(\mathbf{r}_i, \mathbf{r}) = E\Psi, \qquad (22)$$

everywhere. In the internal region it can be expanded in a series

$$\Psi = \Sigma b_s \Phi_s, \qquad (23)$$

which may be non-uniformly convergent on the boundary $r=R$, and in fact will be: the derivative $w'(R)$ (cf. eqn. (4)) cannot be obtained by term-by-term differentiation, cf. (7).

In order to bring in the derivative $w'(R)$, one can use (6) and (22) to obtain

$$\iiint \{\Psi(H\Phi_s)^* - \Phi_s^* H\Psi\}\, d\mathbf{r}_i r^2\, d\omega\, dr = (E_s - E) b_s. \qquad (24)$$

When the left-hand side of (24) is simplified by means of Green's theorem, the only non-vanishing part comes from the term

$$-\frac{\hbar^2}{2M}\left\{r\Psi \frac{\partial^2}{\partial r^2} r\Phi_s^* - r\Phi_s^* \frac{\partial^2}{\partial r^2} r\Psi\right\}$$

in the integrand; integrating this by parts, using (4) and (7), the relation (24) becomes

$$b_s = \frac{w'(R)}{E_s - E}\,\frac{\hbar^2}{2M}\,\frac{R}{\sqrt{(4\pi)}}\iint \Phi_s^*\, \chi_0\, d\mathbf{r}_i\, d\omega = \frac{\hbar^2}{2M}\,\frac{\phi_s^*}{E_s - E}\, w'(R), \qquad (25)$$

where

$$\phi_s = \frac{R}{\sqrt{(4\pi)}}\iint \chi_0^* \Phi_i\, d\mathbf{r}_i\, d\omega \qquad (26)$$

and can be considered as the average of Φ_s over the entrance ($r=R$) of that channel which corresponds to incidence and elastic scattering.

Inserting the value of $\Psi(\mathbf{r}_i, R)$ from (23) and (25) in (4) now gives the standard dispersion formula connecting the wave function with the reduced widths γ_s^2:

$$\frac{w(R)}{w'(R)} = \Sigma_s \frac{\gamma_s^2}{E_s - E}, \qquad (27)$$

$$\gamma_s^2 = \frac{\hbar^2}{2M} |\phi_s|^2. \qquad (28)$$

From this, the Breit–Wigner formula for slow neutron scattering can be deduced, and the neutron width Γ_s identified as $\Gamma_s = 2k\gamma_s^2$ which in this case has a simple physical interpretation: Γ_s is proportional to $|\phi_s|^2$ which is a measure of the probability of finding the neutron in the channel entrance, and to the velocity $\hbar k/M$ with which it might escape.

(ii) *Application to the Medium Interaction Model*

It will greatly simplify the analysis if we adopt the assumption of a sharp boundary to the nucleus (the necessary correction can be made afterwards), and if we further assume that the reaction radius is not appreciably larger, so that $r=R$ represents both the surface of the nucleus and the sphere necessary to seal off the internal region from the reaction channels.

The Hamiltonian can be divided into parts as in § 3 :

$$H=H^{(i)}+H^{(V)}+H', \qquad (5)$$

when $H^{(i)}$ is the exact Hamiltonian of the target nucleus, and has eigenfunctions χ_j

$$H^{(i)}\chi_j(\mathbf{r}_i)=E_j^{(i)}\chi_j.$$

$E_0^{(i)}$ can be conveniently taken to be zero. $H^{(V)}$ describes a neutron in a suitably chosen potential well

$$H^{(V)}=-(\hbar^2/2M)\nabla^2+V(r),$$

so that H' can be treated as a perturbation.

We now have two complete orthonormal sets of functions in the internal region, as in (6), (7) and 8 : namely the eigenfunctions of the unperturbed problem $(H^{(i)}+H^{(V)})$ which can be written more explicitly as

$$\Phi_{jn}^{(0)}=\chi_j(\mathbf{r}_i)\frac{v_n(r)}{r\sqrt{(4\pi)}}=\chi_j(\mathbf{r}_i)\left(\frac{2}{R}\right)^{1/2}\frac{\sin K_n r}{r\sqrt{(4\pi)}}, \qquad (29)$$

where

$$K_n=(n+\tfrac{1}{2})\pi/R \qquad (n=0,\ 1,\ 2,\ \ldots), \qquad (30)$$

and the eigenfunctions of the actual problem (H) which are

$$\Phi_s=\sum_{j.n} c_{jn,s}{}^*\Phi_{jn}{}^{(0)}.$$

When Φ_s is analysed in this way into a combination of the $\chi_j v_n$, the only terms which contribute anything to its 'mean' value ϕ_s at the channel entrance are the terms in $\chi_0 v_n$ (target left in its ground state). Thus from (26)

$$\phi_s=(2/R)^{1/2}\sum_n c_{0n,s}{}^*.$$

The statistical result (21) then gives, for the average value of the reduced width,

$$\text{Av}\ \gamma_s{}^2=\frac{\hbar^2}{MR}\text{Av}\sum_n|c_{0n,s}|^2=\frac{2MgD}{\pi\hbar^2R}\sum_{n=0}\frac{1}{(K^2-K_n{}^2)+M^2g^2/\hbar^4}, \qquad (31)$$

where K denotes the internal wave number $[2M(W+E_s)]^{1/2}/\hbar$, and W is the well depth.

The summation can be performed by means of the formula

$$Im\frac{\tan(\xi+i\sigma)}{\xi+i\sigma}=\sum_{n=0}^{\infty}\frac{4\xi\sigma}{[(n+\frac{1}{2})^2\pi^2-\xi^2+\sigma^2]^2+4\xi^2\sigma^2}, \qquad (32)$$

which can either be proved from Mittag-Leffler's theorem or derived from the series $\cot z=\Sigma 1/(z-m\pi)$. The result is

$$\text{Av}\ \gamma_s{}^2=\frac{DR}{\pi}Im\frac{\tan(\xi+i\sigma)}{\xi+i\sigma}=\frac{DR}{\pi}\frac{\xi}{\xi^2+\sigma^2}\frac{\sinh 2\sigma}{\cos 2\xi+\cosh 2\sigma}$$
$$\times\left\{1-\frac{2\sigma}{\sinh 2\sigma}\frac{\sin 2\xi}{2\xi}\right\}. \qquad (33)$$

Here ξ and σ are positive numbers defined by means of

$$\xi+i\sigma=(K^2+iMg/\hbar^2)^{1/2}R. \qquad (34)$$

In practice $\sigma^2 \ll \xi^2$, so that $\xi \simeq KR$, and the first two factors in (33) yield $D/\pi K$; 2ξ is large enough for the last factor to be neglected. The mean level width for neutron emission is then found to be

$$\bar{\Gamma}=2k\overline{\gamma^2}=\frac{2Dk}{\pi K}\,\frac{\sinh 2\sigma}{\cosh 2\sigma+\cos 2KR} \qquad (35)$$

which agrees with the Weisskopf formula (3) in the limit $\sigma\to\infty$.

It is now necessary however to allow for the effect of the simplifying assumption made above, that the nucleus had a sharp boundary. The gradual nature of the transition of the field $V(r)$ from the well-depth $-W$ to zero can be taken into account as in Scott (1954 b), and has two effects : it replaces the factor $1/K$ by a larger constant S, and it adds a constant to the phase angle KR, so that $\xi \simeq KR-\alpha$. In the experimental reports, the velocity-variation of Γ is often allowed for and the value of $\Gamma^{(1)}=\Gamma\sqrt{(E_1/E)}$ is quoted, calculated for a standard energy of $E_1=1$ ev. With this convention,

$$\text{Av}\,\frac{\Gamma^{(1)}}{D}=\frac{2k_1S}{\pi}\,\frac{\sinh 2\sigma}{\cosh 2\sigma+\cos 2\xi}, \qquad (36)$$

where $\xi=KR-\alpha=(0{\cdot}6A^{1/3}-0{\cdot}8)\pi$ and $k_1=(2ME_1)^{1/2}/\hbar=2{\cdot}2\times10^9$ cm^{-1}.

§ 6. NUMERICAL VALUES AND DISCUSSION

The first factors in (36) correspond to the $2k_1/\pi K$ of the sharp-boundary theory (Blatt and Weisskopf 1952, and eqn. (35)), which would be $1{\cdot}4\times10^{-4}$ with a well depth of 20 MeV as used in the literature, or $0{\cdot}9\times10^{-4}$ with the value 51 MeV which we believe to be more correct (Scott 1954 b). With the diffuse boundary however, using $S=18{\cdot}9\times10^{-14}$ cm as in the latter paper, the actual value of the factors in (36) is rather larger, namely $2{\cdot}6\times10^{-4}$.

The value of the interaction-strength σ can be estimated by the method given previously (Scott 1954 b), but only roughly because of inadequate statistics : for nuclei with $50<N\leqslant82$, $\tanh\sigma=0{\cdot}16\pm0{\cdot}04$, and for $N>82$, $\tanh\sigma=0{\cdot}7\pm0{\cdot}25$. This suggests that $\Gamma^{(1)}/D$ should have a maximum of 4 ± 1 near $A=165$, a somewhat larger maximum at $A=56$, and a broad minimum of $0{\cdot}4\pm0{\cdot}1$ at $A=102$. This is in fair agreement with preliminary results from Brookhaven (Harvey, Porter and Hughes 1954).

When the widths of enough levels have been measured it may be possible to work backwards and deduce σ from Γ_n. But, in considering experimental values of Γ_n/D, the statistical uncertainties in both D and Γ_n when deduced from a sample of say 5 or 10 levels must be borne in mind, as well as the experimental error of an individual Γ_n which often depends on an assumed value for the radiation width, so that the task of determining $\bar{\Gamma}_n/D$ accurately will be difficult and laborious.

In certain cases, e.g. Zn, the predicted mean level widths are rather insensitive to the choice of a value for σ, and a better prediction is possible. For Zn, (36) gives $\Gamma^{(1)}/D=3{\cdot}7\times10^{-4}$, with a probable error of $\sim 10\%$ arising mostly from S. This may be compared with $(5\pm2)\times10^{-4}$ from four levels in ^{67}Zn observed by Dahlberg and Bollinger (1954).

It is not possible to compare the present theory with the cloudy crystal ball of Feshbach, Porter and Weisskopf, since details of the application of the latter to the resonance region are not yet available to us. Some of our formulae, e.g. (34) and (35) do indeed suggest an optical analogue with an extinction coefficient $\propto \sigma R$ or a complex potential $W+\frac{1}{2}ig$ but it should be noted that σ and g do not correspond to the neutron being lost from the entrance channel to other channels (inelastic scattering or radiative capture).

It is noteworthy that the argument from the graph of $z(E)$, which gave (3), also suggests that when two or three levels happen to be unusually close together $(E_{s+1}-E_s \ll D)$, their widths should be below average, whereas the present analysis does not lead one to expect any such correlation. This point could probably be tested experimentally. It is also natural to suppose that the real and imaginary parts of $c_{0n,s}$ in (31) will follow a Gaussian distribution, and therefore that Γ will follow $dP=(1/\bar{\Gamma})\exp(-\Gamma/\bar{\Gamma})\,d\Gamma$, but this does not seem to be strictly deducible from the considerations given here.

It is a pleasure to thank Professor D. J. Hughes for several valuable discussions.

APPENDIX

Estimation of σ from the Thermal Scattering Data

In this appendix the probability distribution of the coherent scattering length will be obtained. It is a consequence of the present theory which was quoted without proof in Scott (1954 b) (referred to as II). According to II, § 3, this problem is equivalent to finding the distribution of the values of β, the phase of the neutron wave function when extrapolated inwards to the centre.

The relation between the notation of II and that of Blatt and Weisskopf (1952) is as follows :

	II=S. (1954 b)	B. & W. (1952)
Phase just outside	$-\theta$	$z(0)-\frac{1}{2}\pi$
Phase extrapolated to centre	β	$\zeta(0)-\frac{1}{2}\pi$
Difference of these	$KR-\alpha=\xi$	KR
Phase shift in traversing nuclear surface	$\alpha-\pi$	0

The result of the present paper can be interpreted in terms of the graphs of the Feshbach–Weisskopf functions $z(E)$ and $\zeta(E)$, and their systematic fluctuations in slope. These fluctuations of average slope are periodic in $\zeta=z-\xi=z-KR+\alpha$. The results (33) and (35) gave the average value (γ^2/S) of dE/dz at those points where z is a multiple of π (i.e. the resonances)

$$\mathrm{Av}\,\frac{dE}{d\zeta}\simeq\mathrm{Av}\,\frac{dE}{dz}=\frac{D}{\pi}\,\frac{\sinh 2\sigma}{\cos 2\zeta+\cosh 2\sigma}\,.$$

Now if the energy of a thermal neutron, $E\simeq0$, falls randomly among the resonance levels, the corresponding value of ζ, namely $\zeta(0)=\beta+\frac{1}{2}\pi$, does not fall randomly on the scale of ζ : instead, the chance that it lies in a range $d\zeta$ is proportional to $dE/d\zeta$, and the probability distribution of β is therefore

$$\frac{\sinh 2\sigma}{\pi}\,\frac{d\beta}{\cosh 2\sigma-\cos 2\beta}\,.$$

This is the formula which was used in II to estimate σ.

REFERENCES

BLATT, J. M., and WEISSKOPF, V. F., 1952, *Theoretical Nuclear Physics*, 1st ed. (New York : Wiley), esp. pp. 398–406.
BOHR, A., and MOTTELSON, B., 1953, *Dan. mat. fys. Medd.*, **27,** No. 16.
DAHLBERG, D. A., and BOLLINGER, L. M., 1954, *Bull. Amer. Phys. Soc.*, **29,** No. 4, 57.
FESHBACH, H., PEASLEE, D. C., and WEISSKOPF, V. F., 1947, *Phys. Rev.*, **71,** 145.
HARVEY, J. A., PORTER, C. E., and HUGHES, D. J., 1954, *Bull. Amer. Phys. Soc.* **29,** No. 4, 57.*
KAPUR, P. L., and PEIERLS, R., 1938, *Proc. Roy. Soc.* A, **166,** 277.
SCOTT, J. M. C., 1954 a, *Phil. Mag.*, **45,** 441 ; 1954 b, *Ibid.*, **45,** 751.
WEISSKOPF, V. F., 1937, *Phys. Rev.*, **52,** 295.
WEISSKOPF, V. F., and WIGNER, E., 1930, *Z. Phys.*, **63,** 54.

*Now reprinted in *Phys. Rev.*, **95,** 645.

CXLIX. *The Characteristic Temperature of Platinum from X-Ray Reflections*

By K. Alexopoulos and P. Euthymiou
Physical Laboratory, University of Athens *

[Revised draft received August 10, 1954]

Summary

The characteristic temperature θ of solids is generally derived from measurements of the specific heat. It can also be derived from the temperature factor of the diffraction of x-rays. The first method gives uncertain results in the case of the transition metals, because in these the electronic heat constitutes a considerable part of the total specific heat, and therefore corrections have to be made in order to obtain the specific heat due to the lattice vibrations alone. In the present paper the intensity of the Debye–Scherrer lines diffracted from platinum were determined at different temperatures. The gradual change of the ratio of intensities of two lines gives the desired value of θ.

The intensity of the diffraction lines was determined from the density of blackening on a photographic film. The temperatures were determined from the expansion of the lattice constant.

Exposures were made at 13 different temperatures between 298° and 1133°K. From the ratio of the integrated intensities of Debye–Scherrer lines (111) and (311) a value of $\theta = 152 \pm 9°$ results. From the pair of lines (200) and (311) the more uncertain value of $192 \pm 29°$ resulted. The weighted mean of the two measurements after taking systematic errors in consideration gives $156 \pm 26°$.

These results can be compared to values of θ from specific heat measurements.

In the T^3 range specific heat measurements give $\theta = 233°$. At higher temperatures the thermal measurements have to be corrected for electronic heat. Accepting for the degeneration temperature $T_0 = 1750°$K and for the number of electrons $q = 0{\cdot}18$, values around $\theta = 235°$K result. The θ values from x-ray diffraction are thus decidedly lower than the thermal values. The same disagreement has been observed with the metals Li and Na.

§ 1. Introduction

According to the Debye theory the thermal vibrations of solids have a spectrum that ends abruptly at a maximum frequency, ν_m. The expression $h\nu_m/k$ is called the Debye characteristic temperature where h and k are Planck's constant and Boltzmann's constant respectively. Once

---

* Communicated by the Authors.

θ is known the above theory permits the calculation of the specific heat C_v of the solid (from now on called *lattice heat*) at all temperatures. Conversely measurements of the specific heat gives the value of the parameter θ. According to the above theory, the values of θ obtained from these measurements should be constant at all temperatures. For a large number of solids this has indeed been found to be the case but in certain interesting instances θ varies. Blackman (1937) has given convincing reasons for these deviations. Another point that complicates the correlation between specific heat measurements and characteristic temperature is the existence of an *electronic specific heat.* This is, for most solids, small in relation to the lattice heat (except at temperatures near the absolute zero) so that this complication is not important. The transition metals however, in which the density of the 3d-states at the highest occupied level is high, is an exception to the above rule and will have considerable electronic heat. It is clear that to calculate the characteristic temperature of the lattice vibrations in this last category of elements, we must first subtract the electronic heat from the measured specific heat. The residue is due exclusively to the lattice heat and can be used to calculate the characteristic temperature θ. This has been successfully done by Clusius for Pd (1947), Ni, Fe, Co (1952 a) and in (1952 b).

Another way of investigating the lattice vibrations is based on a completely different principle : The reflection of x-rays on a lattice plane at an appropriate Bragg angle, assumes that all the atoms are at their equilibrium position, i.e. on the reflecting lattice plane. As temperature rises the heat waves will constitute a perturbation and the resulting reflection will be less intense. Debye and Waller calculated the change of the integrated intensity I of a diffraction line against temperature and correlated it with a characteristic temperature θ_M according to the formula $I=I_0 \exp(-2M)$, where

$$M=\frac{6h^2}{mk\theta_M}\,\frac{\sin^2\vartheta}{\lambda^2}\left(\frac{\phi(x)}{x}+\frac{1}{4}\right).$$

This calculation was made for an isotropic simple cubic lattice but experiments showed that it is also valid for a large number of other lattices. Thus James and Brindley (1928, 1929) and others found that it could be applied to NaCl, KCl and Al throughout a wide range of temperatures. The values of θ_M that resulted from their measurements practically coincided with the values of θ obtained from specific heat measurements. X-ray measurements have also been made by Andriesen (1935) on Ag and by Owen and Williams (1947) on Cu, Au, and Al in the range 293–920°K. The accuracy obtained in the measurements by Owen and Williams was sufficient to detect the small gradual change in the value of θ_M due to the thermal expansion of the lattice. In all these cases, the characteristic temperature derived in this way was in good agreement with the characteristic temperature derived from specific heat measurements.

On the other hand, other measurements are much less satisfactory. Arakatsu and Scherrer (1930) applied the above formula to the diffraction lines of Li at room temperature and obtained $\theta_M=510°$, although a value around 350 can be shown to fit their results as well. A more sensitive approach was undertaken by one of the authors (Alexopoulos 1932), who compared the intensity of lines at two different temperatures, 90° and 293°K, obtaining $\theta_M=355\pm18°$. Pankow (1936) repeated the same measurement and got $352\pm12°$. He also compared the intensities in smaller temperature intervals and obtained $\theta_M=315\pm11°$ in the interval 90–190°K, and $\theta_M=378\pm16°$ in the interval 190–293°K. These results show that θ_M gets larger with increasing temperature and $\theta_M=352°$ should be considered as a mean for the two other values. These results should be compared to the values of θ derived from specific heat measurements. Simon and Swain (1935) show that the curve $C_v=f(T)$ cannot be described with a constant value of θ. At very low temperatures ($T=15°$K) θ is approximately 330° and it gets larger as temperature rises to reach 430° at 190°K from where on it stays practically constant. In the range of the x-ray measurements it has a mean value of about 410° in the interval of 90° to 190°K and 430° in the interval from 190° to 293°K.

A second similar case is Na. Dawton (1937) using x-rays investigated the region between 117 and 291°K and found $\theta_M=140°$ at the lowest temperature and a gradual drop to $\theta_M=120°$ at room temperature. These values are all smaller than $\theta=159°$ that results from specific heat measurements (Simon and Zeidler 1926) in the temperature range between 20 and 200°K.

The present paper reports on the investigation of Pt in the range between 298° and 1133°K. For this transition metal the total specific heat considerably exceeds, at higher temperatures, the classical value of 5, 96 cal/deg. mol., indicating a large contribution from the electrons. Hence, before using specific heat values for the determination of θ, an appropriate correction for the electronic heat has to be made.

§ 2. DETERMINATION OF θ FROM DIFFRACTION EXPERIMENTS AT DIFFERENT TEMPERATURES

The power of a beam of x-rays diffracted under a Bragg angle ϑ from a crystalline powder at a temperature T is

$$P=I_0\frac{le^4\lambda^3n^2j\,dV}{16\pi rm^2c^4}\,\frac{1+\cos^2 2\vartheta}{\sin\vartheta\,.\,\sin 2\vartheta}$$

$$\times A(\lambda,\vartheta)\,.\,[\Sigma F_k\exp\{2\pi i(hx_k+ky_k+lz_k)\}]^2\,.\exp(-2M), \quad . \quad . \quad (1)$$

where I_0 is the intensity of the incident x-radiation ; e, m, c, λ, dV (h, k, l) have their usual significance, l is the length of the Debye–Scherrer line, j is the multiplicity factor for the crystal planes (h, k, l) corresponding to the glancing angle ϑ, n is the number of cells per unit volume, r is the radius of the Debye–Scherrer camera, A is the absorption factor depending on λ and ϑ and F_k is the scattering factor of an atom k at rest whose reduced coordinates in the unit cell are x_k, y_k, z_k.

If we compare the powers of two different lines at glancing angles ϑ_1 and ϑ_2 taken at the same temperature T, but with different wavelengths K_a and K_β, and calculate the logarithm of their ratio, L, we have

$$L=C+\frac{12h^2}{4mk\theta_M}\left(\frac{\sin^2\vartheta_1}{\lambda_\beta^2}-\frac{\sin^2\vartheta_2}{\lambda_\alpha^2}\right)-\frac{12h^2}{mk\theta_M}\times\left(\frac{\sin^2\vartheta_1}{\lambda_\beta^2}-\frac{\sin^2\vartheta_2}{\lambda_\alpha^2}\right)\cdot\frac{\phi(\theta_M/T)}{\theta_M/T}, \quad . \quad . \quad . \quad (2)$$

where C is a constant practically independent of T. Only the third term contains the temperature and is an apparently complicated function of T. Nevertheless if we limit the temperature range from 300°K to 1000°K and keep the values of the parameter θ_M between 100° and 250°, the function $T/\theta_M{}^2 \,.\, \phi(\theta_M/T)$ plotted against temperature, gives a family of curves which are very approximately rectilinear. Their slopes depend on the respective value of the parameter θ_M.

According to the above calculation, if the ratio of the intensity of two diffraction lines is measured at different temperatures and is plotted on a semilogarithmic scale against T a straight line should result with a slope equal to the slope of the third term of eqn. (2). Thus by comparing the slope of the experimental line $L=f(T)$ with that of the corresponding theoretical line we get the value of θ_M.

§ 3. EXPERIMENTAL PART

The power of the Debye–Scherrer lines diffracted from platinum was measured by the blackening on a photographic film.

The scattering specimen was a vertical platinum wire of 200 μ diameter (fig. 1) continuously rotated by means of a pulley. The rotation was necessary because at high temperatures a certain amount of recrystallization occurred resulting in spottiness of the Debye–Scherrer lines. The wire was kept taut by a small weight which dipped into a container with mercury. This served at the same time as the second lead for the electric current that heated the wire. Water circulating in the brass body kept it cool. The film was pressed around the camera's external surface by means of a thin brass sheet covered with black velvet. Elastic tape held everything in position. The camera was exposed to unfiltered iron radiation, working at a voltage of 40 kv and a current of 5 mA. The duration of each exposure was 1 hour.

The temperature, T, of the wire was determined from the current i that flowed through the wire. In a first series of measurements (Euthymiou 1952) the calibrating curve $T=f(i)$ was determined experimentally by means of a thermoelectric method : a junction of the platinum wire with a thin constantan wire (40 μ) was heated in a suitable oven to various temperatures, and the resulting thermoelectric force was measured. Then the wire was heated under normal conditions in the scattering chamber and the thermoelectric power measured against heating current. In this way the relation $T=f(i)$ was obtained. This method was found to introduce serious systematic errors, as the temperature at the junction of the heated platinum wire was found to be considerably lower than along the rest of its length, where the scattering volume was situated. This method was then abandoned in favour of a direct determination of the temperature from the expansion of the lattice constant. Owen and Yates' measurements (1934) of the lattice constants of platinum at different temperatures, permitted us to calculate the distance of two suitable Debye–Scherrer lines on the photograph and to plot distance against temperature. The temperature for each value of the heating current i was found by measuring the distance s on the corresponding film. Four exposures were made at each value of i resulting in eight values of s. Because of errors in the measurements of s on

Fig. 1

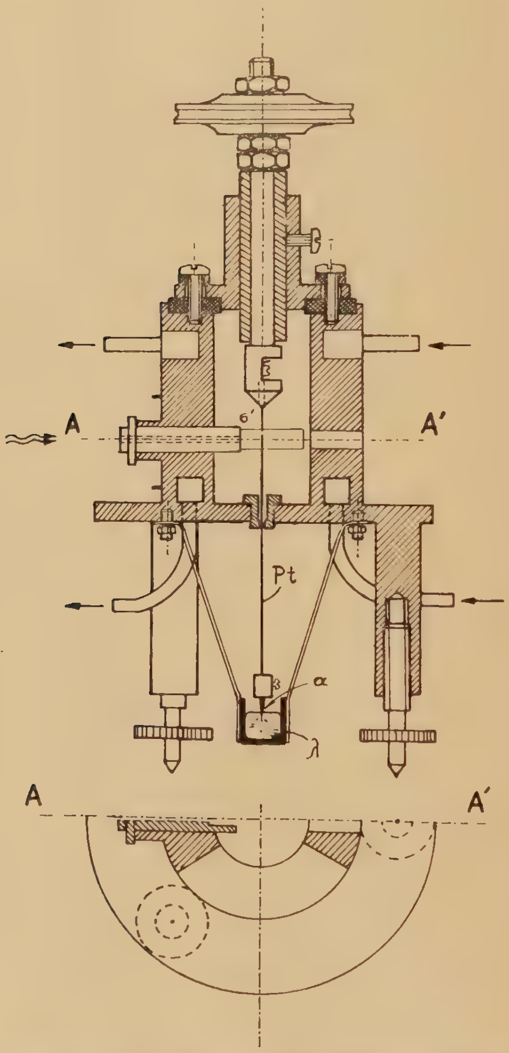

a comparator, there was a large scattering in the temperature values thus determined. Nevertheless, this is not very troublesome, as the method is, at least, exempt from systematic errors. The radius of the cylindrical film does not enter into the calculation since exposures were made at room temperature, and the distances *s* referred to them.

Exposures were taken at 13 different heating currents in the range from room temperature to about 1133°K. No higher temperature could be attained because the rate of recrystallization became excessive. At each value of the heating current four exposures were made, each giving two semi-circumferential films, so that a total of eight films could be used for each temperature. The density curve of each Debye–Scherrer line was measured with a microphotometer. The lines (111), (200), (220), (311), produced by the K_α radiation and the line (331) produced by the K_β radiation were measured. In order to find the relation between the indications of the galvanometer and the quantity of radiation (intensity × time), a number of films were exposed to direct blackening with the aid of a rotating, graded sector. With the aid of such a calibrating curve the density curves for each Debye–Scherrer line were reduced to intensity curves and then their areas were measured with a planimeter. Each area represents the integrated intensity I of the corresponding Debye–Scherrer line, which is proportional to the power of the diffracted x-radiation.

Fig. 2

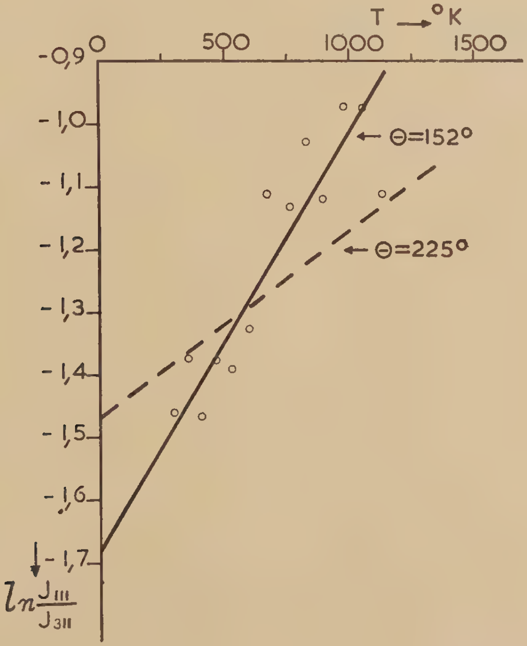

Figure 2 is a plot for lines (111) and (311), where the abscissa is temperature, and the ordinate is ln (I_{111}/I_{311}) calculated from the mean values on eight films. The slope of the most probable straight line through these points was found by the method of least squares. Each point was given a different weight depending on the divergence of the eight values from the mean value. By comparing this slope with the slopes of the calculated family of straight lines (§ 2) we found the value of $\theta_M = 152°$. The probable error in the slope was found to produce a probable error of $\Delta\theta_M = \pm 9°$.

This value of $\Delta\theta_M$ results from fig. 2 if the values of the temperature are considered without error. In reality errors exist because the temperature was computed, as mentioned, from the ‘ most probable curve ’ $i=f(T)$ that passes through scattered points of the lattice expansion measurements. On both sides of this curve two curves were traced so as to contain all the scattered points. The distance of these from the ‘ most probable curve ’ gives indication of the maximum possible error in temperature. At 1130°K this error is about 120°. If the temperature of 1130°K is thus changed to 1250°K, and if the other intermediate temperatures are correspondingly corrected, new values of θ_M result. By considering in this way the maximum possible systematic error in the temperature measurement, θ_M could either be larger or smaller by 8°. In fig. 3 we plot experimental results for the second pair of lines (200) and (311). The same calculations as above were made for this pair of lines. All the results are grouped in the table. We have also plotted the results for the other three pairs of lines (220)–(311), (222)–(311) and (331)–(311), but the points were so broadly scattered and the resulting error so large that results would be without significance.

Fig. 3

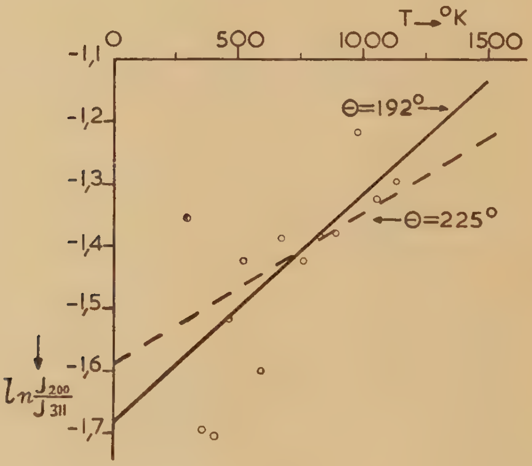

The two measurements of the table after being given appropriate weights give the mean value $\theta_M = 156° \pm 23°$. If the systematic error is also taken in consideration, the total error reaches 26°.

§ 4. DISCUSSION OF RESULTS

In § 3 we showed that the change of the intensity of x-rays diffracted from platinum leads to a characteristic temperature of 156°. This value will now be compared to values of θ found in other ways. The most important methods are specific heat measurements in the T^3 range and in the medium temperature range up to $T \cong \theta$.

Lines	θ_M	Random error	Maximum systematic error
(111)–(311)	152	±9	±8
(200)–(311)	192	±29	±10·6

The specific heat of a solid is given by two terms, the first due to the lattice and the second to the free electrons. The first term is given by C_v, lattice$=6R/2\times D(T/\theta)$ where D is the Debye function. At very low temperatures (i.e. $T \ll \theta$) this term simplifies to C_v, lattice$=446(T/\theta)^3$.

The electronic heat cannot be easily given in an explicit form. At temperatures that are low relatively to the degeneration temperature T_0 (approximately up to $T_0/3$) the electronic heat is a linear function of T

$$C_e=(\tfrac{1}{2})\pi^2 RqT/T_0=\gamma T, \qquad \ldots\ldots \quad (3)$$

where q is the number of free electrons per atom. At higher temperatures C_e asymptotically takes the classical value $C_e=(3/2)R\,.\,q$.

The curve $C_e=f(T)$ in the whole range of temperatures is given in a large number of books (e.g. Mott and Jones 1936, p. 180).

Specific heats at very low temperatures will thus follow a law

$$C_v=446(T/\theta)+\gamma T.$$

Measurements by Kok and Keesom (1936) in the liquid He-range give $\theta=233°$ and after a correction by Wohlfarth (1948) one gets $T_0/q=7000$. This latter value in conjunction with the magnetic measurements of Hoare and Matthews (1952) gives $T_0=1750°$ and $q=0, 25$. In order to determine θ from the specific heat measurements at medium temperatures the electronic heat should be subtracted from the experimental C_v. We notice that if T_0 is equal to 1750°, measurements from about 500°K upwards should not be corrected according to the formula (3) but by using the exact expression. Since this last point although understood, has not been carried out by others exactly, we will undertake here a new evaluation of the values of θ at different temperatures. The total specific heat of platinum has been measured in the range from 20 to 200°K by Simon and Zeidler (1926) and up to 1870°K recently by Jaeger and Rosenbohm (1939). Curve C_{tot} of fig. 4 shows the best fit through their measurements. If the electronic heat is now subtracted, a curve for the lattice heat only will result.

By using $T_0=1750$°K and $q=0{\cdot}18$ we obtain a curve for the lattice heat that approaches the classical value 5955 cal/deg.mol. fairly well for temperatures up to 800°K. It should be noticed that if the value $q=0{\cdot}25$ proposed by Hoare and Matthews had been used, the agreement would have been less satisfactory.

Fig. 4

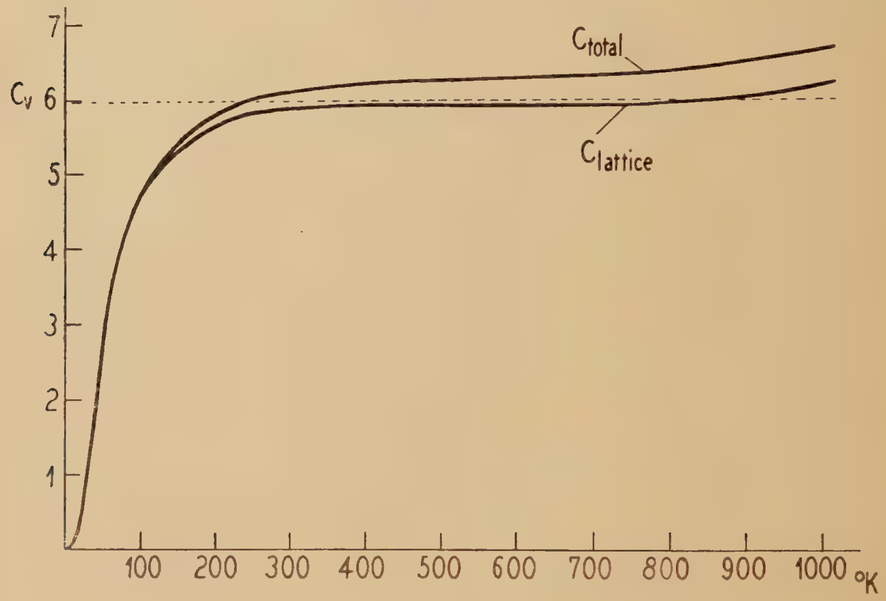

Fig. 5

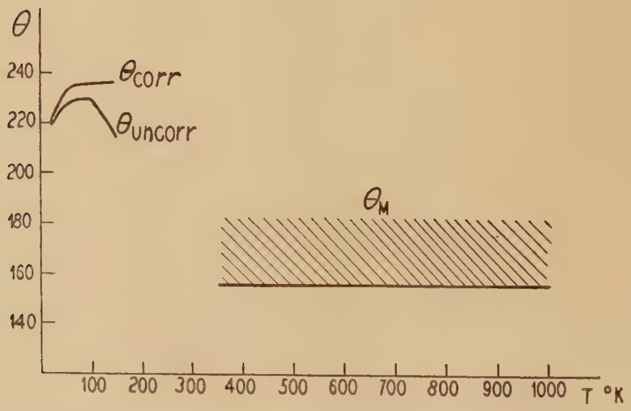

In the range where the slope is sufficient, the corrected curve can be used to calculate θ at different temperatures. The results are given in fig. 5. On the same plot the values of θ are shown as obtained by Simon and Zeidler from their measurements without correcting for the electronic heat. We notice that in this range θ should be given higher values around 235°

than the value 225° generally accepted. This gives also a better agreement with the value 233° found in the T^3 region. On the same figure we insert the results of this paper in the form of a shaded area.

The position of this area shows that the characteristic temperature θ_M, derived from the temperature factor of x-ray experiments, is decidedly lower than the value derived from specific heat measurements. In figs. 2 and 3 lines with a slope corresponding to $\theta_M=225°$ have been traced. It is obvious that in no case can this value be brought to agree with the x-ray results.

A possible reason for such a discrepancy could be the large difference in the temperatures at which the characteristic temperatures were determined from specific heat data and from x-ray intensities. The resulting change in θ due to expansion can be accounted for in the $T>\theta$ region by assuming an Einstein model for the vibrations with a frequency equal to $k\theta/h$. By using the formula (Mott and Jones, p. 19)

$$d \ln \nu_{\max}/d \ln V = -\alpha V_0/\chi_0 C_v,$$

the change of θ is calculated to $d\theta = -\alpha\theta(\alpha V_0/\chi_0 C_v)\, dT$. By inserting the experimental values (Mott and Jones, p. 318) a change of 9° (from 235 to 226) results when the temperature is changed from 0 to 700°K—the mean temperature of the x-ray experiments. This change is not sufficient to explain the far smaller value $\theta_M=156°$ found from the x-ray experiments.

The possibility of the anharmonic terms of vibration being excessively large should also be considered. Since no direct way of calculating these terms for Pt exists, the amplitude of vibration of Pt was compared to the amplitudes of Al, KCl, Cu, Ag, and Au for which the experimental results have been found to be well expressed by a Debye–Waller formula up to a quite high limiting temperature. The ratios of mean square displacements at the limiting temperature to the mean square displacements at the melting point have been computed for the cases mentioned and all fall in the region 0·55 to 0·67. The same ratio for Pt is 0·44 thus making it improbable that the anharmonic terms should be more important in Pt than in the other solids. Also the ratio of mean square displacements at the limiting temperature to the square of the interatomic distances are 0·15% for Pt against 0·23 to 0·48% for the other cases.

Platinum with Li and Na thus constitutes a third case of disagreement between θ_M and θ. All three give a θ_M value that is too low.

REFERENCES

ALEXOPOULOS, K., 1932, *Diplomarbeit* (E. T. H. Zurich).
ANDRIESEN, R., 1935, *Physica*, **2,** 417.
ARAKATSU, B., and SCHERRER, P., 1930, *Helv. Phys. Acta*, **3,** 428.
BLACKMAN, M., 1937, *Proc. Roy. Soc.* A, **152,** 416 ; 1951, *Proc. Phys. Soc.* A, **64,** 681.
CLUSIUS, K., and SCHACHINGER, L., 1947, *Z. Nat.*, 2 a, 90 ; 1952 a, *Ibid.*, 7a, 185; 1952 b, *Z. Ang. Phys.*, **4,** 442.
DAWTON, R. H. V. M., 1937, *Proc. Phys. Soc.*, **49,** 294.

Euthymiou, P., 1952, *Thesis* (Athens).
Hoare, F. E., and Matthews, J. C., 1952, *Proc. Roy. Soc.* A, **212,** 137.
Jaeger, E. M., and Rosenbohm, E., 1939, *Physica,* **4,** 1123.
James, R. W., and Brindley, G. W., 1928, *Proc. Roy. Soc.* A, **121,** 155.
James, R. W., Brindley, G. W., and Wood, R. G., 1929, *Proc. Roy. Soc.* A, **125,** 401.
Kok, J. A., and Keesom, W. H., 1936, *Physica,* **3,** 1035.
Mott, N. F., and Jones, H., 1936, *The Theory of the Properties of Metals and Alloys* (Oxford : Clarendon Press).
Owen, E. A., and Yates, E., 1934, *Phil. Mag.,* **17,** 113.
Owen, E. A., and Williams, R. W., 1947, *Proc. Roy. Soc.,* **188,** 509.
Pankow, G., 1936, *Helv. Acta,* **9,** 87.
Simon, F., and Swain, R. C., 1935, *Z. phys. Ch.* B, **28,** 189.
Simon, F., and Zeidler, W., 1926, *Z. phys. Chem.* A, **123,** 383.
Wohlfarth, E. P., 1948, *Proc. Leeds Phil. Soc.,* **5,** 89.

CL. CORRESPONDENCE

The Lattice Thermal Conductivity of Dilute Copper Alloys at Low Temperatures

By G. K. White* and S. B. Woods
Division of Physics, National Research Council, Ottawa, Canada

[Received September 20, 1954]

The lattice thermal conductivity, K_g, of metals at low temperatures has a particular interest as it appears to be limited at such temperatures by free electron scattering of the lattice waves or phonons, and therefore yields information on the interaction between phonons and free electrons. Apart from measurements on copper–nickel alloys (see, for example, Estermann and Zimmerman 1952) and recent work on silver–palladium alloys (Kemp *et al.* 1954), there appears to be little experimental knowledge of this interaction. It has been suggested (e.g. Gurevich 1945, Frederikse 1953, MacDonald 1954) that the phonon–electron interaction may play an important part in explaining the departures of the observed thermoelectric forces from those theoretically predicted.

As part of an investigation of the electrical resistance minimum and thermoelectric power, dilute copper–iron alloys having a relatively large residual electrical resistance have been produced in this laboratory; these seemed to us ideal subjects for study of the low temperature thermal conductivity and subsequent deduction of the lattice component.

The measurements of thermal and electrical conductivity were made between 2 and 150°K on rods of two different alloys in an apparatus which will be described more fully elsewhere. The method of measurement of the thermal conductivity was similar to that described by White (1953 a) and the electrical resistance was measured with a galvanometer amplifier (MacDonald 1947).

The total thermal conductivity is given by the sum of the lattice component, K_g, and the electronic component, K_e,

$$K=K_e+K_g, \qquad (1)$$

where the electronic thermal resistivity is

$$1/K_e=W_e=W_0+W_i. \qquad (2)$$

W_i is the ideal electronic thermal resistivity due to scattering by lattice vibrations; W_0 is the residual electronic thermal resistivity due to impurity scattering and should be related to the residual electrical resistance ρ_0 at a temperature T by the relation

$$\rho_0/W_0T=L, \qquad (3)$$

where L is the Lorentz number.

---

[*] National Research Laboratories Postdoctorate Fellow, at present on leave from Commonwealth Scientific and Industrial Research Organization (Australia).

The two alloys investigated were homogenized and annealed specimens containing nominally 0·056% and 0·0043% iron which gave residual electrical resistances at helium temperature of $0{\cdot}56\times10^{-6}$ and $0{\cdot}041\times10^{-6}$ ohm cm respectively (cf. pure copper at room temperature, $\rho=1{\cdot}72\times10^{-6}$ ohm cm). The respective alloys exhibited a resistance minimum at approximately 25° and 15°K, the resistance at 2°K being 5 to 8% higher than at the minimum.

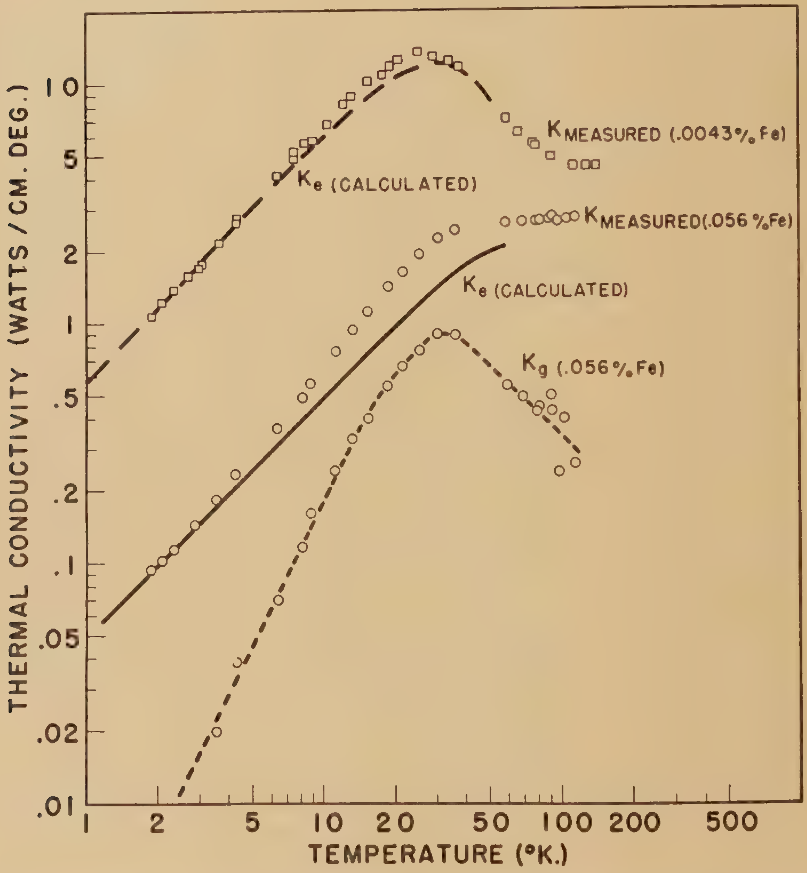

Experimental results for thermal conductivity of two dilute copper–iron alloys, and values deduced for electronic and lattice conductivities.

At temperatures below 20°K, $W_i \ll W_0$ and hence $K=K_0+K_g$. This, together with the fact that we expect $K_g \propto T^2$ (e.g. Makinson 1938, Klemens 1954) and to be very much less than K_0 below 4°K, enables us to obtain K_0/T or W_0T directly from the experimental values. This latter quantity, like ρ_0, should be constant if we neglect the possible effect of an anomaly associated with the resistance minimum. For the 0·056% and the 0·0043% alloys we obtain values for W_0T of 21·7 and 1·52 cm deg²/watt respectively, which give values for L (eqn. (3)) within a few per cent of the theoretical value of $2{\cdot}45\times10^{-8}$.

Values for W_i used to calculate the electronic conductivity, K_e, at temperatures above 20°K have been taken from previous work on pure copper (Berman and MacDonald 1952 and White 1953 b). This work indicates that for $T<50$°K, W_i can be well represented by $7{\cdot}1\times10^{-6}T^{2{\cdot}4}$ watt/cm deg. The calculated curves for K_e in the figure are then the function

$$K_e=1/W_e=(W_0+7{\cdot}1\times10^{-6}T^{2{\cdot}4})^{-1}$$

where $W_0=21{\cdot}7/T$ for the 0·056% alloy and $1{\cdot}52/T$ for the 0·0043% alloy. Values for K_g calculated from (1) are shown only for the 0·056% alloy in which the lattice contribution is comparable to the electronic contribution and hence the calculated results will not be seriously affected by small uncertainties in W_i or W_0.

In the region below 15°K, where the lattice waves are scattered predominantly by free electrons, we expect K_g to vary with T^2. The results, shown in the figure, are well represented by

$$K_g=1{\cdot}8\times10^{-3}T^2 \qquad (T<15°\mathrm{K}). \qquad . \; . \; . \; . \quad (4)$$

This compares with the value of $1{\cdot}4\times10^{-3}\,T^2$ calculated by Klemens from the ideal electronic conductivity K_i, assuming that the free electrons interact equally with transverse and longitudinal phonons.

It is of interest that if $K_g=1{\cdot}8\times10^{-3}T^2$, the phonon mean free path below 20°K will be approximately given by $2\times10^{-3}T^{-1}$ cm. The relatively strong phonon–electron interaction which we infer from these results lends substance to the suggestion of Gurevich that the equilibrium of phonons in the lattice may be disturbed by a flow of electrons at low temperatures. This may not only affect the thermoelectric power, but also the ideal electronic thermal conductivity, there being a marked disparity between theory and experiment in both these quantities.

ACKNOWLEDGMENTS

We are grateful to Dr. D. K. C. MacDonald and Dr. P. G. Klemens who have helped to stimulate our interest in the problem of electron–phonon interaction, and to Dr. W. B. Pearson who produced the copper–iron alloys.

REFERENCES

BERMAN, R., and MACDONALD, D. K. C., 1952, *Proc. Roy. Soc.* A, **211,** 122.
ESTERMANN, I., and ZIMMERMAN, J. E., 1952, *J. Appl. Phys.*, **23,** 578.
FREDERIKSE, H. P. R., 1953, *Phys. Rev.*, **92,** 248.
GUREVICH, L., 1945, *J. Phys. U.S.S.R.*, **9,** 477.
KEMP, W. R. G., KLEMENS, P. G., SREEDHAR, A. K., and WHITE, G. K., 1954, *Proc. Phys. Soc.* A, **67,** 728.
KLEMENS, P. G., 1954, *Aust. J. Phys.*, **7,** 57.
MACDONALD, D. K. C., 1947, *J. Sci. Instrum.*, **24,** 232 ; 1954, *Physica* (Proc. of Amsterdam Conf. on Semi-Conductors).
MAKINSON, R. E. B., 1938, *Proc. Camb. Phil. Soc.*, **34,** 474.
WHITE, G. K., 1953 a, *Proc. Phys. Soc.* A, **66,** 559 ; 1953 b, *Aust. J. Phys.*, **6,** 397.

CLI. *Notices of New Books and Periodicals received*

Twinning and Diffusionless Transformations in Metals. By E. O. Hall. (Butterworths Scientific Publications, London.) [Pp. ix+191.] Price 30*s*.

The study of the related fields covered by the title, after a long period of inactivity, has revived in the last decade, and the extensive advances made justify this detailed review. Dr. Hall's monograph is written in a self-contained form, including chapters on elementary crystallography and on the 'way of life' which has grown up around the experimental investigation of metallic single crystals.

The crystallographic treatment of twinning mostly covers classical material (however, some of the twinning elements of titanium listed in Table V and referred to on p. 75, seem to have been arrived at by an unsatisfactory method of inspired guesswork), but recent advances make up the bulk of the chapter on Formation of Twins under Stress. The fragmentary nature of the information here presented is no reflection on the author, but rather serves to emphasize that this topic is at the frontier of present knowledge. By contrast, in the chapter on annealing twins a much more unified picture is presented. The chapter on Theories of Twin Formation is prefaced by an introduction to dislocation theory which is, perhaps necessarily, too condensed to be of much help to the complete beginner. The dislocation theory of twinning is well presented, and the author reflects the present incomplete state of theoretical understanding by referring to the Russian elastic treatment of twinning and commenting that a synthesis between the two approaches remains to be made.

The chapter on diffusionless transformations deals largely with crystallography; Dr. Hall expounds this involved subject fully and clearly. Purely metallurgical aspects, as for instance the stabilization of austenite, are excluded. No unified theory of the crystallographic nature of these transformations was available to the author when he wrote, and it is a measure of the pace of current research that in the past year no fewer than three rival theories have been published.

The book can be confidently recommended as a reliable source of information and as a stimulating introduction for research workers entering the field.

R. W. C.

Theoretical Elasticity. By A. E. Green and W. Zerna. (Oxford: University Press.) Price 50*s*.

Interest in the theory of elasticity as distinct from the applications of the theory has, during recent years, very greatly increased, largely for two reasons. The first is the development of complex variable methods in this country by Stevenson, Green and others and to the belated discovery of the work of Muskhelishvili in Russia. The second is the work of Green, Rivlin and others on finite deformations facilitated by the systematic use of the tensor notation.

These two developments and elastic shell theory are the main topics discussed in this very useful and timely book which should be widely read. It is, as the title implies, a book on the theory of the subject and is written for those whose interests are primarily mathematical.

It is clear and as easy to follow as the nature of the subject permits though, in the reviewer's opinion, it would be improved by the addition of a bibliography at the end of each chapter. The book is well produced and is at a reasonable price and is a worthy successor to the recent volumes of applied mathematics from the same publishers.

W. M. S.

The Theory of Cohesion. By M. A. JASWON. (Pergamon Press.) [Pp. 245.] Price 37*s*. 6*d*.

"AN outline of the cohesive properties of electrons in atoms, molecules and crystals", is the subtitle of this book. It is intended to be an introduction to the subject, preparatory to reading the standard treatises; but surely three initial chapters on wave mechanics are superfluous nowadays. The various approximations for the helium atom and hydrogen molecule are given at length, with a chapter on Molecular Orbitals. After a sketch of the theory of metals, the results are given of the cellular approximation applied to alkali, divalent, and noble metals, and certain alloys. The final chapter deals with covalent structures. But the text is very incomplete. For the student, there is no general account of types of binding forces (cohesive energy itself is only defined in a footnote), so that he will find it difficult to see the relevance of each succeeding topic. On the other hand, some modern work of great interest, such as the theory of plasma oscillations, is deliberately excluded. There is no reference at all to Slater's MIT reports. This book may provide useful summaries of certain topics for research workers, but is too inelegant and incoherent to be recommended as an introduction. J. M. Z.

[*The Editors do not hold themselves responsible for the views expressed by their correspondents.*]

INDEX TO VOL. 45.

Abdou (A. H.), slip lines and pits, 105.

Alexopoulos (K). and Euthymiou (P.), characteristic temperature of platinum, 1332.

Alkali metals, cohesion (March), 325.

Almond (M.), *see* Clegg, 583.

Aluminium, plastically deformed, etchpit attack (Forsyth), 344.

Aluminium–copper alloys, direct evidence of dislocations (Wilsdorf and Kuhlmann-Wilsdorf), 1096.

Andersson (G.), electromagnetic separation of spallation products, 621.

Angular correlation experiment, the source (Breitenberger), 497.

Angular distribution experiments, reduction by least squares (Price), 237.

Angular and energy distributions, energetic pion interactions (Morrish), 47.

Anomalous electron-scattering in metals (MacDonald and Pearson), 491.

Anomalous spin of ^{47}Ti (Flowers), 329.

Appapillai (V.), Mailvaganam (A. W.), and Wolfendale (A. W.), cloud chamber study of inter actions of fast μ–mesons, 1059.

Armenteros (R.), *see* Podolanski, 13.

Atmospherics with long trains of pulses (Hepburn and Pierce), 917.

Atomic systems, slow elastic collisions (Massey and Bates), 111.

Barron (T. H. K.) and Domb (C.), velocity of elastic waves in solidified inert gases, 654.

Bassani (F.) and Fumi (F. G.), alkali halide crystals, impurities, ion vacancies, association energy, 228.

Bates (D. R.) and Massey (H. S. W.), slow elastic collisions between atomic systems, 111.

Bennett (J. E.), *see* Ingram, 545.

Bergenlid (U.), Hill (R. W.), Webb (F. J.) and Wilks (J.), specific heat of graphite below 90°K, 851.

^{9}Be, disintegration by 6 MeV γ rays (Carver, Kondarah and McDaniel), 948.

β-decay of K meson (Friedlander *et al.*), 1043.

—— (Dahanayake *et al.*), 1219.

Bhatia (A. B.) and Tauber (G. E.), characteristic temperatures for cubic crystals, 1211.

Biggs (W. D.) and Broom (T.), Yield strength of partly ordered Cu$_3$Au wires, 246.

Bijl (D.) and Pullan (H.), thermal expansion of solids at low temperatures, 290.

Bilby (B. A.) and Bullough (R.), formation of twins by a moving crack, 631.

Bishop (G. R.), Daniels (J. M.), Durand (H.), Johnson (C. E.) and Perez (J.), polarized γ rays from oriented ^{54}Mn, 1197.

Bleaney (B.), Llewellyn (P. M.) and Pryce (M. H. L.), paramagnetic resonance in Plutonyl rubidium nitrate and spin of ^{239}Pu, 773.

——, nuclear spin of ^{241}Pu, 991.

——, and Hall, paramagnetic resonance in neptunyl rubidium nitrate, 992.

Bocchieri (P.) and Feldman (G.), double pion production and pseudoscalar coupling, 1145.

Books, new :—Alfven, Origin of the solar system, 996 ; Bickley, Bessel functions and formulae, 661 ; Birks, Scintillation counters, 107 ; Braddick, Physics of Experimental method, 884 ; Carter, Electromagnetic field in its engineering aspect, 885 ; Chadwick, Radioactivity and radioactive substances, 107 ; Chapman and Cowling, Mathematical theory of non-uniform gases, 106 ; Chaundry, Barrett and Batey, Printing of Mathematics, 662; Corson, Tensors, spinors and relativistic wave-equations, 234; Cottrell, Dislocations and plastic flow in crystals, 661; Courant and Hilbert, Methods of mathematical physics, 106; Craggs and Meek, High voltage laboratory technique, 660; Crowther, The sciences of energy, 994; Faraday Society, The first fifty years 1903–53, 236; Frisch, Progress in nuclear physics, 883; Gaydon and Wolfhard, Flames, 110; Gillespie, Signal noise in nuclear counter amplifiers, 550; Gomer and Smith, Structure and properties of solid surfaces, 885; Green and Zerna, Theoretical elasticity, 1346; Gurney, Ionic processes in solution, 346; Hall, Twinning and diffusionless transformations in metals, 1346; Howarth, Modern developments in fluid mechanics, 550; Hughes, Neutron optics, 661; Jaswon, Theory of cohesion, 1346; Jaynes, Ferroelectricity, 235; Jeffreys, The Earth, 662; Ketelaar, Chemical constitution, 108; Kittell, Solid state physics, 109; Klemperer, Electron optics, 234; Kronig, Textbook of physics, 995; Lewis and Wells, Millimicrosecond pulse techniques, 1098; Milne, Differential Equations, 346; Physical Society, Progress in physics, 994; Ramsay, Nuclear moments, 884; Rotblat, Atomic energy, 660; Royal Astronomical Society, occasional notes, 886; Segre, Experimental nuclear physics Vol. II, 110; Shea, Transistor circuits, 235; Stewart, Ferromagnetic domains, 1098; Struik, Concise history of mathematics, 1224; Synge, Geometrical mechanics and de Broglie waves, 994; Verma, Crystal growth and dislocations, 106; Wilson, Theory of metals, 108; Wooley and Stubbs, Outer layers of a Star, 109; Zwikker, Physical properties of solid materials, 996.

^{10}B (α, pγ) ^{13}C, angular correlations and distributions (Stanley), 430.

^{11}B (d, n) ^{12}C, angular distribution of neutrons (Graue), 1205.

Boundary layer growth in three dimensions (Squire), 1272.

Boundary layer growth, spinning body (Illingworth), 1.

Braddick (H. J. J.) and Leontic (B.), cosmic ray interactions underground, 1287.

Bransden (B. H.) and McKee (J. S. C.), elastic scattering of neutrons by α particles, 869.

Breitenberger (E.), the source in an angular correlation experiment, 497.

Brenner (S.), Brown (G. E.) and Elton (L. R. B.), elastic scattering of electrons by mercury, 524.

Broom (T.), *see* Biggs, 246.

Brown (G. E.), *see* Brenner, 524.

Brownian movement of linear and non-linear systems (MacDonald), 63, 345.

—— (Polder), 69.

Buchanan (J. S.), Cooper (W. A.), Millar (D. D.) and Newth (J. A.), *V*-events, fourty-four charged, 1025.

Bullen (T. G.), *see* Skinner, 1070.

Bullough (R.), *see* Bilby, 631.

Burbidge (E. Margaret) and Burbidge (G. R.), Freundlich's proposed red-shift law, observational data, 1019.

Burrow (J. H.) and Mitchell (J. W.), thin films of silver sulphide, silver and gold, 208.

Butement (F. D. S.) and Poë (A. J.), radioactivity of neutron excess iridium, 31.

——, a 7-second iridium isomer, 1090.

Camagni (P.), Chiarotti (G.), Fumi (F. G.) and Giulotto (L.), $F \to Z_1$ conversion in KCl, 225.

Cartwright (D.), Green (L. L.) and Willmott (J. C.), α particles from ^{14}N (d α) angular distribution at low energies, 742.

Carver (J. H.) and Kondaiah (E.), photo-neutron yield from Copper for Li γ rays, 998.

Carver (J. H.), Kondaiah (E.) and McDaniel (B. D.), neutrons and α particles from ^{9}Be by γ rays, 948.

Cerenkov radiation and bremsstrahlung (Lawson), 748.

Chackett (K. F.), Fremlin (J. H.) and Walker (D.), nuclear reactions by N and O ions, 173.

Chackett (K. F.) and Fremlin (J. H.), forward displacement of ^{13}N produced by ^{14}Al, 735.

Chandrasekhar (S.), inhibition of convection by magnetic field II, 1177.

Characteristic temperatures for cubic crystals (Bhatia and Tauber), 1211.

Characteristic temperature of platinum (Alexopoulos and Euthymiou), 1332.

Charged hyperons in emulsions (Friedlander), 418.

Chester (W.), quasi-cylindrical shock tube, 1293.

Chiarotti (G.), *see* Camagni, 225.

Chinneck (A.), *see* Holder, 997.

Clegg (J. A.), Almond (M.) and Stubbs (P. H. S.), remanent magnetism, sedimentary rocks, 583.

Cole (G. H. A.), *see* Eisenschitz, 394.

Collins (L. E.) and Heavens (O. S.), magnetic behaviour of nickel crystal films, 283.

Cooper (W. A.), *see* Buchanan, 1025.

Cosmic radiation, alpha particle component (Waddington), 1312.

Cosmic radio-frequency radiation, isotropic compound (Shakeshaft), 1136.

Cosmic ray interactions underground (Braddick and Leontic), 1287.

Cosmic ray heavy nuclear fragmentations (Gottstein), 347.

Cosmic ray particles, acceleration (Thompson), 1210.

Cosmic rays, time variations of extensive air showers (Cranshaw and Galbraith), 1109.

Cox (H. L.), *see* Pursey, 295.

Cranshaw (T. E.) and Galbraith (W.), extensive air showers, cosmic rays, time variations, 1109.

Critical shear stress and work hardening, temperature dependence (Seeger), 771.

Croft (A. J.), Olsen-Barr (J. L.) and Powell (R. W.), gallium, superconductivity, anisotropy, 123.

Coulomb excitation of isomeric states in Silver (Huus and Lunden), 966.

Counters with random dead time (Ramakrishnan), 1050.

Cu_3Au, ordering effects at 100°c (Dugdale and Green), 163.

Cunliffe (A.), *see* Gould, 818.

Curran (S. C.), *see* Dixon, 683.

Dagg (M.), *see* Maxwell, 551.

Dahanayake (C.), Francois (P. E.), Fujimoto (Y.), Iredale (P.), Waddington (C. J.) and Yasin (M.), heavy mesons and hyperons, associated production, 885.

——, β decay of K mesons, 1219.

Daniels (J. M.), *see* Bishop, 1197.

Dearnaley (G.), elastic scattering of protons by fluorine, 1213.

Delayed disintegration of a nuclear fragment (Solheim and Sörensen), 1284.

Deruyttere (A.) and Greenough (G. B.), Zinc single crystals, cleavage planes, markings, 624.

Deuterons, interactions with Carbon (Freemantle, Gibson and Rotblat), 1200.

Deuteron reactions, angular correlations (Stanley), 807.

Diamond, hardness properties, cube faces (Wilks and Wilks), 844.

Diffusion of nitrogen in alpha iron (Thomas and Leak), 656.

Diffusion of carbon in alpha iron (Thomas and Leak), 986.

Dilute copper alloys, electrical resistance minimum (Pearson), 1087.

Discrete radio sources (Twiss), 249.

Dislocation acceptor centres, statistics of occupation (Read), 1119.

Dislocations in Germanium, theory (Read), 775.

Dixon (D.) and McNair (A.), natural radioactivity in Nd, Rh and Os, 1099.

Dixon (D.), McNair (A.) and Curran (S. C.), natural radioactivity of Lutetium, 683.

Domb (C.), *see* Barron, 654.

Double pion production and pseudoscalar coupling (Bocchieri and Feldman), 1145.

Dugdale (J. S.) and MacDonald (D. K. C.), thermodynamic properties of low boiling point elements, influence of zero-point energy, 811.
Dugdale (R. A.) and Green (A.), Cu^3Au, ordering effects at 100°c, 163.
Durand (H.), *see* Bishop, 1197.
Edwards (S. F.), divergence of perturbation method in field theory, 758.
Eisenschitz (R.) and Cole (G. H. A.), Liquid viscosity, effect of electric field, theory, 394.
Elasticity, slightly anisotropic materials (Pursey and Cox), 295.
Elastic moduli and plastic properties of pure metals (Pugh), 823.
Elastic scattering of neutrons by α particles (Bransden and McKee), 869.
Elastic scattering of protons by fluorine (Dearnaley), 1213.
Electromagnetic separation of spallation products (Andersson), 621.
Electronic wave functions in crystals (Jenkins and Pincherle), 93.
Elton (L. R. B.), *see* Brenner, 524.
Energy band shapes and band widths in metals (Raimes), 727.
Euthymiou (P.), *see* Alexopoulos, 1332.
Fatigue fracture of copper (Wadsworth and Thompson), 223.
Feldman (G.), *see* Bocchieri, 1145.
Feltham (P.), polycrystals, β-flow, Mott's theory, 9.
Finlay-Freundlich (E.), red shifts in spectra of celestial bodies, 303.
Flowers (B. H.), anomalous spin of ^{47}Ti, 329.
19 Fluorine excitation of levels (Jones and Wilkinson), 230.
Formation of twins by a moving crack (Bilby and Bullough), 631.
Forsyth (P. J. E.), aluminium, plastically deformed, etchpit attack, 344.
Francis (J. R. D.), wave motions and aerodynamic drag on free oil surface, 695.
Francois (P. E.), *see* Dahanayake, 885, 1219.
Freemantle (R. G.), Gibson (W. M.) and Rotblat (J.), Deuterons, 19 Mev, interactions with Carbon, 1200.
Freemantle (R. G.), Grothal (T.), Gibson (W. M.), McKeague (R.), Prowse (D. J.) and Rotblat (J.), scattering of deuterons and protons by α particles, 1090.
Fremlin (J. H.), *see* Chackett, 173, 735.
Freundlich's proposed red-shift law (Burbidge and Burbidge), 1019.
Freundlich's red shift (ter Haar), 320, 1023.
Freundlich's red-shift, Astrophysical considerations (McCrea), 1010.
Friedlander (M. W.), charged hyperons in emulsions, 418.
——, Keefe (D.), Menon (M. G. K.) and Merlin (M.), mass of Λ^0-particle, 533.
Friedlander (M. W.), Keefe (D.), Menon (M. G. K.) and van Rossum (L.), β-decay of K meson, 1043.
Frisch (O. R.) and Littler (D. J.), pile modulation and fluctuations, 126.
Fujimoto (Y.), *see* Dahanayake, 885, 1219.
Fumi, (F. G.), *see* Camagni, 225.
——, *see* Bassani, 228.
$F \rightarrow Z_1$ conversion in KCl (Camagni *et al.*), 225.
Gadd (G. E.), *see* Holder, 997.
Galbraith (W.), *see* Cranshaw, 1109.
Gallium, superconductivity, anisotropy (Croft, Olsen-Barr and Powell), 123.
Gamma radiation from $^{228}_{90}Th$ (Newton and Rose), 58.
Gayther (D. B.), lifetimes of θ^0- and Λ^0-particles, 570.
General circulation of atmosphere (Lighthill), 1154.
Gibson (W. M.), *see* Freemantle, 1090, 1200.
Giulotto (L.), *see* Camagni, 225.
Gottstein (K.), heavy cosmic ray nuclei, fragmentation, 347.
Gould (R. N.) and Cunliffe (A.), extended use of perturbation theory, 818.
Grace, (M. A.), Johnson (C. E.), Kurti (N.), Lemmer (H. R.) and Robinson (F. N. H.), nuclear orientation of ^{54}Mn, 1192.

Grain boundary diffusion, concentration contours (Whipple), 1225.
Graue (A.), ^{11}B (d, n) ^{12}C, angular distribution of neutrons, 1205.
Green (A.), *see* Dugdale, 163.
Green (L. L.), *see* Cartwright, 742.
Greenough (G. B.), *see* Deruyttere, 624.
Greenhow (J. S.), wind measurements at altitudes of 80–100 km, 471.
Grey tin, electronic conduction (Kendall), 141.
Grotdal (T.), *see* Freemantle, 1090.
Hall (G. R.), *see* Bleaney, 991, 992.
Hall (I. M.), supersonic flow, flat nosed circular cylinders, 333.
Ham (A. C.) and Jackson (L. C.), Helium film, thickness of saturated, above and below λ point, 1084.
Hanbury Brown (R.), Twiss (R. Q.), Interferometer for Radio astronomy, 663.
Heats of formation, calculation, binary alloys (Varley), 887.
Heavens (O. S.), *see* Collins, 283.
Heavy mesons and hyperons, associated production (Dahanayake *et al.*), 885.
Helium film, thickness, saturated (Ham and Jackson), 1084.
Helium II film, unsaturated, thickness (McCrum and Mendelssohn), 102.
Helium and tritium produced in steel by protons (Martin *et al.*), 410.
Hellawell (A.) and Hume-Rothery (W.), lattice spacings of dilute solid solutions, 797.
Hepburn (F.) and Pierce (E. T.), atmospherics with long trains of pulses, 917.
Hercus (G. R.) and Wilks (J.), specific heat of liquid helium II, as a function of pressure, 1163.
Hill (R. W.) and Ricketson (B. W. A.), solid hydrogen, λ anomaly, specific heat, 277.
Hill (R. W.), *see* Bergenlid, 851.
Hirst (F.), Johnstone (I.) and Poole (M. J.), d-^6Li reactions, 762.
Hitchcock (A.), spins of odd-odd nuclei in j–j coupling model, 379, 385.
Hodgson (P. E.), nuclear disintegrations by protons II, 190.
Holder (D. W.), Chinneck (A.) and Gadd (G. E.), interaction of shock wave with supersonic stream bounded by wall, 997.
Hume-Rothery (W.), *see* Hellawell, 797.
Huus (T.) and Lundén (A.), coulomb excitation of isomeric states in silver, 966.
Ideal crystal at absolute zero (Salter), 360.
Ideal Fermi–Dirac gas (Lidiard), 202.
Illingworth (C. R.), boundary layer growth, spinning body, 1.
Inall (E. K.), ^7Li, ^8Be, ^4He, γ–α angular correlation, 768.
Ingram (D. J. E.) and Bennett (J. E.), paramagnetic resonance in activated carbon, 545.
Ingram (D. J. E.) and Tapley (J. G.), paramagnetic resonance at radiofrequencies in carbon, 1221.
Inhibition of convection by magnetic field II (Chandrasekhar), 1177.
Interaction of an arrested charged hyperon (Johnston and O'Ceallaigh), 424.
Interaction of dislocation and charged solute ion (Landauer), 1216.
Ionisation of fast nitrogen ions (Stephens and Walker), 543.
Ionized gas, collisional effects and conduction current (Ware), 547.
Iredale (P.), *see* Dahanayake, 885, 1219.
Iridium, 7-second isomer (Butement and Poë), 1090.
Isotopic selection rules, ^{10}B (Jones and Wilkinson), 703.
Jackson (L. C.), *see* Ham, 1084.
Jenkins (D. P.) and Pincherle (L.), electronic wave functions in crystals, 93.
Johnson (C. E.), *see* Grace, 1192.
——, *see* Bishop, 1197.
Johnson (F. B.) and Pease (R. S.), pile irradiation of quartz oscillators, 651.
Johnston (J. E.), *see* Skinner, 1070.
Johnston (R. H. W.) and O'Ceallaigh (C.), interaction of an arrested charged hyperon, 424,

Johnstone (I.), *see* Hirst, 762.
Jones (G. A.) and Wilkinson (D. H.), excitation of levels in ^{19}F, by α particles, 230.
——, isotopic selection rules, radiations from ^{10}B, 703.
Jones (G. O.) and Martin (D. L.), specific heat of lithium fluoride at low temperatures, 649.
Keefe (D.), *see* Friedlander, 533, 1043.
Kendall (J. T.), grey tin, electronic conduction, 141.
Klemens (P. G.), thermoelectric power of monovalent metals at high temperature, 881.
Kolsky (H.), propagation of longitudinal elastic waves along cylindrical bars, 712.
Kondaiah (E.), *see* Carver, 948, 988.
Kuhlmann-Wilsdorf (Doris), *see* Wildorf, 1096.
Kurti (N.), *see* Grace, 1192.
Λ^0-particle, mass (Friedlander, Keefe, Menon and Merlin), 533.
Λ^0-particles, new estimate of life time (Page), 863.
Landauer (R.), interaction of dislocation and charged solute ion, 1216.
Landsberg (P. T.), third law of thermodynamics, restricted quantum statistical proof, 1129.
Lattice spacings of dilute solid solutions (Hellawell and Hume-Rothery), 797.
Lattice thermal conductivity of dilute copper alloys at low temperatures (White and Woods), 1343.
Lawson (J. D.), Cerenkov radiation and bremsstrahlung, 748.
^{207}Lead, photo-production of isomeric state (Reid and McNeill), 957.
Leak (G. M.), *see* Thomas, 656, 986.
Lemmer (H. R.), *see* Grace, 1192.
Leontic (B.), *see* Braddick, 1287.
Lidiard ((A. B.), ideal Fermi–Dirac gas, 202.
Lifetimes of θ^0- and Λ^0-particles (Gayther), 570.
Lighthill (M. J.), general circulation of atmosphere, 1154.
Liquid helium in narrow gaps (McCrum), 1302.
Liquid viscosity, theory, effect of electric field (Eisenschitz and Cole), 394.
d-^{6}Li reactions (Hirst, Johnstone and Poole), 762.
^{7}Li, ^{8}Be, ^{4}He, γ–α angular correlation (Inall), 768.
^{7}Li (pγ) ^{8}Be, special mechanisms (Wilkinson), 259.
Littler (D. J.), *see* Frisch, 126.
Llewellyn (P. M.), *see* Bleaney, 773, 991, 992.
Longitudinal elastic waves along cylindrical bars, propagation (Kolsky), 712.
Lundén, *see* Huus, 966.
McCrea (W. H.), Freundlich's red-shift, astrophysical considerations, 1010.
McCrum (N. G.), liquid helium in narrow gaps, 1302.
McCrum (N. G.) and Mendelssohn (K.), thickness of unsaturated He II film, 102.
McDaniel (B. D.), *see* Carver, 948.
McDiarmid (I. B.), large angle scattering of μ-mesons in lead, 933.
MacDonald (D. K. C.), Brownian movement of linear and non-linear systems, 63, 345.
—— and Pearson (W. B.), anomalous electron-scattering in metals, 491.
—— *see* Dugdale, 881.
Machin (K. E.) and O'Brien (P. A.), radio frequency radiation from sunspots, emission polar diagram, 973.
McKeague (R.), *see* Freemantle, 1090.
McKee (J. S. C.) *see* Bransden, 869.
McNair (A.), *see* Dixon, 683, 1099.
McNeill (K. G.), *see* Reid, 957.
Magnetic properties of alloys, Cu and Ni with Pl and Pt (Wohlfarth), 647.
Magnetic viscosity in precipitation alloys (Phillips, Street and Woolley), 505.
Magnetism, remanent, sedimentary rocks (Clegg, Almond and Stubbs), 583.

Mailvaganam (A. W.), *see* Appapillai, 1059.
March (N. H.), alkali metals, cohesion, Thomas–Fermi–Dirac theory, 325.
Martin (D. L.), *see* Jones, 649.
Martin (G. R.), Thomson (S. J.), Wardle (G.) and Mayne (K. I.), helium and tritium produced in steel by protons, 410.
Massey (H. S. W.), *see* Bates, 111.
Mathematical Tables, unpublished, Royal Society depository, 599.
Matthews (P. M.), *see* Ramakrishnan, 1053.
Maxwell (A.), turbulence in the upper ionosphere, 1247.
Maxwell (A.) and Dagg (M.), radio-astronomical investigation of drift movements in upper atmosphere, 551.
Mayne (K. I.), *see* Martin, 410.
Mechanism of rolling friction (Tabor), 1081.
Mendelssohn (K.), *see* McCrum, 102.
Menon (M. G. K.), *see* Friedlander, 533, 1043.
Mercury, elastic scattering of electrons by (Brenner, Brown and Elton), 524.
Merlin (M.), *see* Friedlander, 533.
Metal surface in conduction theory, physical nature (Müser), 1237.
Millar (D. D.), *see* Buchanan, 1025.
Mitchell (J. W.), *see* Burrow, 208.
Mitchell (R. S.), polytypism of cadmium iodide, 1093.
Morrish (A. H.), pion interactions angular distribution, energetic, 47.
Multiple scattering, measurement (Överas), 158.
μ-mesons, anomalous scattering (Rochester and Wolfendale), 980.
μ-mesons, interactions of fast (Appapillai, Mailvaganam and Wolfendale), 1059.
μ-mesons, large angle scattering in lead (McDiarmid), 933.
Müser (H. A.), metal surface in conduction theory, physical nature, 1237.
NaCl and KCl crystals (Bassani and Fumi), 228.
Natural radioactivity of Lutetium (Dixon, McNair and Curran), 683.
Natural radioactivity, Nd, Rh, Os, search (Dixon and McNair), 1099.
Neutral V-particles, decay in emulsions (Yasin), 413.
Neutron scattering and the weak interaction model of the nucleus (Scott), 751.
Neutron widths and density of nuclear levels (Scott), 1322.
Newth (J. A.), *see* Page, 38.
——, *see* Buchanan, 1025.
Newton (J. O.) and Rose (B.), γ radiation from $^{228}_{90}$Th, 58.
Nickel single-crystal films, magnetic behaviour (Collins and Heavens), 283.
^{13}N, forward displacement produced by ^{14}Al (Chackett and Fremlin), 735.
^{14}N(d, α) α particles, angular distribution (Cartwright, Green and Wilmott), 742.
Nuclear disintegrations by protons II (Hodgson), 190.
Nuclear orientation of ^{54}Mn (Grace *et al.*), 1192.
Nuclear reactions by ions (Chackett, Fremlin and Walker), 173.
Nuclear spin of ^{241}Pu (Bleaney, Llewellyn and Pryce), 991.
O'Brien (P. A.), *see* Machin, 973.
O'Ceallaigh (C.), *see* Johnston, 424.
Olsen-Barr (J. L.), *see* Croft, 123.
One dimensional fluid, molecular distribution functions (Ramakrishnan), 401, 1053.
Överas (H.), multiple scattering, measurement, 158.
Page (D. I.), Λ^0-particles, lifetime, new estimate, 863.
—— and Newth (J. A.), $V_1{}^0$-particles, life time, 38.
Paramagnetic resonance at radio-frequencies (Ingram and Tapley), 1221.
—— in activated carbon (Ingram and Bennett), 545.
—— plutonyl rubidium nitrate (Bleaney, Llewellyn and Pryce), 773.
Pearson (W. B.), electrical resistance minimum in dilute copper alloys, 1087.
——, *see* MacDonald, 491.
Pease (R. S.), *see* Johnson, 651.

Penrose (O.), quantization of sound waves, 80.
Perez (J.), *see* Bishop, 1197.
Perturbation method in field theory, divergence (Edwards), 758.
Perturbation theory, extended use (Gould and Cunliffe), 818.
Phillips (J. H.), Street (R.) and Woolley (J. C.), magnetic viscosity in precipitation alloys, 505.
Photo-neutron yield from Copper for Li γ rays (Carver and Kondaiah), 988.
Pierce (E. T.), *see* Hepburn, 917.
Pile irradiation of quartz oscillators (Johnson and Pease), 651.
Pile modulation and fluctuations (Frisch and Littler), 126.
Pincherle (L.), *see* Jenkins, 93.
Plaskett (J. S.), self trapped electrons in a Fermi gas, 1255.
Podolanski (J.) and Armenteros (R.), *V*-events, analysis, 13.
Poë (A. J.), *see* Butement, 31, 1090.
Polarized γ rays from ^{54}Mn (Bishop *et al.*), 1197.
Polder (D.), Brownian movement in linear and non-linear systems, 69.
Polycrystals, β-flow, Mott's theory (Feltham), 9.
Polytypism of Cadmium Iodide (Mitchell), 1093.
Poole (M. J.), *see* Hirst, 762.
Powell (R. W.), *see* Croft, 123.
Price (P. C.), angular distribution experiments, reduction by least squares, 237.
Pritchard (H. O.) and Sumner (F. H.), property of ‘ repeating ’ secular determinants, 466.
Propagation of heat in liquid helium (Ziman), 100.
Property of ‘ repeating ’ secular determinants (Pritchard and Sumner), 466.
Prowse (D. J.), *see* Freemantle, 1090.
Pryce (M. H. L.), *see* Bleaney, 773, 991, 992.
Pugh (S. F.), elastic moduli and plastic properties of pure metals, 823.
Pullan (H.), *see* Bijl, 290.
Pursey (H.) and Cox (H. L.), elasticity measurements, slightly anisotropic materials, 295.
Quantization of sound waves I (Penrose), 80.
Quasi-cylindrical shock tube (Chester), 1293.
Radioactivity of neutron excess iridium isotopes (Butement and Poë), 31.
Radio astronomy, new type of interferometer (Hanbury Brown and Twiss), 663.
Radiofrequency radiation from sunspots (Machin and O'Brien), 973.
Raimes (S.), energy band shapes and band widths in metals, 727.
Ramakrishnan (A.), one dimensional fluid, molecular distribution functions, 401.
—— counters with random dead time, 1050.
—— and Matthews (P. M.), molecular distribution functions of one dimensional fluid, 1053.
Read, (W. T.) Jr., dislocations in germanium, 775.
——, dislocations in acceptor centres, 1119.
Red shifts in spectra of celestial bodies (Finlay-Freundlich), 303.
Reid (J. M.) and McNeill (K. G.), photo-production of isomeric state in ^{207}Lead, 957.
Ricketson (B. W. A.), *see* Hill, 277.
Robinson (F. N. H.), *see* Grace, 1192.
Rochester (G. D.) and Wolfendale (A. W.), μ-mesons, anomalous scattering, 980.
Rose (B.), *see* Newton, 58.
Rosenberg (H. M.), conductivity at low temperatures, magnesium, 73.
—— ——, gallium crystal, 767.
Rotblat (J.), *see* Freemantle, 1090, 1200.
Royal Society, depository for mathematical tables, 599.
Salter (L.), ideal crystal at absolute zero, 360.
——, Simon melting equation, 369.
Scattering of deuterons and protons by α particles (Freemantle *et al.*), 1090.
Scott (A. B.), surface energy of sodium, 1173.
—— ——, of colloidal metals in ionic lattices, 610.

Scott (J. M. C.), surface of a nucleus, 441.
——, neutron scattering and the weak interaction model, 751.
——, neutron widths and density of nuclear levels, 1322.
Seeger (A.), critical shear stress and work hardening, temperature dependence, 771.
Self trapped electrons in a Fermi gas (Plaskett), 1255.
Shakeshaft (J. R.), cosmic radio-frequency radiation, isotropic component, 1136.
Shock wave interaction with supersonic stream (Holder, Chinneck and Gadd), 997.
Simon melting equation (Salter), 369.
Skinner (H. W. B.), Bullen (T. G.) and Johnston (J. E.), soft x-ray spectra, notes, Fe group, 1070.
Slip lines and pits (Abdou), 105.
Soft x-ray spectra, particularly of the Fe group (Skinner, Bullen and Johnston), 1070.
Solheim (A.) and Sörensen (S. O.), delayed disintegration of a nuclear fragment, 1284.
Solid hydrogen, specific heat, λ-anomaly (Hill and Ricketson), 277.
Sörensen (S. O.), *see* Solheim, 1284.
Specific heat of graphite below 90°K (Bergenlid, Hill, Webb and Wilks, J.), 851.
Specific heat of liquid helium—II, pressure (Hercus and Wilks), 1163.
Specific heat of lithium fluoride at low temperatures, 649.
Spins of odd–odd nuclei (Hitchcock), 379, 385.
Squire (L. C.), boundary layer growth in three dimensions, 1272.
Stanley (A. G.), angular correlations, deuteron reactions, 807.
——, ^{10}B (α, pγ) ^{13}C, 430.
Stephens (K. G.) and Walker (D.), ionization of fast nitrogen ions in matter, 543.
Street (R.), *see* Phillips, 505.
Stubbs (P. H. S.), *see* Clegg, 583.
Sumner (F. H.), *see* Pritchard, 466.
Supersonic flow, flat nosed cylinders (Hall), 333.
Surface energy of colloidal metals in ionic lattices (Scott, A. B.), 610.
Surface energy of sodium (Scott, A. B.), 1173.
Surface of a nucleus (Scott, J. M. C.), 441.
Tabor (D.), mechanism of rolling friction, 1081.
Tapley (J. G.), *see* Ingram, 1221.
Tauber (G. E.), *see* Bhatia, 1211.
ter Haar (D.), Freundlich's red shift, 320, 1023.
Thermal conductivity of gallium crystal at low temperatures (Rosenberg), 767.
Thermal and electrical conductivity of magnesium (Rosenberg), 73.
Thermal expansion of solids at low temperatures (Bijl and Pullan), 290.
Thermodynamic properties of low boiling point elements (Dugdale and MacDonald), 811.
Thermoelectric power of monovalent elements at high temperature (Klemens), 881.
Thin films of silver sulphide, silver and gold (Burrow and Mitchell), 208.
Third law of thermodynamics, restricted quantum statistical proof, (Landsberg), 1129.
Thomas (W. R.) and Leak (G. M.), diffusion of nitrogen in alpha-iron, 656.
——, —— carbon in alpha-iron, 986.
Thompson (W. B.), cosmic ray particles, acceleration, 1210.
Thompson (N.), *see* Wadsworth, 223.
Thomson (S. J.), *see* Martin, 410.
Turbulence in the upper ionosphere (Maxwell), 1247.
Twiss (R. Q.), discrete radio sources, 249.
——, *see* Hanbury Brown, 663.
Upper atmosphere, drift movements (Maxwell and Dagg), 551.
Van Rossum (L.), *see* Friedlander, 1043.
V-events, analysis (Podolanski and Armenteros, 13.
V-events, fourty-four charged (Buchanan *et al.*), 1025.
V_1^0-particles, life time (Page and Newth), 38.

Varley (J. H. O.), heats of formation of binary alloys, calculation, 887.

Velocity of elastic waves in solidified inert gases (Barron and Domb), 654.

Waddington (C. J.), cosmic radiation, α particle component, 1312.

——, *see* Dahanayake, 885, 1219.

Wadsworth (N. J.) and Thompson (N.), fatigue fracture of copper, 223.

Walker (D.), *see* Chackett, 173.

——, *see* Stephens, 543.

Wardle (G.), *see* Martin, 410.

Ware (A. A.), ionized gas, collisional effects and conduction current, 547.

Wave motions and aerodynamic drag on free oil surface (Francis), 695.

Webb (F. J.), *see* Bergenlid, 851.

Whipple (R. T. P.), diffusion, concentration contours in grain boundary, 1225.

White (G. K.) and Woods (S. B.), copper alloys dilute, lattice thermal conductivity, low temperatures, 1343.

Wilkinson (D. H.), *see* Jones, 230, 703.

——, reaction ^{7}Li (pγ) ^{8}Be, special mechanisms, 259.

Wilks (E. M.) and Wilks (J.), hardness properties of diamond, cube faces, 844.

Wilks (J.), *see* Wilks (E. M.), 844.

——, *see* Bergenlid, 851.

——, *see* Hercus, 1163.

Willmott (J. C.), *see* Cartwright, 742.

Wilsdorf (H.) and Kuhlmann-Wilsdorf (Doris), dislocations in aluminium–copper alloys, direct evidence, 1096.

Wind measurements at altitudes of 80–100 km (Greenhow), 471.

Wohlfarth (E. P.), magnetic properties of alloys, Co and Ni with Pl and Pt, 647.

Wolfendale (A. W.), *see* Rochester, 980.

——, *see* Appapillai, 1059.

Woods (S. B.), *see* White, 1343.

Woolley (J. C.), *see* Phillips, 505.

Yasin (M.), decay of neutral *V*-particles, 413.

——, *see* Dahanayake, 885, 1219.

Yield strength of partly ordered Cu_3Au wires (Biggs and Broom), 246.

Ziman (J. M.), propagation of heat in liquid helium, 100.

Zinc crystals, cleavage planes, markings (Deruyttere and Greenough), 624.

END OF THE FORTY-FIFTH VOLUME

Printed by Taylor & Francis, Ltd.
Red Lion Court, Fleet Street, London, E.C.4

U. of Haw. 5

PERIODICAL